

## A transparent, tough, and impact-resistant bio-inspired glass composite with tunable mechanical properties

By

## Ali Amini Harandi

## Department of Mechanical Engineering McGill university

31 August 2020

A thesis submitted to McGill University in partial fulfillment of the requirements for a doctoral degree

© Ali Amini Harandi, 2020

## **Dedication**

To **Sahar**, my best friend and love of my life.

To **Hana**, the joy of my life.

To my parents for their love and support

## **Table of contents**

Abstract	vi
Résumé	viii
Acknow	ledgementsx
Contribu	ntions of Authorsxi
List of F	ïgures xiv
List of T	ablesxxii
1 Chapter 1:	A review on Structural bio-inspired materials and their methods of fabrication 1
1.1 Struct	ural biological materials2
1.1.1 I	ntroduction2
1.1.2 N	Nacre
1.1.3 I	Bone 6
1.1.4	Teeth 8
1.2 Fabric	cation techniques for bio-inspired materials9
1.2.1 I	ntroduction9
1.2.2 F	Freeze casting9
1.2.3	D printing11
1.2.4	Self-assembly

1.2	.5 Other techniques	. 15
1.3	Bio-inspiration; a new approach toward a tough and impact-resistant glass structure	. 17
1.4	Thesis Objectives	. 17
1.5	Thesis Organization	. 18
1.6	References	. 19
I	Link between chapter 1 and chapter 2	. 33
2 Cha	apter 2: Centrifugation of index-matched acrylic and glass flakes yields a strong and	
transpar	ent bioinspired nacreous composite	. 34
2.1	Abstract	. 36
2.2	Introduction	. 37
2.3	Results and discussions	. 38
2.4	Conclusions	. 49
2.5	Supplementary materials	. 51
2.5	.1 Materials and Methods	. 51
2.5	.2 Fracture mechanics calculations	. 54
2.5	.3 Index-matching	. 55
2.5	.4 Mechanical and fracture characterization supplementary results	. 57
2.6	Acknowledgements	. 58
2.7	References	. 59
Ţ	Link between chapter 2 and chapter 3	. 62

3 Ch	apter 3: Poly(methyl methacrylate)-based polymers with improved toughno	ess and impact
resistano	ce and tunable mechanical properties	63
3.1	Abstract	65
3.2	Introduction	66
3.3	Materials and methods	68
3.3	.1 Copolymerization and crosslinking of PMMA	69
3.3	.2 Tensile test	69
3.3	.3 Three-point bending (3PB) test	69
3.3	.4 Single-edge notched beam (SENB) test	70
3.3	.5 Weight-drop impact test	70
3.3	.6 Evaluation of solvent resistance	71
3.4	Results and Discussions	71
3.5	Optical clarity and solvent resistance	72
3.6	Mechanical properties	73
3.7	Fracture toughness	78
3.8	Impact resistance	79
3.9	Conclusions	82
3.10	Supplementary information	83
3.11	Acknowledgements	86
2 12	Deferences	97

L	ink from chapter 3 to chapter 4	90
Cha	pter 4: An impact resistant bio-inspired transparent composite material with tunable	
echanic	cal properties	91
4.1	Abstract	93
4.2	Introduction	94
4.3	Materials and Methods	97
4.3.	1 Materials	97
4.3.	2 Glass composite fabrication	98
4.3.	Mechanical, fracture toughness, and impact resistance characterization of the	
glas	s composite	99
4.4	Results and discussion	00
4.4.	1 Impact-resistant nacreous glass composite	00
4.4.	2 Effect of soft phase on mechanical properties of the glass composite	03
4.4.	Effect of different soft phases on fracture properties of the glass composite 1	04
4.4.	4 Conclusions 1	06
4.5	Acknowledgements	07
4.6	References	08
Cha	pter 5: Conclusion	10
5.1	Summary of accomplishments	11
5.2	Thesis contributions	13
	Chaechanio 4.1 4.2 4.3 4.3. 4.3. 4.4. 4.4. 4.4. 4.4. 5.1	4.2 Introduction

5.	.3	Future work	114
6	Supp	plementary experimental information	118

## **Abstract**

Glasses have numerous applications due to their exceptional transparency and stiffness; however, poor fracture and impact resistance limit their applications. One strategy to improve their mechanical properties is through bio-inspiration. Structural biological composites such as nacre, the protective inner layer of mollusk shells, offer far superior mechanical properties relative to their constituents. This has motivated researchers to mimic the design principles in natural composites to create tough transparent materials. However, current bio-inspired composites suffer from poor optical transmission and trade-offs between rigidity, toughness, and fabrication scalability. Here, we present an optically transparent tough nacreous glass composite material with a four-fold increase in fracture toughness, a three-fold increase in flexural strength compared to conventional structural glasses, and a 73% average optical transmittance. Our composite is fabricated with a simple scalable approach: the composite consists of glass flakes and poly (methyl methacrylate) (PMMA) structured utilizing a centrifugation fabrication method that aligns and compacts the flakes into layers. To optimize the transparency of the structure, the refractive indices of the PMMA and glass are matched by adding a dopant to the PMMA. Our glass composite also outcompeted annealed glass and PMMA in impact resistance; it absorbs 34 times more energy than annealed glass and five-fold more energy than PMMA under impact loads. Based on these results, this nacreous glass composite is proposed as a potential alternative in diverse architectural, vehicular, and electronics applications.

In the second part of this thesis, we developed a class of PMMA-based polymers by copolymerizing with acrylonitrile (AN) and crosslinking with 1,4 butanediol dimethacrylate (BUT) to enhance and tune the PMMA's mechanical properties as our composite's soft phase. We proposed a simple method to increase PMMA's fracture toughness and impact resistance without

sacrificing other mechanical properties, and with the least modification in its simple fabrication method. Such an approach enhanced PMMA's fracture toughness and impact resistance by 30% and 40%, respectively, while the strength remained constant. In the third part of current thesis, we incorporated our PMMA-based polymers into the glass composite to study the soft phase's role on composite's mechanics and tuning the structural properties. In this way, we successfully increased the composite's rupture strain by 30% while retaining the flexural strength of the material. We could also increase the Work of Fracture (WOF) as a measure of fracture toughness by 40%. PMMA-based polymers, however, appeared to have no effect on the impact resistance of the material.

## Résumé

Les verres ont de nombreuses applications en raison de leur transparence et de leur rigidité exceptionnelle; cependant, une mauvaise résistance à la fracture et aux chocs limite leurs applications. Une stratégie pour améliorer leurs propriétés mécaniques est par la bio-inspiration. Les composites biologiques structuraux tels que la nacre, la couche intérieure protectrice des coquilles de mollusques, offrent des propriétés mécaniques bien supérieures par rapport à leurs constituants. Cela a motivé les chercheurs à imiter les principes de construction des composites naturels pour créer des matériaux transparents résistants. Cependant, les composites bio-inspirés actuels souffrent d'une mauvaise transmission optique et d'un compromis entre la rigidité, la résistance aux chocs, et la possibilité de la fabrication industrielle. Ici, nous présentons un matériel composite de verre nacré dur, optiquement transparent, avec une augmentation de la résistance à la fracture de quatre fois, une augmentation de la résistance à la flexion de trois fois par rapport aux verres structurels conventionnels, et une transmittance optique moyenne de 73%. Notre composite est fabriqué avec une approche simple et évolutive: le composite se compose de flocons de verre et de poly (méthacrylate de méthyle) (PMMA), structuré en utilisant une méthode de fabrication par centrifugation qui aligne et compacte les flocons en couches. Pour optimiser la transparence de la structure, les indices de réfraction du PMMA et du verre sont egalisés en ajoutant un dopant au PMMA. Notre verre composite a également surpassé le verre recuit et le PMMA en termes de résistance aux chocs; il absorbe 34 fois plus d'énergie que le verre recuit et cinq fois plus d'énergie que le PMMA sous des charges d'impact. Sur la base de ces résultats, ce composite de verre nacré est proposé comme une alternative potentielle dans diverses applications architecturales, automobiles et électroniques.

Dans la deuxième partie de cette thèse, nous avons développé une classe de polymères à base de PMMA en copolymérisant avec de l'acrylonitrile (AN) et en réticulant avec du 1,4 butanediol diméthacrylate (BUT) pour améliorer et ajuster les propriétés mécaniques du PMMA en tant que phase molle de notre composite. Nous avons proposé une méthode simple pour augmenter la ténacité à la rupture et la résistance aux chocs du PMMA sans sacrifier d'autres propriétés mécaniques, et avec la moindre modification à la méthode de fabrication simple. Une telle approche a amélioré la ténacité et la résistance aux chocs du PMMA de 30% et 40%, respectivement, tandis que la résistance est restée constante ou a connu une augmentation modeste. Dans la troisième partie de cette thèse, nous avons incorporé nos polymères à base de PMMA dans

le composite de verre pour étudier le rôle de la phase molle sur les propriétés mécaniques du composite et sur le réglage des propriétés structurelles. De cette manière, nous avons réussi à augmenter la contrainte de rupture du composite de 30% tout en conservant la résistance à la flexion du matériel. Nous pourrons également augmenter le travail de fracture (WOF) comme mesure de la résistance à la rupture de 40%. Cependant, les polymères à base de PMMA semblaient n'avoir aucun effet sur la résistance aux chocs du matériel.

## Acknowledgements

My Ph.D. journey was long, arduous, and reaching this point was not possible without the help and support of many people, to whom I would like to express my deepest gratitude and appreciation.

Firstly, I would like to thank my supervisor Allen Ehrlicher for all the support and guidance during my Ph.D. Without a doubt, this project could not be accomplished without his ideas, advice, and help. His support was not limited to my academic life: he has been a good friend and has always been there when I faced a problem and needed a helping hand in my personal life. A special thanks to my dearest friends Chris Sitaras and Adele Khavari, who helped me over the course of my Ph.D. with their priceless emotional and technical help.

I would like to extend my appreciation to all of my colleagues in the Bio Active Materials lab. It was a great pleasure working with them, and without their support, this project would have been extremely difficult: Ajinkya Ghagre, Haruka Yoshie, Newsha Koushki, Pouria Tirgar, Luv Kishore, and Amy Sutton.

I would like to thank the Faculty of Engineering at McGill University, Natural Sciences and Engineering Research Council of Canada, Canada Research Chairs Program, and the Fonds Québécois de la Recherche sur la Nature et les Technologies for their financial support for this project.

I would like to thank professor Francois Barthelat and Professor Pascal Hubert for granting me access to their labs and their research facilities.

Lastly, I would like to thank the staff at Nanoqam and UQAM Chemstore for their invaluable help.

## **Contributions of Authors**

This thesis comprises of three manuscripts, and the contribution of authors for each one is listed below:

• Centrifugation of index-matched acrylic and glass flakes yields a strong and transparent bioinspired nacreous composite

Ali Amini<sup>1,2</sup>, Adele Khavari<sup>1</sup>, Francois Barthelat<sup>2,3</sup>, Allen J. Ehrlicher<sup>1,2</sup>

- 1. Bio-Active Materials Laboratory, Department of Bioengineering, McGill University, Montreal, Quebec, H3A 0C3, Canada.
- 2. Department of Mechanical Engineering, McGill University, Montreal, Quebec, H3A 0C3, Canada.
- 3. Department of Mechanical Engineering, University of Colorado Boulder, Boulder, Colorado, US.

### **Contributions:**

AA: Conceptualized the problem, designed and performed the experiments for sample preparation, performed the characterization tests, analyzed the results, discussed the results, prepared the figures and wrote the manuscript.

AK: Designed experiments, provided technical and scientific advice, reviewed and edited the manuscript.

FB: Provided technical and scientific advice, reviewed and edited the manuscripts, provided resources and funding.

AE: Conceptualized the problem, developed the methodology, provided scientific and technical advice, wrote the manuscript, provided resources and funding.

In revision in *Science* Journal

• Poly(methyl methacrylate)-based polymers with improved toughness and impact resistance and tunable mechanical properties

Ali Amini<sup>1,2</sup>, Adele Khavari<sup>2</sup>, Pouria TirgarBahnamiri<sup>2</sup>, Allen J Ehrlicher\*<sup>1,2</sup>

1-Department of Mechanical Engineering, McGill University, Quebec, Canada.

2- BioActive Materials Lab., Department of Bioengineering, McGill University, Quebec,

Canada.

**Contributions:** 

AA: Conceptualized the problem, designed and performed the experiments for sample preparation, performed the characterization tests, analyzed the results, discussed the results, prepared the figures and wrote the manuscript.

AK: Conceptualized the problem, designed experiments, provided technical and scientific advice, reviewed and edited the manuscript.

PTB: Provided technical and scientific advice, performed experiments for sample preparation.

AE: Conceptualized the problem, developed the methodology, provided scientific and technical advice, wrote the manuscript, provided resources and funding.

Manuscript in preparation.

• An impact resistant bio-inspired transparent composite material with tunable mechanical properties

Ali Amini<sup>1,2</sup>, Adele Khavari<sup>2</sup>, Francois Barthelat<sup>2,3</sup>, Allen J Ehrlicher\*<sup>1,2</sup>

1-Department of Mechanical Engineering, McGill University, Quebec, Canada.

2- BioActive Materials Lab., Department of Bioengineering, McGill University, Quebec, Canada.

xii

3. Department of Mechanical Engineering, University of Colorado Boulder, Boulder, Colorado, US.

## **Contributions:**

AA: Conceptualized the problem, designed and performed the experiments for sample preparation, performed the characterization tests, analyzed the results, discussed the results, prepared the figures and wrote the manuscript.

AK: Conceptualized the problem, provided technical and scientific advice, reviewed and edited the manuscript.

FB: Provided technical and scientific advice, reviewed and edited the manuscripts, provided resources and funding.

AE: Conceptualized the problem, developed the methodology, provided scientific and technical advice, wrote the manuscript, provided resources and funding.

Manuscript in preparation.

## **List of Figures**

Figure 1-1. Nacre, the inner layer in mollusk shells. A) A red abalone shell from top. B) Nacre is
located beneath the protective calcite layer. C) A schematic of brick and mortar structure in
nacre. D) Arrangement of ceramic tablets in a tessellated way in red abalone nacre. D) SEM
image of a fractured surface in a red abalone shell shows a perfect brick and mortar structure.
Image acquired from [28].
Figure 1-2. Structure of bone from nanoscale to microscale. Outer surface is composed of
compact bone with highly oriented fibrillar structure in different length-scales. The inner part is
composed of the spongy bone. Image acquired for [2]
Figure 1-3.Human teeth. There is a protective hard layer on the top that acts as a shield against
penetrations. Beneath that, there is dentin, which is a tough tubular material with some
interesting toughening mechanisms such as crack arresting. Image acquired from [5]
Figure 2-1. Centrifuged-based fabrication method of nacreous glass composite. (A) Cleaned
glass flakes were dispersed in toluene. (B) Glass flakes surface-treated with y-MPS and then
with a solution of MMA in toluene to promote polymerization from the glass surface. (C)
Surface-treated glass flakes were involved in free radical polymerization of PMMA at 50°C. (D)
Glass-PMMA mixture transferred to a casting mold with a pre-designed cavity on the bottom (E)
Glass-PMMA mixture was centrifuged to impose alignment in flakes and densify the mixture.
(F) Polymerization process finalized in oven: 12 hours at 50°C, 4 hours at 70°C and 2 hours at
100°C
Figure 2-2. Dopant percentage and composite thickness affect composite transparency and
haziness. (A) 1mm thick glass composites with 0% dopant (top), and 12% dopant (bottom). (B)

Transmittance for the soda-lime glass, doped PMMA (12%), 12% glass composite, laserengraved laminated glass [17], and bio-inspired transparent composite [14]. Our composite compares well with soda-lime monolithic glass and is superior to its bio-inspired counterparts. 41 Figure 2-3. Centrifugation increases the glass volume fraction by decreasing the polymer thickness layer between tablets. (A) Glass volume fraction increases almost two-fold when the sample centrifuged (2000g). Also, polymer layer thickness decreases about 50% when centrifuged with 2000g force. (B) Section SEM image of a non-centrifuged composite (top, about 24% glass volume fraction). We observed a noticeable number of areas with no flakes, and also many flakes with random orientation in the material. Polar distribution of orientation in the flakes also confirms this observation (bottom). (C) Section SEM image of centrifuged composite (2000g, about 43% glass volume fraction). Flakes are more oriented in one direction, and areas with no flakes are rarely observed. Polar distribution of orientation in the flakes for different centrifuging speeds also shows insignificant difference between 1000g, 2000g and 4000g forces. Figure 2-4. Surface functionalization and centrifuging process improve the mechanical properties of the glass composite. (A) Flexural stress-flexural strain curves for the composites with and without surface-functionalized glass and centrifugation. Surface-treated composite experiences a linear deformation regime followed by a non-linear one up to the failure, whereas the composite with no glass functionalization and centrifugation deforms non-linearly to the fracture while possessing lower strength and stiffness values. (B) strength and flexural modulus increase with centrifugation. While the higher centrifuging speed yields higher strength and flexural modulus, 2000g appears to be the saturation point. (C) SENB test load-displacement curves for pure PMMA, non-centrifuged and centrifuged composites, illustrating an increased fracture strength

with composite formulation and subsequent centrifugation. (D)  $K_{IC}$  and WOF values increase Figure 2-5. Transparent nacreous glass mimics key aspects of nacre's microstructure and toughening mechanisms. (A) SEM micrograph of the sample cross-section in a fractured surface in our glass composite. Staggered glass platelets with polymer layers in between and numerous pulled-out glass tablets due to fracture. (B) Fracture surface of natural nacre. (C) While tablets are experiencing delamination due to lateral deformation, the polymer layer acts as a bridge between tablets and contributes to the composite toughness (white arrow). (D) Tablet sliding in large scale leads to tablet pull-out and hence deflection of crack growth path. (E) Macroscopic Figure 2-6. Ashby plot of fracture toughness versus strength for numerous synthetic and natural materials. Our transparent nacreous composite (centrifuged at 2000g) outperforms annealed soda-lime [28], tempered [2], laminated [3], bio-inspired transparent composite [14], and laser-Figure 2-7. Glass composite doped with Phenanthrene is highly transparent, but hazy. (A) Transmittance values for 1mm thick samples and different phenanthrene weight percentages. (B) Haze factor values for 1mm thick composites and different dopant weight percentages. (C) PMMA refractive index increases linearly by increasing phenanthrene weight percentage. (D) Average transmittance values in terms of dopant weight percentage. 12% appears to be the optimum dopant amount. (E) Comparison of transmittance and haze factor for the 12% glass composite, doped PMMA (12%), soda-lime glass, bio-inspired transparent composite (14), and laser-engraved laminated glass [17]. Although the transmittance of our glass composite is similar to the soda-lime glass, its haze factor is higher by a factor of 20. Our glass composite, however,

is superior to its bio-inspired rivals both in transmittance and haze factor. (F) Haze factor values
for 1mm thick composites and different dopant weight percentages. 12 wt% of dopant yields the
lowest haze factor value. Data point and error bars demonstrate the mean value and the standard
deviation respectively
Figure 2-8. Effect of centrifugation on rupture strain of the composite. Centrifuging appears to
have insignificant effect on the composite's rupture strain
Figure 2-9. Nacreous glass composite outperforms normal, tempered and laminated glass under
fracture. (A) Crack initiation fracture toughness vs final strength for normal annealed soda-lime
[28], tempered [2], laminated [3], bio-inspired transparent composite [14], and our composite
glass (2000g). The composite demonstrated here outperforms other state of the art glasses in both
fracture toughness and final strength. (B) WOF versus final strength for normal annealed [32],
laminated (3), and laser-engraved laminated [17] glasses, as well as the pure PMMA and our
composite glass(2000g). The only glass that exceeds our composite in terms of WOF is Ref. 17,
but it possesses far less strength compared to our composite. Data points and error bars
demonstrate the mean value and the standard deviation respectively
Figure 3-1. Chemical structure of polymers. A) Neat PMMA. B) PMMA copolymerized with
acrylonitrile (PA polymer). C)PMMA crosslinked with 1,4 butanediol dimethacrylate (PBDM
polymer). D) PA polymer crosslinked with 1,4 butanediol dimethacrylate (PABDM polymer). 71
Figure 3-2. Optical transparency and solvent resistance of polymers. A) All synthesized
polymers showed excellent optical clarity without any noticeable difference with PMMA. B)
Unlike PA polymers that performed poorly when exposed to a solvent, the rest of polymers
showed better solvent resistance that neat PMMA. The effect of toluene at room temperature,
however, appeared to negligible even on PA polymers

Figure 3-3. PA and PBDM show different behavior under tensile loading. A) PA polymers experience a huge plastic deformation after yielding, while PBDMS polymers are similar to PMMA and break shortly after yielding. B) PABDM polymers' stress-strain profile could be similar to PA or PBDM depending on the proportion of the chemical components. C) PA polymers experience stress whitening and craze after yielding. D) No stress-whitening was Figure 3-4. Mechanical properties of polymers from tensile testing. A) small molar percentages of AN almost retain yield/rupture strength, while similar to PBDM polymers, higher molar percentages of AN have a negative effect on strength values. PABDM polymers mostly show an improvement in strength values for higher BUT concentrations compared to the corresponding PA polymer. B) PA polymers undergo a huge plastic deformation and hence experience a considerable rupture strain. BUT crosslinker, on the contrary, does not affect the yield/rupture strain. All PABDM polymers with lower proportions of BUT showed high extensions at failure. Figure 3-5. Crosslinking improves flexural modulus. increasing AN concentrations would decrease the flexural modulus of PA polymers. Increasing BUT concentration would increase the flexural modulus in PBDM polymers. Crosslinking with BUT compensates the negative effect of AN on modulus, and hence, PABDM polymers possess higher (or similar) modulus values compared to PA and PMMA polymers......78 Figure 3-6. Effect of copolymerization and crosslinking on PMMA's fracture toughness. PA fracture toughness increases as the AN concentration increases in the polymer. Crosslinking, however, appeared to have an adverse effect on the fracture toughness. High AN content, along

with low crosslinking agent concentrations, yielded a PABDM polymer with higher toughness
than PA counterparts79
Figure 3-7. Performance of PMMA-based polymers under impact loading. A) PA impact
resistance generally increases by increasing the AN content. The impact energy could be further
increases by crosslinking the PA polymer with low amounts of BUT (PABDM polymer). BUT
alone, however, has a negative effect on the impact resistance of PMMA (left) and
PA polymers (middle) turn to fewer and bigger pieces when breaking under impact loads,
compared to PBDM and PABDM (right) polymers, which turn to smaller and more fragments
with the same loading and boundary conditions
Figure 3-8. Mechanical properties of polymers from tensile testing. A) small molar percentages
of AN could retain yield strength and cause a smaller decline in final strength. PBDM polymers
also possess lower strength values compared to PMMA. PABDM polymers mostly show an
improvement in strength values for higher BUT concentrations. B) PA polymers undergo a huge
plastic deformation and hence experience a considerable rupture strain. BUT crosslinker, on the
contrary, does not affect the yield/rupture strain. All PABDM polymers with lower proportions
of BUT showed high extensions at failure. However, increasing the BUT molar percentage
diminishes the rupture strain. Bar graphs are mean values, and error bars demonstrate standard
deviation
Figure 3-9. Crosslinking improves flexural modulus. PA polymers are inferior to PMMA in
flexural modulus, and the decline in modulus values is more for higher AN concentrations.
PBDM polymers, on the other hand, possess higher modulus compared to PMMA. Crosslinking
with BUT compensates the negative effect of AN on modulus, and hence, PABDM polymers

possess higher (or similar in some cases) modulus values compared to PA and PMMA. Bar
graphs are mean values, and error bars demonstrate standard deviation
Figure 3-10. Effect of copolymerization and crosslinking on PMMA's fracture toughness. A) PA
polymers appeared to have higher WOF compared to pure PMMA. Crosslinking, however, had a
negative impact on WOF. High AN content, along with low crosslinking agent, yielded a
PABDM polymer with higher toughness than PA counterparts. Data points are mean values and
the error bars are standard deviation
Figure 3-11. Performance of PMMA-based polymers under impact loading. Increasing AN
content in PA would increase the impact resistance of the material. The impact resistance was
further increase by incorporating low contents of crosslinking agent in PABDM polymers. BUT,
however, appeared to have a negative effect on impact resistance of the PBDM polymers. Data
points are mean values and error bars demonstrate standard deviation
Figure 4-1. Our glass composite mimics the structure and toughening mechanisms of natural
nacre. A) Centrifuging imposes order on the structure, and a brick-and-mortar structure is
obtained. B) Due to our index-matching strategy, the glass composite possesses high levels of
transparency, compared to the one without index-matching that is entirely white and hazy. C)
Due to the activation of toughening mechanisms throughout the material, crack deflection is
observed in macroscale. 97
Figure 4-2. Nacreous glass composite outperforms annealed glass in impact energy. A) Load-
displacement profiles of annealed glass, PMMA, and nacreous glass. Annealed glass and PMMA
experience a sharp and sudden drop in load after reaching maximum load, while glass composite
goes through numerous variations in load and possesses much larger displacement at the failure
point. B) Centrifugation increases the impact energy. While centrifuging increases the impact

energy by more than 100%, using crosslinked and co-polymerized PMMA does not affect the impact resistance of the glass composite. Bar graphs demonstrate mean energy values normalized by samples' thickness. C) Images of normal glass, PMMA, and composite glass with 2mm of thickness before (top), write after (middle), and after (bottom) impact, while simply supported. Bar graphs demonstrate mean values and error bars are standard deviation. ............ 102 Figure 4-3. Effect of PMMA-based polymers on mechanical properties of glass composite. A) Low percentages of AN, along with PABDM (with moderate percentages of AN and BUT), appear to have no effect on the composite's strength. PBDM, however, negatively affected the composite's strength. B) Rupture strain increases as we increase the AN content in PA polymer. PBDM and PABDM polymers (in low BUT concentrations) do not have any adverse effect on the rupture strain. C) While PAs reduce the composite's flexural modulus, PBDM polymers slightly enhance the flexural modulus. Bar graphs demonstrate mean values and error bars are standard deviation. 104 Figure 4-4. PA polymers increase the WOF. A) Glass composites experience non-catastrophic crack growth and fracture. As apparent from the load-deflection profiles, PMMA undergoes a sudden and rapid crack growth and fracture after reaching maximum load, while glass composites experience a smooth and slower crack growth till complete failure. B) PA polymers increase the WOF, and the increase is more significant for higher AN concentrations. PBDM polymers affect the WOF negatively regardless of the molar percentage of BUT. A notable increase in WOF was observed when high amounts of AN with a low amount of BUT was used 

## **List of Tables**

Table 2-1. Strength, rupture strain, and flexural modulus values for composite with no surface
functionalization and centrifuging, surface-functionalized and centrifuged, and PMMA samples.
Table 3-1. Monomer concentrations in polymeric samples

# Chapter one Introduction

A review on Structural bio-inspired materials and their

methods of fabrication

## 1.1 Structural biological materials

## 1.1.1 Introduction

Natural materials are excellent sources of inspiration for designing novel and advanced materials, and even solving engineering problems. Based on this fact, bio-inspired materials as a field of research has attracted a tremendous amount of attention. Mimicking the design principles in natural materials which have benefitted from millions of years of evolutionary processes and refinements is the main focus in this area of research.

One could categorize bio-inspired materials into two main groups of functional and structural materials. Areas like sensing, optics and robotics fall into the category of functional materials. Some famous examples are the robots built from soft or hard materials to emulate the motion of jellyfish[1]. Unlike the functional bio-inspired materials, the main goal in design of structural materials is usually simple: building a final structure with a level of toughness or strength, significantly more than that of main constituent elements, simply through design principles and strategies[2]. In this literature review, the main focus will be on structural bio-inspired materials, design principles employed by nature in natural materials and novel fabrication methods for mimicking these design strategies.

There are some key features which are in common between most of structural biological materials. They usually have a hierarchical structure, their structure forms through a bottom-up self-assembly process and hydration has a key role in their mechanical properties[3]. Also, in their formation only the main elements of C, O, H, P, N, S, Ca and Si have been used which highlights the role of geometry and design principles for the successful functionality[4].

According to *Naleway*, although there are many different natural living species, the strategies they have employed to fight with natural challenges could be categorized into only 8 groups[5]. These

8 groups are 1)fibrous like tendons, 2)helical like insect exoskeletons to resist torsional loads, 3)gradient like human teeth, 4)layered like nacre, 5)tubular like mammalian horn and hoof, 6)cellular like organs of birds, 7)suture like leatherback turtles and 8)overlapping like shark skin. But no matter which of the abovementioned strategies is used by nature, there is one simple similarity between all of structural biological materials: they are composed of soft and hard phases[4]. The soft part is usually a biopolymer like collagen, elastin and keratin and the hard part is mostly mineral materials like calcium carbonate, carbonated hydroxyapatite and silica. The soft part is responsible for strength, while the hard part takes care of stiffness and toughness.

Nacre, bone, and teeth are three examples of natural structural materials that have been extensively studied by researchers. Here, we briefly review their structure, properties, and the reasons that have made these materials an excellent source of inspiration for making new synthetic materials.

## **1.1.2** Nacre

Nacre is a very good examples of a structural bio-material and how a proper combination of geometry and design can lead to remarkable mechanical properties of the structure in comparison with its building blocks.

Nacre, the tough inner layer produced by mollusk shells, is an organic-inorganic composite material (Fig. 1-1). The mineral part (aragonite) forms about 95% of its volume, and just a minor part of the volume is soft biopolymer. Although fragile elements form a major part of nacre, it is 3000 times tougher than hard ceramic platelets[6] and it can undergo up to 1% of strain which is incredible in comparison with its ceramic building blocks[7].

Many researchers have tried to characterize the mechanical properties of nacre on macroscopic samples. Mechanical properties of nacre have been thoroughly investigated under tension[8, 9], bending[10-12] and compression[13]. Also, experimental methods in finer scales have been used to measure the mechanical properties of individual components of the nacre. For example, nanoindentation methods have been utilized to study the deformation and fracture of single tablets in the nacre structure[14-16].

The role of soft biopolymer in nacre has not drawn as much attention as the hard part. Smith studied the force-extension behavior of natural adhesives by AFM[17], revealing that folding-unfolding behavior of proteins play a role in both strength and toughness of nacre. According to Evans, viscoelastic glue between ceramic tablets improves the nacre's toughness[18]. Using a finite element analysis of nacre, Tushtev showed that the biopolymer is really important in stress distribution in nacre[19]. Meyers also studied the role of biopolymer in strength of nacre, but he concluded that the role of biopolymer is more in growth of aragonite crystals in the c direction than in nacre's strength and toughness[20, 21]. Lopez by measuring the strength of isolated organic and inorganic parts in nacre concluded that biopolymer doesn't have any major contribution in strength of nacre and its role is more in crack deflection[22]. The behavior of biopolymer in nacre was studied experimentally (AFM) and modeled by Xu[23]. Dastjerdi conducted experiments on biopolymer in three different kinds of nacres to characterize its role in the high toughness of nacre[24]. He showed that biopolymer is really weak in terms of fracture toughness and that's why it can contribute to extrinsic toughening mechanisms like crack bridging or crack deflection by leading the crack to propagate in itself instead of the brick part. Niebel studied the role of soft biopolymer in fracture toughness of nacre-like materials by infiltrating 3 different polymeric materials into the porous ceramic scaffold made by magnetically assisted slip casting method[25].

He used polymeric materials with different degree of stiffness and strength. According to his results, by increasing the stiffness of the soft phase, the strength of the composite will increase and also using tough polymeric materials leads to a composite structure with high crack initiation toughness. But using an elastomer with an intermediate degree of toughness and stiffness will trigger and activate the extrinsic toughening mechanisms one would expect in nacre-like structures.

Also several mechanisms have been proposed to explain the incredible performance of nacre under mechanical loads. One mechanism is related to the tough organic biopolymer between the tablets [10]. There is a strong adhesion between tablets and the biopolymer which cause a resistance against shear movement of the tablets with respect to each other. Also, like many other proteins, this biopolymer unfolds several times when extended that will contribute to energy dissipation[17]. Another important mechanism is the resistance against movement of the tablets due to the contact between nano-asperities on the tablet surface[18, 26]. Bridges between the tablets is the next factor[27]. Since these bridges will not contribute to load bearing and hardening after they break, one should consider their role just in low strain regimes [28]. The last, and according to Espinosa[28] and Barthelat [7], most important mechanism is the interlocking between the platelets due to the small waviness of them. Fratzl on the other hand, discussed a key characteristic in common between many natural materials using the aforementioned mechanisms: tessellation[29]. This feature has been described in many cases like nacre. The behavior of nacre under tension is related to periodic change in mechanical properties and more specifically young's modulus which happens in any brick and mortar structure with periodic transition from hard to soft part of material and vice versa. This variation in modulus controls the crack driving force and can finally arrest the crack. Following the work of Jager & Fratzl [30], many researchers like Ji & Gao[31] studied the nacre structure by considering it as a simple structure of staggered hard tablets with a soft material in between. In another similar work, Gao analyzed such structure from the tablet size and geometry point of view and concluded that the nanometer size of tablets make them insensitive to flaws and cracks[32].

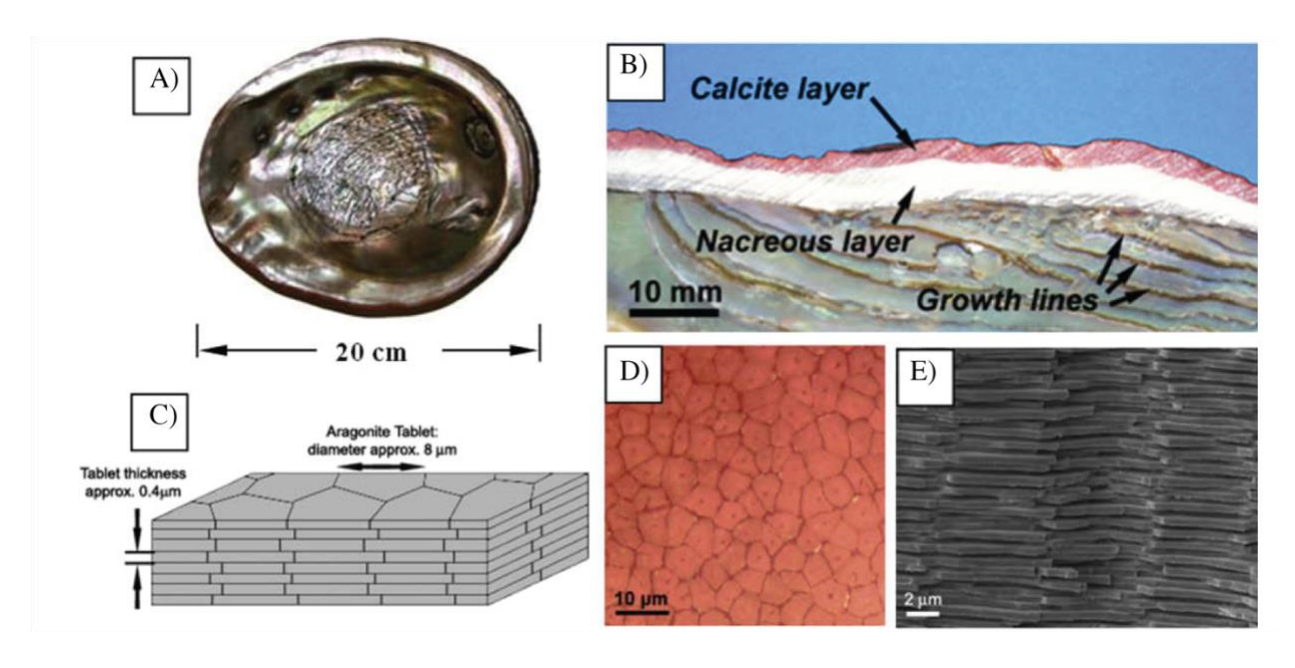


Figure 1-1. Nacre, the inner layer in mollusk shells. A) A red abalone shell from top. B) Nacre is located beneath the protective calcite layer. C) A schematic of brick and mortar structure in nacre. D) Arrangement of ceramic tablets in a tessellated way in red abalone nacre. D) SEM image of a fractured surface in a red abalone shell shows a perfect brick and mortar structure.

Image acquired from [28].

## 1.1.3 Bone

Bone also is an organic (mainly collagen type I)/inorganic(hydroxyapatite) composite [1]. Water is another important element, consisting 10-15% of bone's volume (Fig. 1-2). There are two types of mammalian bone: cortical or compact bone which is found in long bones like the femur and fibula and cancellous or porous bone which can be found in the core of bones and also flat bones and are composed of bony trabecular struts and marrow-filled cavities[33]. Although the porosity of the cancellous part reduces the strength, it makes the bone a lightweight structure[33]. From the

macroscopic point of view, the mechanical properties of bone won't be the same for different bones and it even varies in different parts of one specific bone[34]. Rho studied the site-specific mechanical and physical properties of some human bones like femur and tibia[35]. At the microscale, mineralized collagen fibers form plate-like lamellae in a few micrometers in size. The lamellae could either be arranged in an organized way like osteon in which plate-like lamellae form concentric layers around a canal (haversian system) or in a less organized way like woven bone[35]. Ascenzi studied the behavior of single Haversian systems under all the major modes of mechanical loading[36-39]. Also, there are many studies on mechanical properties of trabecular bone according to which, the modulus of elasticity is estimated between 1 to 20 GPa [40-42]. According to [33], both the strength and toughness of the bone are dependent on the degree of mineralization. Also, the mechanical properties of bone are quite strain-rate dependent [43]. Many research groups have studied the fracture behavior of bone. For instance, Behiri studied the bovine bone fracture toughness [44] and Nalla studied the quasi-static fracture toughness of human cortical bone [45]. Nalla investigated the different mechanisms contributing to fracture toughness of bone, namely un-cracked ligament bridging, crack deflection, collagen-fibril bridging and constrained micro-cracking [45]. According to this study, the most important mechanism is crack deflection which contributes about 50% to the fracture toughness.

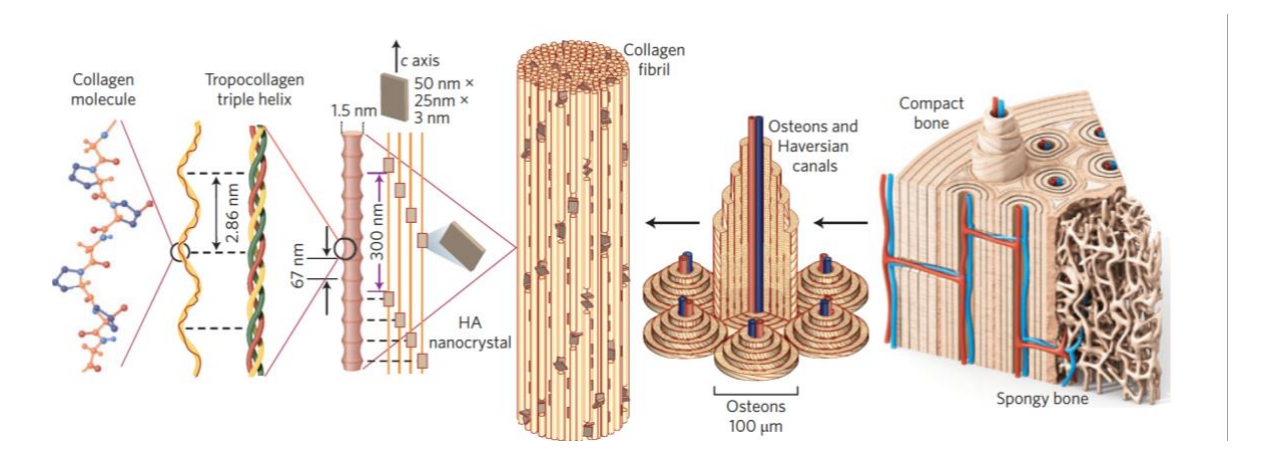


Figure 1-2. Structure of bone from nanoscale to microscale. Outer surface is composed of compact bone with highly oriented fibrillar structure in different length-scales. The inner part is composed of the spongy bone. Image acquired for [2].

## 1.1.4 Teeth

Teeth consist of one hard and highly mineralized outer layer called enamel and one inner and tougher layer called dentin(Fig. 1-3) [33]. Enamel is formed by woven hydroxyapatite rods with an average diameter of 5 microns[46]. Unlike the enamel, dentin is more similar to bone since it contains collagen hydroxyapatite and water with almost the same volume fraction. The microstructure of dentin is consisting of some units called tubulars embedded in a matrix of collagen reinforced with hydroxyapatite plate-like crystals. The tubulars themselves are surrounded by hydroxyapatite crystals[47]. Hardness and fracture toughness of tooth have been measured by *Nalla* [45] and *Imbeni* [47].

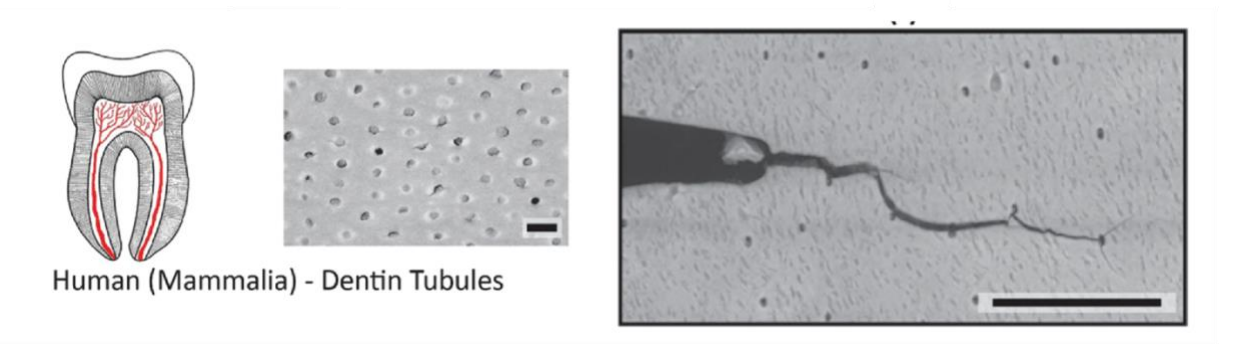


Figure 1-3. Human teeth. There is a protective hard layer on the top that acts as a shield against penetrations. Beneath that, there is dentin, which is a tough tubular material with some interesting toughening mechanisms such as crack arresting. Image acquired from [5].

## 1.2 Fabrication techniques for bio-inspired materials

## 1.2.1 Introduction

Considering the importance of natural material based on what is mentioned above, many researchers have tried to employ current fabrication techniques, modify existing methods or even create new methods to mimic the design and strategies in natural materials. In the following paragraphs, a review of these techniques will be presented.

## 1.2.2 Freeze casting

Freeze casting or ice templating is one of the more promising techniques for emulating the structural biomaterials like nacre and bone. In this technique, a slurry of ceramic and water is frozen from the bottom and due to the formation of lamellar ice crystals, ceramic particles are entrapped between ice crystals. After a freeze-drying process and sublimation of water, a porous template of the ice structure will remain and after sintering could be used for many purposes. In this way, one could mimic the nacre structure by infiltrating a second soft phase into the structure to fill the pores. The theory behind this technique can be found in [48] and [49]. He also used alumina and AlSi to produce ceramic/metal composites and also controlled the pore size of

hydroxyapatite porous structure to build artificial bone [50]. Munch mimicked the nacre structure very well by modifying the sintering part and including additives to the ceramic slurry, [51]. He used sucrose to control the roughness of the tablet surfaces and also controlled the adhesiveness of the soft phase to ceramic phase by grafting methacrylate groups on ceramic surfaces before polymer infiltration. Another novelty of his work lies in one extra process of pressing and sintering the scaffold in order to increase the ceramic content for having a brick and mortar structure instead of a lamellar structure. The capability of freeze casting in emulating porous structures like bone and layered structures like nacre has made many researchers try different ceramics and freezing vehicles and also study the different factors effective in controlling the structure of porous structure. Water, camphene, camphor-naphthalene and tert-butyl alcohol have been used as freezing vehicles to obtain lamellar[52], cellular[53, 54], dendritic[55] and prismatic[56] structures respectively. Effects of ceramic particle size, freezing front velocity and ceramic load (concentration) has been also studied[57, 58]. Effects of different additives such as glycerol, sucrose, sodium chloride, citric water, ethanol and PVA on the final microstructure has been studied thoroughly[59-61]. Controlling the temperature gradient is one of the effective ways of controlling the microstructure. Waschkies [62] and Deville [58] by using double-sided cooling and Moon[63] by radial freezing are some of important examples. Also Bai used a wedge in order to create a temperature gradient in 2 directions [64]. In this way, he was able to start the ice nucleation on a line instead of a plane and so, obtained a very well aligned lamellar structure. By the help of this novel idea and also doing something similar to [51], he made a hydroxyapatite/PMMA composite that mimics the structure of the nacre extremely well. Using electric[65] and magnetic[66, 67] fields is another way of manipulating the microstructure. Hunger self-assembled the alumina platelets using shear force from ice crystal propagations and obtained an alumina

porous structure with good mechanical properties[68]. The same idea used by *Bouville* to create an inorganic composite material very similar to nacre[69]. He didn't use any organic materials as soft part and hence their final structure could retain its mechanical properties even in high temperatures. In their work, alumina platelets were used as the main part of composite and alumina nano-particles and glass precursors filled the gaps between platelets.

## **1.2.3 3D** printing

3D printing is another important and popular technique which has been widely used. Currently, there are four main 3D printing methods available: stereolithography (STL), inkjet printing, selective laser sintering (SLS), and deposition modeling [70]. STL is based on layer by layer curing of photo-resist ink due to illumination of desired shape by a laser. Although using DLP technology a relatively big area with high precision could be cured, this technique is limited to using one material and also printed parts are usually brittle[71]. In SLS a high power laser is used to sinter the powder and so there is no need for toxic glues, though so many heating and cooling processes might affect the precision of this technique[70, 72]. Deposition modeling printers work based on layer by layer extrusion of molten polymers to form the 3D structure[70].

Cooke used stereolithography (SLA) method to print biodegradable structures to be used in tissue engineering for bony substrates[73]. Using fused deposition modeling (FDM) technology, Kalita developed polymer-ceramic scaffolds with controlled porosity for bone grafts[74]. By designing hydrogel based ceramic slurry, Fu used direct ink writing technique to 3D print a glass porous scaffold with mechanical properties and structure comparable to cortical and trabecular bone respectively[75]. Dimas conducted a computational study on brick and mortar structures and validated their results by 3D printing method[76]. He produced brick and mortar structures using a multi-material 3D printer and printed both soft and hard phase of the structure simultaneously

and achieved a final structure which its mechanical properties far exceeded the main constituents. Inspired by the hierarchical structure of balsa wood, *Compton* developed an epoxy-based ink reinforced by high aspect ratio fibers and 3D-printed cellular structures[77]. *Mirzaifar* did the same computational and experimental study on defect tolerance of hierarchical brick and mortar structure[78]. Due to alignment of fibers in the direction of printing, their final structures achieved exceptional mechanical properties. *Gergely* created sacrificial templates for bone regeneration using FDM printing technique[79]. *Martin* developed a novel 3D printing technique by combining SLA and magnetic field[80]. He used an ink containing alumina platelets coated by nano-size magnetic sensitive particles. By applying magnetic field, he was able to orient the platelets in desired direction and then cure the photo-sensitive ink. In this way, he mimicked many natural tough structures like nacre and bone. The same idea utilized by *Kokkinis* on direct ink writing method to build a magnetic multi-material 3D printer that is able to print complex 3D structures with enhanced mechanical properties in desired parts[81].

## 1.2.4 Self-assembly

Self-assembly is a bottom-up technique which can be used to emulate natural materials. It is a process in which some pre-existing elements form a structure according to a design without any direct intervention. Although self-assembly of micron size and even bigger objects would be interesting for applications like biomimetic composites, most of the works done so far have been on sub-micron length scales like self-assembly of molecules. Concept of self-assembly could be extended to 3D structures using Layer-by layer (LBL) assembly and could be used for making bio-inspired composite materials. In this technique, a substrate is dipped sequentially into two solutions containing the same objects but with different properties like electrical charges. So every time the substrate is immersed in one of the solutions, one layer of the objects will form on the

substrate[82]. The main drawback of this method is the necessity of repetition of dipping the substrate in solutions in order to reach to an acceptable thickness[83]. Tang obtained montmorillonite (MMT) clay-poly-diallydimethylammonium chloride films using LBL assembly technique and made films with up to 200 layers with mechanical properties comparable to nacre[84]. Podsiadlo used the same technique to make composite films made of MMT clay and polyvinyl alcohol (PVA) [85]. In both mentioned works the link between soft and hard phase is created just like nacre, but the main difference is the thickness of the "brick" part which in the case of clay is way thinner. Bonderer attempted to make organic-inorganic composite films by sequentially deposition of alumina platelets and chitosan biopolymer in order to mimic the structure of nacre[86]. He observed a considerable increase in mechanical properties of chitosan by the addition of only 15% of alumina platelets. *Podsiadlo* fabricated a transparent brick and mortar structure by clay platelets and PVA[87]. He showed that weak bonding interaction like hydrogen and van der Waals bonds between clay and matrix and also the ionic bonds in matrix can act as sacrificial bonds and increase the overall mechanical properties of the structure. Following the work of Ebina[88], transparent films with nacre like structures were made using evaporation self-assembly technique[89, 90]. Nano-clay platelets were the brick part of their composite films. Wang employed the same technique to create transparent nacre like composites with nano-fibrillar cellulose (NFC) and PVA in between the clay platelets [91]. By bridging clay platelets, NFCs cause a resistance against sliding of clay platelets with respect to each other. Assembly of the main building blocks of a structure could be also done using Deoxyribonucleic acid (DNA) strands. DNA strands could be designed in a way to be complementary and two single stranded DNAs form a helix double stranded one through hybridization process. This capability can be employed for programmable assembly of different particles as main elements of a whole structure. This technique has been used to assemble isotropic[92], anisotropic[93] and attaching particles with different shapes [94]. Although has not drawn enough attention yet, this technique is capable of being used in structural applications as well. Since objects with various shapes could be attached with the aid of DNA, one can utilize soft lithography techniques to make custom-size and custom-shape particles. Micro-contact printing[72], replica molding[95], micro-transfer molding[96] are some of the soft-lithography techniques widely used for fabricating micro and nano-sized particles. In [97], protocols related to many important soft-lithography techniques can be found. Yang made SiBNC ceramic plate-like particles using micro-transfer molding and vacuum assisted micro-molding in capillary techniques[98]. Guan employed micro contact hot printing to make polypropyl methacrylate particles with the size of a few tens of microns and disperse them in water[99]. Rolland proposed a new contact printing process with non-wetting templates called particle replication in non-wetting templates (PRINT) to fabricate particles with sizes below 200nm and with precise control on their size and shape [100]. In order to overcome the topological limitations of soft-lithography, Laftratta proposed a new technique, membrane assisted micro-transfer molding, to make complex 3D shapes with closed loops in just one step process[101]. Hernandez made particles with shapes of Latin alphabet letters made of photo-resist SU8 and dispersed them in aqueous media[102]. One important concern regarding DNA assembly would be how to attach DNA oligos to solid surfaces like glass or other polymeric materials. Attaching DNA to glass surface is of great importance considering the wide range application of glass which is due to its known chemical composition and versatility. DNA strands can be attached to glass surface either through modification of glass surface by silanization chemistry or using silanizied DNA oligos[103]. Amino and thiol modified DNA oligos are routinely used for these purposes. Amino modified DNA strands could be bonded to epoxy silane-derivatized glass[104,

105] or isothiocyanate coated glass[103]. Depending on the desired application, similar strategies can be employed for bonding DNAs to other solid supports like polymeric materials. One example is photo-resist SU8 which has a great importance in microelectromechanical systems (MEMS). Marrie attached DNA oligos to cured SU8 surfaces through simple reaction between amine group of modifies DNAs and epoxide group of SU8 surface[106]. Different approaches also proposed by other researchers for bonding DNA to glass through a dry method or using oligos with different functional groups like aminoalkyl and thiophosphoryl groups[107, 108].

### 1.2.5 Other techniques

There are many other experimental techniques used for bio-inspired purpose which can't be categorized in abovementioned groups. Using a technology similar to one for making multilayer capacitors, Clegg made squares of ceramics by silicon carbide powder and coated the surface of plates by graphite for a weak interface and then formed the final structure by stacking the plates and sintering them under pressure [109]. Almqvist utilized some simple fabrication methods like centrifugation, dipping, sedimentation, shearing and spinning to make bioinspired composites using talc as the main building block [110]. Ekiz combined slip casting and hot pressing methods to fabricate alumina/epoxy composite materials with enhanced orientation of tablets in epoxy and achieve good level of toughness and strength[111]. Bonderer used a combination of gel-casting and hot pressing techniques to fabricate composite structures with sub-micron sized alumina platelets with aligned orientation and up to 50 percent of alumina volume fraction[112]. Libanori made some composite films with an elasticity modulus spanning over several orders of magnitude by using various hard phases in different length scales and assembled the films with a simple technique of solvent welding [113]. Erb showed that by optimizing the size of hard phase in organic/inorganic composites, their orientation can be manipulated easily and just by the use of very weak magnetic fields[114]. He coated the surface of alumina platelets and calcium sulfate rods both with the biggest dimensions being less than 10 microns and successfully oriented the particles with a weak magnetic field of 30 mT. Using this technique, he was able to make highly oriented structures like nacre with different orientation in different layers like human teeth. Livanov employed a simple method to stack millimeter size alumina platelets with different thicknesses and a soft phase in between to emulate the structure of sponge spicules[115]. Behr utilized sedimentation technique to obtain centimeter-size samples with well aligned alumina platelets. He also applied high pressure and temperature on the samples to increase the volume fraction of platelets in the final structures[116]. Ferrand combined slip casting technique and magnetic field to manipulate orientation of ceramic platelets and make gradient structures with programmed structure[117]. Using a simple shear casting approach, Abba made chitosan-alumina composite films to mimic nacre structure and studied the effect of hard phase volume fraction and humidity on mechanical properties[118]. He successfully mimicked the structure of natural materials like human teeth and nacre and reached to hard phase volume fraction of 100 %. Demirors combined electric and magnetic fields in process of making composite material with alumina platelets as hard phase to control the spatial distribution and orientation of magnetized platelets respectively[119]. He used micron-sized electrodes to produce a desired electric field and self-assemble the platelets in designed spatial locations using dielectrophorsis process. With this approach, he produced a composite structure with a local stiffness comparable to teeth on one side and softer than skin on the other side while the whole structure being capable of great extensibility. In another top-down approach, Mirkhalaf carved suture-like patterns in glass sheets to increase the fracture toughness of glass [6]. Mirkhalaf also used laser engraving technique on glass sheets to carve 3D interlocking millimeter sized building blocks in order to enhance the energy absorption and the impact resistance of glass sheets[120]. Impact resistance of carved glass increased up to 4 times and they observed a progressive damage instead of a catastrophic one.

## 1.3 Bio-inspiration; a new approach toward a tough and impact-resistant glass structure

Glass has many interesting properties and a wide range of applications, thanks to its excellent optical clarity, rigidity, and abundance. However, glasses are brittle, with low fracture toughness and impact resistance, limiting their applications. Since high toughness is one of the most pronounced characteristics of natural materials such as nacre, glass is of the candidates to be integrated into a nacre-inspired composite material. We already showed in the previous sections that some researchers developed tough and transparent nacre-inspired composites. However, most of the bio-inspired transparent composites suffer from a general trade-off between toughness, rigidity, and scalability. Here, we propose a straightforward methodology for fabricating a nacreous composite material with superior strength, fracture toughness, and impact resistance to the normal glasses. Our material is scalable, and our fabrication technique is not complex. We use glass flakes and poly (methyl methacrylate) as the building blocks of our material. We employ centrifugation as a vital part of the fabrication procedure for ordering the microstructure, and we propose a simple method for making the composite optically transparent.

## 1.4 Thesis Objectives

The main objective of this thesis is to design and fabricate a nacre-inspired tough and transparent glass composite using a simple and scalable fabrication method. To achieve this objective, following three parts were accomplished:

- 1- Design and fabrication of a nacreous glass composite with high levels of optical transparency, toughness, and strength using a simple and scalable fabrication technique based on the centrifugation method. Identify the deformation and extrinsic toughening mechanisms in the glass composite.
- 2- Develop a class of polymethyl methacrylate (PMMA)-based polymers with improved fracture toughness, impact resistance, and chemical resistance, while the chemical synthesis simplicity and optical transparency of PMMA are retained.
- 3- Evaluate the performance of the nacreous glass composite under impact loading. To incorporate the PMMA-based polymers developed in the second part into the glass composite to study the role of soft phase on the mechanical properties, fracture toughness, and impact resistance of the glass composite.

### 1.5 Thesis Organization

This is a manuscript-based thesis consisting of six chapters. The first chapter reviews the structure and properties of some important structural biological materials, namely nacre, bone, and teeth. The chapter is continued by reviewing the fabrication methods for mimicking the design and structure of natural structural materials and their common advantages and challenges. Chapter 2 presents a centrifuged-based fabrication technique to develop a transparent and tough glass composite. Different aspects of the glass composite such as mechanical and optical properties are evaluated. The optical transmittance and haziness are evaluated and studied as a function of dopant percentage, thickness, and light wavelength. The effect of centrifugation on the microstructure and the glass volume fraction is studied. The mechanical properties and fracture toughness also are measured. The microstructure is studied and the key extrinsic toughening mechanisms responsible for high levels of fracture toughness are identified. The

novel glass composite is then compared with some state-of-the-art counterparts and commercially available glasses in terms of strength, toughness, and optical transparency. In chapter 3, a series of PMMA-based polymers are developed, aiming to tune the mechanical properties of the soft phase in the glass composite. PMMA is copolymerized with Acrylonitrile (AN) and crosslinked with 1,4 Butanediol Dimethacrylate (BUT). The optical transparency of the polymers is optimized and the chemical resistance of the polymers is evaluated. The effects of AN and BUT on the mechanical properties, fracture toughness, and impact resistance of PMMA are extensively studied.

In Chapter 4, first, the impact resistance of the glass composite is evaluated and compared with normal glass and PMMA. Then, the role of the soft phase on the mechanical properties, fracture toughness, and impact resistance of the glass composite is studied by incorporating the developed PMMA-based polymers into the glass composite.

Chapter 5 includes a summary of the accomplishments and the contributions of the thesis. Some suggestions for the future works are also presented.

Chapter 6 provides some supplementary information on the challenging journey of this PhD project and briefly describes some aspects and parts that are not included in this thesis but could be helpful and potentially insightful for those continuing this work.

### 1.6 References

[1] M.A. Meyers, P.-Y. Chen, Biological Materials Science: Biological Materials, Bioinspired Materials, and Biomaterials, Cambridge University Press, Place Published, 2014.

[2] U.G. Wegst, H. Bai, E. Saiz, A.P. Tomsia, R.O. Ritchie, Bioinspired structural materials, Nature materials, 14 (2015) 23-36.

- [3] M.A. Meyers, J. McKittrick, P.-Y. Chen, Structural biological materials: critical mechanics-materials connections, science, 339 (2013) 773-779.
- [4] J. McKittrick, P.-Y. Chen, L. Tombolato, E. Novitskaya, M. Trim, G. Hirata, E. Olevsky, M. Horstemeyer, M. Meyers, Energy absorbent natural materials and bioinspired design strategies: a review, Materials Science and Engineering: C, 30 (2010) 331-342.
- [5] S.E. Naleway, M.M. Porter, J. McKittrick, M.A. Meyers, Structural design elements in biological materials: application to bioinspiration, Advanced Materials, 27 (2015) 5455-5476.
- [6] M. Mirkhalaf, A.K. Dastjerdi, F. Barthelat, Overcoming the brittleness of glass through bioinspiration and micro-architecture, Nature communications, 5 (2014).
- [7] F. Barthelat, H. Tang, P. Zavattieri, C.-M. Li, H. Espinosa, On the mechanics of mother-of-pearl: a key feature in the material hierarchical structure, Journal of the Mechanics and Physics of Solids, 55 (2007) 306-337.
- [8] F. Barthelat, H. Espinosa, An experimental investigation of deformation and fracture of nacre—mother of pearl, Experimental mechanics, 47 (2007) 311-324.
- [9] J. Currey, Mechanical properties of mother of pearl in tension, Proceedings of the Royal Society of London B: Biological Sciences, 196 (1977) 443-463.
- [10] A. Jackson, J. Vincent, R. Turner, A physical model of nacre, Composites Science and Technology, 36 (1989) 255-266.
- [11] R. Menig, M. Meyers, M. Meyers, K. Vecchio, Quasi-static and dynamic mechanical response of Strombus gigas (conch) shells, Materials Science and Engineering: A, 297 (2001) 203-211.
- [12] R. Wang, Z. Suo, A. Evans, N. Yao, I. Aksay, Deformation mechanisms in nacre, Journal of Materials Research, 16 (2001) 2485-2493.

- [13] R. Menig, M. Meyers, M. Meyers, K. Vecchio, Quasi-static and dynamic mechanical response of Haliotis rufescens (abalone) shells, Acta Materialia, 48 (2000) 2383-2398.
- [14] F. Barthelat, D. Zhu, A novel biomimetic material duplicating the structure and mechanics of natural nacre, Journal of Materials Research, 26 (2011) 1203-1215.
- [15] B. Bruet, H. Qi, M. Boyce, R. Panas, K. Tai, L. Frick, C. Ortiz, Nanoscale morphology and indentation of individual nacre tablets from the gastropod mollusc Trochus niloticus, Journal of Materials Research, 20 (2005) 2400-2419.
- [16] X. Li, W.-C. Chang, Y.J. Chao, R. Wang, M. Chang, Nanoscale structural and mechanical characterization of a natural nanocomposite material: the shell of red abalone, Nano Letters, 4 (2004) 613-617.
- [17] B.L. Smith, T.E. Schäffer, M. Viani, J.B. Thompson, N.A. Frederick, J. Kindt, A. Belcher, G.D. Stucky, D.E. Morse, P.K. Hansma, Molecular mechanistic origin of the toughness of natural adhesives, fibres and composites, Nature, 399 (1999) 761-763.
- [18] A. Evans, Z. Suo, R. Wang, I. Aksay, M. He, J. Hutchinson, Model for the robust mechanical behavior of nacre, Journal of Materials Research, 16 (2001) 2475-2484.
- [19] K. Tushtev, M. Murck, G. Grathwohl, On the nature of the stiffness of nacre, Materials Science and Engineering: C, 28 (2008) 1164-1172.
- [20] M. Meyers, C. Lim, A. Li, B.H. Nizam, E. Tan, Y. Seki, J. McKittrick, The role of organic intertile layer in abalone nacre, Materials Science and Engineering: C, 29 (2009) 2398-2410.
- [21] M.A. Meyers, A.Y.-M. Lin, P.-Y. Chen, J. Muyco, Mechanical strength of abalone nacre: role of the soft organic layer, Journal of the Mechanical behavior of biomedical materials, 1 (2008) 76-85.

- [22] M.I. Lopez, P.E.M. Martinez, M.A. Meyers, Organic interlamellar layers, mesolayers and mineral nanobridges: Contribution to strength in abalone (Haliotis rufescence) nacre, Acta biomaterialia, 10 (2014) 2056-2064.
- [23] Z.H. Xu, X. Li, Deformation strengthening of biopolymer in nacre, Advanced Functional Materials, 21 (2011) 3883-3888.
- [24] A.K. Dastjerdi, R. Rabiei, F. Barthelat, The weak interfaces within tough natural composites: experiments on three types of nacre, Journal of the mechanical behavior of biomedical materials, 19 (2013) 50-60.
- [25] T.P. Niebel, F. Bouville, D. Kokkinis, A.R. Studart, Role of the polymer phase in the mechanics of nacre-like composites, Journal of the Mechanics and Physics of Solids, 96 (2016) 133-146.
- [26] F. Barthelat, C.-M. Li, C. Comi, H.D. Espinosa, Mechanical properties of nacre constituents and their impact on mechanical performance, Journal of Materials Research, 21 (2006) 1977-1986.
- [27] F. Song, Y. Bai, Effects of nanostructures on the fracture strength of the interfaces in nacre, Journal of Materials Research, 18 (2003) 1741-1744.
- [28] H.D. Espinosa, J.E. Rim, F. Barthelat, M.J. Buehler, Merger of structure and material in nacre and bone–Perspectives on de novo biomimetic materials, Progress in Materials Science, 54 (2009) 1059-1100.
- [29] P. Fratzl, O. Kolednik, F.D. Fischer, M.N. Dean, The mechanics of tessellations bioinspired strategies for fracture resistance, Chem Soc Rev, 45 (2016) 252-267.
- [30] I. Jäger, P. Fratzl, Mineralized collagen fibrils: a mechanical model with a staggered arrangement of mineral particles, Biophysical journal, 79 (2000) 1737-1746.

- [31] B. Ji, H. Gao, Mechanical properties of nanostructure of biological materials, Journal of the Mechanics and Physics of Solids, 52 (2004) 1963-1990.
- [32] H. Gao, B. Ji, I.L. Jager, E. Arzt, P. Fratzl, Materials become insensitive to flaws at nanoscale: lessons from nature, Proc Natl Acad Sci U S A, 100 (2003) 5597-5600.
- [33] M.A. Meyers, P.-Y. Chen, A.Y.-M. Lin, Y. Seki, Biological materials: structure and mechanical properties, Progress in Materials Science, 53 (2008) 1-206.
- [34] S. Goldstein, The mechanical properties of trabecular bone: dependence on anatomic location and function, Journal of biomechanics, 20 (1987) 1055-1061.
- [35] J.-Y. Rho, L. Kuhn-Spearing, P. Zioupos, Mechanical properties and the hierarchical structure of bone, Medical engineering & physics, 20 (1998) 92-102.
- [36] A. Ascenzi, P. Baschieri, A. Benvenuti, The bending properties of single osteons, Journal of biomechanics, 23 (1990) 763-771.
- [37] A. Ascenzi, P. Baschieri, A. Benvenuti, The torsional properties of single selected osteons, Journal of biomechanics, 27 (1994) 875-884.
- [38] A. Ascenzi, E. Bonucci, The tensile properties of single osteons, The Anatomical Record, 158 (1967) 375-386.
- [39] A. Ascenzi, E. Bonucci, The compressive properties of single osteons, The Anatomical Record, 161 (1968) 377-391.
- [40] K. Choi, J. Kuhn, M. Ciarelli, S. Goldstein, The elastic moduli of human subchondral, trabecular, and cortical bone tissue and the size-dependency of cortical bone modulus, Journal of biomechanics, 23 (1990) 1103-1113.
- [41] P. Mente, J. Lewis, Experimental method for the measurement of the elastic modulus of trabecular bone tissue, Journal of Orthopaedic Research, 7 (1989) 456-461.

- [42] J.Y. Rho, R.B. Ashman, C.H. Turner, Young's modulus of trabecular and cortical bone material: ultrasonic and microtensile measurements, Journal of biomechanics, 26 (1993) 111-119.
- [43] R.R. Adharapurapu, F. Jiang, K.S. Vecchio, Dynamic fracture of bovine bone, Materials Science and Engineering: C, 26 (2006) 1325-1332.
- [44] J.C. Behiri, W. Bonfield, Crack velocity dependence of longitudinal fracture in bone, Journal of Materials Science, 15 (1980) 1841-1849.
- [45] R.K. Nalla, J.H. Kinney, R.O. Ritchie, Mechanistic fracture criteria for the failure of human cortical bone, Nat Mater, 2 (2003) 164-168.
- [46] M.L. Snead, D. Zhu, Y. Lei, S.N. White, C.M. Snead, W. Luo, M.L. Paine, Protein self-assembly creates a nanoscale device for biomineralization, Materials Science and Engineering: C, 26 (2006) 1296-1300.
- [47] V. Imbeni, R.K. Nalla, C. Bosi, J.H. Kinney, R.O. Ritchie, In vitro fracture toughness of human dentin, Journal of Biomedical Materials Research Part A, 66A (2003) 1-9.
- [48] U.G. Wegst, M. Schecter, A.E. Donius, P.M. Hunger, Biomaterials by freeze casting, Philos Trans A Math Phys Eng Sci, 368 (2010) 2099-2121.
- [49] S. Deville, E. Maire, G. Bernard-Granger, A. Lasalle, A. Bogner, C. Gauthier, J. Leloup, C. Guizard, Metastable and unstable cellular solidification of colloidal suspensions, Nat Mater, 8 (2009) 966-972.
- [50] S. Deville, E. Saiz, R.K. Nalla, A.P. Tomsia, Freezing as a Path to Build Complex Composites, Science, 311 (2006) 515-518.
- [51] E. Munch, M.E. Launey, D.H. Alsem, E. Saiz, A.P. Tomsia, R.O. Ritchie, Tough, bio-inspired hybrid materials, Science, 322 (2008) 1516-1520.

- [52] S. Deville, E. Saiz, A.P. Tomsia, Freeze casting of hydroxyapatite scaffolds for bone tissue engineering, Biomaterials, 27 (2006) 5480-5489.
- [53] K. Araki, J.W. Halloran, Porous Ceramic Bodies with Interconnected Pore Channels by a Novel Freeze Casting Technique, Journal of the American Ceramic Society, 88 (2005) 1108-1114.
- [54] E.-J. Lee, Y.-H. Koh, B.-H. Yoon, H.-E. Kim, H.-W. Kim, Highly porous hydroxyapatite bioceramics with interconnected pore channels using camphene-based freeze casting, Materials Letters, 61 (2007) 2270-2273.
- [55] K. Araki, J.W. Halloran, New Freeze-Casting Technique for Ceramics with Sublimable Vehicles, Journal of the American Ceramic Society, 87 (2004) 1859-1863.
- [56] R. Guo, C.A. Wang, A. Yang, Piezoelectric properties of the 1–3 type porous lead zirconate titanate ceramics, Journal of the American Ceramic Society, 94 (2011) 1794-1799.
- [57] S. Deville, Freeze-Casting of Porous Biomaterials: Structure, Properties and Opportunities, Materials, 3 (2010) 1913-1927.
- [58] S. Deville, E. Saiz, A.P. Tomsia, Ice-templated porous alumina structures, Acta Materialia, 55 (2007) 1965-1974.
- [59] Q. Fu, M.N. Rahaman, F. Dogan, B.S. Bal, Freeze casting of porous hydroxyapatite scaffolds. II. Sintering, microstructure, and mechanical behavior, J Biomed Mater Res B Appl Biomater, 86 (2008) 514-522.
- [60] K. Lebreton, J.M. Rodríguez-Parra, R. Moreno, M.I. Nieto, Effect of additives on porosity of alumina materials obtained by freeze casting, Advances in Applied Ceramics, 114 (2015) 296-302.

- [61] E. Munch, E. Saiz, A.P. Tomsia, S. Deville, Architectural Control of Freeze-Cast Ceramics Through Additives and Templating, Journal of the American Ceramic Society, 92 (2009) 1534-1539.
- [62] T. Waschkies, R. Oberacker, M.J. Hoffmann, Control of Lamellae Spacing During Freeze Casting of Ceramics Using Double-Side Cooling as a Novel Processing Route, Journal of the American Ceramic Society, 92 (2009) S79-S84.
- [63] J.-W. Moon, H.-J. Hwang, M. Awano, K. Maeda, Preparation of NiO–YSZ tubular support with radially aligned pore channels, Materials Letters, 57 (2003) 1428-1434.
- [64] H. Bai, Y. Chen, B. Delattre, A.P. Tomsia, R.O. Ritchie, Bioinspired large-scale aligned porous materials assembled with dual temperature gradients, Science advances, 1 (2015) e1500849.
- [65] Y. Zhang, L. Hu, J. Han, Preparation of a dense/porous bilayered ceramic by applying an electric field during freeze casting, Journal of the American Ceramic Society, 92 (2009) 1874-1876.
- [66] M.M. Porter, P. Niksiar, J. McKittrick, G. Franks, Microstructural Control of Colloidal-Based Ceramics by Directional Solidification Under Weak Magnetic Fields, Journal of the American Ceramic Society, 99 (2016) 1917-1926.
- [67] M.M. Porter, M. Yeh, J. Strawson, T. Goehring, S. Lujan, P. Siripasopsotorn, M.A. Meyers, J. McKittrick, Magnetic freeze casting inspired by nature, Materials Science and Engineering: A, 556 (2012) 741-750.
- [68] P.M. Hunger, A.E. Donius, U.G. Wegst, Platelets self-assemble into porous nacre during freeze casting, J Mech Behav Biomed Mater, 19 (2013) 87-93.

- [69] F. Bouville, E. Maire, S. Meille, B. Van de Moortele, A.J. Stevenson, S. Deville, Strong, tough and stiff bioinspired ceramics from brittle constituents, Nat Mater, 13 (2014) 508-514.
- [70] G.X. Gu, I. Su, S. Sharma, J.L. Voros, Z. Qin, M.J. Buehler, Three-Dimensional-Printing of Bio-Inspired Composites, Journal of biomechanical engineering, 138 (2016) 021006.
- [71] F.P.W. Melchels, J. Feijen, D.W. Grijpma, A review on stereolithography and its applications in biomedical engineering, Biomaterials, 31 (2010) 6121-6130.
- [72] S. Kumar, Selective laser sintering: A qualitative and objective approach, JOM, 55 (2003) 43-47.
- [73] M.N. Cooke, J.P. Fisher, D. Dean, C. Rimnac, A.G. Mikos, Use of stereolithography to manufacture critical-sized 3D biodegradable scaffolds for bone ingrowth, Journal of Biomedical Materials Research Part B: Applied Biomaterials, 64 (2003) 65-69.
- [74] S.J. Kalita, S. Bose, H.L. Hosick, A. Bandyopadhyay, Development of controlled porosity polymer-ceramic composite scaffolds via fused deposition modeling, Materials Science and Engineering: C, 23 (2003) 611-620.
- [75] Q. Fu, E. Saiz, A.P. Tomsia, Bioinspired Strong and Highly Porous Glass Scaffolds, Adv Funct Mater, 21 (2011) 1058-1063.
- [76] L.S. Dimas, G.H. Bratzel, I. Eylon, M.J. Buehler, Tough Composites Inspired by Mineralized Natural Materials: Computation, 3D printing, and Testing, Advanced Functional Materials, 23 (2013) 4629-4638.
- [77] B.G. Compton, J.A. Lewis, 3D-printing of lightweight cellular composites, Adv Mater, 26 (2014) 5930-5935.

- [78] R. Mirzaeifar, L.S. Dimas, Z. Qin, M.J. Buehler, Defect-Tolerant Bioinspired Hierarchical Composites: Simulation and Experiment, ACS Biomaterials Science & Engineering, 1 (2015) 295-304.
- [79] R.C. Gergely, S.J. Pety, B.P. Krull, J.F. Patrick, T.Q. Doan, A.M. Coppola, P.R. Thakre, N.R. Sottos, J.S. Moore, S.R. White, Multidimensional vascularized polymers using degradable sacrificial templates, Advanced Functional Materials, 25 (2015) 1043-1052.
- [80] J.J. Martin, B.E. Fiore, R.M. Erb, Designing bioinspired composite reinforcement architectures via 3D magnetic printing, Nat Commun, 6 (2015) 8641.
- [81] D. Kokkinis, M. Schaffner, A.R. Studart, Multimaterial magnetically assisted 3D printing of composite materials, Nat Commun, 6 (2015) 8643.
- [82] C. Jiang, V.V. Tsukruk, Freestanding Nanostructures via Layer-by-Layer Assembly, Advanced Materials, 18 (2006) 829-840.
- [83] I. Corni, T. Harvey, J. Wharton, K. Stokes, F. Walsh, R. Wood, A review of experimental techniques to produce a nacre-like structure, Bioinspiration & biomimetics, 7 (2012) 031001.
- [84] Z. Tang, N.A. Kotov, S. Magonov, B. Ozturk, Nanostructured artificial nacre, Nat Mater, 2 (2003) 413-418.
- [85] P. Podsiadlo, A.K. Kaushik, E.M. Arruda, A.M. Waas, B.S. Shim, J. Xu, H. Nandivada, B.G. Pumplin, J. Lahann, A. Ramamoorthy, N.A. Kotov, Ultrastrong and Stiff Layered Polymer Nanocomposites, Science, 318 (2007) 80-83.
- [86] L.J. Bonderer, A.R. Studart, L.J. Gauckler, Bioinspired design and assembly of platelet reinforced polymer films, Science, 319 (2008) 1069-1073.
- [87] P. Podsiadlo, A.K. Kaushik, B.S. Shim, A. Agarwal, Z. Tang, A.M. Waas, E.M. Arruda, N.A. Kotov, Can nature's design be improved upon? High strength, transparent nacre-like

- nanocomposites with double network of sacrificial cross links, J Phys Chem B, 112 (2008) 14359-14363.
- [88] T. Ebina, F. Mizukami, Flexible Transparent Clay Films with Heat-Resistant and High Gas-Barrier Properties, Advanced Materials, 19 (2007) 2450-2453.
- [89] P. Das, S. Schipmann, J.M. Malho, B. Zhu, U. Klemradt, A. Walther, Facile access to large-scale, self-assembled, nacre-inspired, high-performance materials with tunable nanoscale periodicities, ACS Appl Mater Interfaces, 5 (2013) 3738-3747.
- [90] J. Wang, Q. Cheng, L. Lin, L. Chen, L. Jiang, Understanding the relationship of performance with nanofiller content in the biomimetic layered nanocomposites, Nanoscale, 5 (2013) 6356-6362.
- [91] J. Wang, Q. Cheng, L. Lin, L. Jiang, Synergistic toughening of bioinspired poly (vinyl alcohol)–clay–nanofibrillar cellulose artificial nacre, ACS nano, 8 (2014) 2739-2745.
- [92] J.W. Kim, J.H. Kim, R. Deaton, DNA-linked nanoparticle building blocks for programmable matter, Angew Chem Int Ed Engl, 50 (2011) 9185-9190.
- [93] M.R. Jones, R.J. Macfarlane, B. Lee, J. Zhang, K.L. Young, A.J. Senesi, C.A. Mirkin, DNA-nanoparticle superlattices formed from anisotropic building blocks, Nat Mater, 9 (2010) 913-917.
- [94] F. Lu, K.G. Yager, Y. Zhang, H. Xin, O. Gang, Superlattices assembled through shape-induced directional binding, Nat Commun, 6 (2015) 6912.
- [95] Y. Xia, J.J. McClelland, R. Gupta, D. Qin, X.M. Zhao, L.L. Sohn, R.J. Celotta, G.M. Whitesides, Replica molding using polymeric materials: A practical step toward nanomanufacturing, Advanced Materials, 9 (1997) 147-149.

- [96] X.M. Zhao, Y. Xia, G.M. Whitesides, Fabrication of three-dimensional micro-structures: Microtransfer molding, Advanced Materials, 8 (1996) 837-840.
- [97] D. Qin, Y. Xia, G.M. Whitesides, Soft lithography for micro-and nanoscale patterning, Nature protocols, 5 (2010) 491-502.
- [98] H. Yang, P. Deschatelets, S.T. Brittain, G.M. Whitesides, Fabrication of high performance ceramic microstructures from a polymeric precursor using soft lithography, Advanced Materials, 13 (2001) 54-58.
- [99] J. Guan, A. Chakrapani, D.J. Hansford, Polymer microparticles fabricated by soft lithography, Chemistry of materials, 17 (2005) 6227-6229.
- [100] J.P. Rolland, B.W. Maynor, L.E. Euliss, A.E. Exner, G.M. Denison, J.M. DeSimone, Direct fabrication and harvesting of monodisperse, shape-specific nanobiomaterials, Journal of the American Chemical Society, 127 (2005) 10096-10100.
- [101] C.N. LaFratta, L. Li, J.T. Fourkas, Soft-lithographic replication of 3D microstructures with closed loops, Proceedings of the National Academy of Sciences, 103 (2006) 8589-8594.
- [102] C.J. Hernandez, T.G. Mason, Colloidal alphabet soup: Monodisperse dispersions of shape-designed lithoparticles, The Journal of Physical Chemistry C, 111 (2007) 4477-4480.
- [103] Z. Guo, R.A. Guilfoyle, A.J. Thiel, R. Wang, L.M. Smith, Direct fluorescence analysis of genetic polymorphisms by hybridization with oligonucleotide arrays on glass supports, Nucleic acids research, 22 (1994) 5456-5465.
- [104] W.G. Beattie, L. Meng, S.L. Turner, R.S. Varma, D.D. Dao, K.L. Beattie, Hybridization of DNA targets to glass-tethered oligonucleotide probes, Molecular biotechnology, 4 (1995) 213-225.

[105] J.B. Lamture, K. LBeattie, B.E. Burke, M.D. Eggers, D.J. Ehrlich, R. Fowler, M.A. Hollis, B.B. Kosicki, R.K. Reich, S.R. Smith, Direct detection of nucleic acid hybridization on the surface of a charge coupled device, Nucleic acids research, 22 (1994) 2121-2125.

[106] R. Marie, S. Schmid, A. Johansson, L. Ejsing, M. Nordström, D. Häfliger, C.B. Christensen, A. Boisen, M. Dufva, Immobilisation of DNA to polymerised SU-8 photoresist, Biosensors and Bioelectronics, 21 (2006) 1327-1332.

[107] M. Joshi, N. Kale, R. Lal, V.R. Rao, S. Mukherji, A novel dry method for surface modification of SU-8 for immobilization of biomolecules in Bio-MEMS, Biosensors and Bioelectronics, 22 (2007) 2429-2435.

[108] D. Sethi, A. Kumar, R. Gandhi, P. Kumar, K. Gupta, New protocol for oligonucleotide microarray fabrication using SU-8-coated glass microslides, Bioconjugate chemistry, 21 (2010) 1703-1708.

[109] W. Clegg, K. Kendall, N.M. Alford, T. Button, J. Birchall, A simple way to make tough ceramics, Nature, 347 (1990) 455-457.

[110] N. Almqvist, N.H. Thomson, B.L. Smith, G.D. Stucky, D.E. Morse, P.K. Hansma, Methods for fabricating and characterizing a new generation of biomimetic materials, Materials Science and Engineering: C, 7 (1999) 37-43.

[111] O. Oner Ekiz, A.F. Dericioglu, H. Kakisawa, An efficient hybrid conventional method to fabricate nacre-like bulk nano-laminar composites, Materials Science and Engineering: C, 29 (2009) 2050-2054.

[112] L.J. Bonderer, K. Feldman, L.J. Gauckler, Platelet-reinforced polymer matrix composites by combined gel-casting and hot-pressing. Part I: Polypropylene matrix composites, Composites Science and Technology, 70 (2010) 1958-1965.

- [113] R. Libanori, R.M. Erb, A. Reiser, H. Le Ferrand, M.J. Süess, R. Spolenak, A.R. Studart, Stretchable heterogeneous composites with extreme mechanical gradients, Nature communications, 3 (2012) 1265.
- [114] R.M. Erb, R. Libanori, N. Rothfuchs, A.R. Studart, Composites reinforced in three dimensions by using low magnetic fields, Science, 335 (2012) 199-204.
- [115] K. Livanov, H. Jelitto, B. Bar-On, K. Schulte, G.A. Schneider, D.H. Wagner, R. Ballarini, Tough Alumina/Polymer Layered Composites with High Ceramic Content, Journal of the American Ceramic Society, 98 (2015) 1285-1291.
- [116] S. Behr, U. Vainio, M. Muller, A. Schreyer, G.A. Schneider, Large-scale parallel alignment of platelet-shaped particles through gravitational sedimentation, Sci Rep, 5 (2015) 9984.
- [117] H. Le Ferrand, F. Bouville, T.P. Niebel, A.R. Studart, Magnetically assisted slip casting of bioinspired heterogeneous composites, Nat Mater, 14 (2015) 1172-1179.
- [118] M.T. Abba, P.M. Hunger, S.R. Kalidindi, U.G. Wegst, Nacre-like hybrid films: Structure, properties, and the effect of relative humidity, J Mech Behav Biomed Mater, 55 (2015) 140-150. [119] A.F. Demirörs, D. Courty, R. Libanori, A.R. Studart, Periodically microstructured composite films made by electric-and magnetic-directed colloidal assembly, Proceedings of the National Academy of Sciences, 113 (2016) 4623-4628.
- [120] M. Mirkhalaf, J. Tanguay, F. Barthelat, Carving 3D architectures within glass: Exploring new strategies to transform the mechanics and performance of materials, Extreme Mechanics Letters, 7 (2016) 104-113.

### Link between chapter 1 and chapter 2

Glasses have a wide range of applications in everyday life, from small screens of electronic devices to giant glass panes in buildings. However, ductility is a major problem in most normal glasses. Different tempering methods have been developed to improve the mechanics of glasses; however, glass brittleness has remained to be an issue in many cases. Some works have been done on developing bio-inspired glass composites, but they usually leave one of the key characteristics (transparency, strength, toughness, and scalability in the fabrication process) of ideal bio-inspired glass behind. In the next chapter, we present a simple, scalable, and yet efficient method for the fabrication of a nacre-inspired glass with high levels of toughness, strength, and optical transparency at the same time.

## Chapter 2

Centrifugation of index-matched acrylic and glass flakes yields a strong and transparent bioinspired nacreous composite

# Centrifugation of index-matched acrylic and glass flakes yields a strong and transparent bioinspired nacreous composite

Ali Amini<sup>1,2</sup>, Adele Khavari<sup>1</sup>, Francois Barthelat<sup>2,3</sup>, Allen J. Ehrlicher<sup>1,2</sup>

1. Bio-Active Materials Laboratory

Department of Bioengineering, McGill University

Montreal, Quebec, H3A 0C3, Canada

E-mail: Allen.Ehrlicher@mcgill.ca

2. Department of Mechanical Engineering, McGill University

Montreal, Quebec, H3A 0C3, Canada

3. Department of Mechanical Engineering, University of Colorado Boulder

Boulder, Colorado, US.

**Keywords**: Bio-inspired, composite materials, nacre, glass, PMMA, fracture toughness

### 2.1 Abstract

Glasses have numerous applications due to their exceptional transparency and stiffness, however, poor fracture and impact resistance limit their applications. One strategy to improve their mechanical properties is through bio-inspiration. Structural biological composites such as nacre, the protective inner layer of mollusk shells, offer far superior mechanical properties relative to their constituents. This has motivated researchers to mimic the design principles in natural composites to create tough transparent materials. However, current bio-inspired composites suffer from poor optical transmission and tradeoffs between strength and toughness. Here, we present an optically transparent tough nacreous glass composite material with a four-fold increase in fracture toughness, a three-fold increase in flexural strength compared to conventional structural glasses, and a 73% average optical transmittance. Our composite is fabricated with a simple scalable approach: the composite consists of glass flakes and poly (methyl methacrylate) (PMMA) structured utilizing a centrifugation fabrication method that aligns and compacts the flakes into layers. To optimize the transparency of the structure, the refractive indices of the PMMA and glass are matched by adding a dopant to the PMMA. Based on these results, this nacreous glass composite is proposed as a potential alternative in diverse architectural, vehicular, and electronics applications.

### 2.2 Introduction

Glasses are brittle materials with low fracture toughness and low resistance against impact, which limits the range of their applications. Thermal or chemical tempering is a common strategy to increase the strength of glasses [1], however, this does not dramatically improve fracture toughness [2] and can lead to catastrophic, "explosive" types of failures. Laminating glass creates a polymeric glass sandwich-like composite structure [3], the greatest advantage of which is safety: upon fracture, the polymeric layers prevent small pieces of the fractured glass from shattering in catastrophic failure. However, there are only modest mechanical improvements in laminated glasses [4–6].

To improve glass toughness and impact resistance, researchers have explored bioinspiration - implementing design principles observed in biology. Nacre, the tough material comprising the inner layer of mollusk shells, is a classic example of a tough structural biomaterial; nacre is 3000 times tougher than the components [7], breaks at 1% of strain – a remarkable improvement relative to the individual ceramic building blocks, and its elastic modulus is approximately 1000 times larger than that of the connective proteins alone [8].

Many techniques of varying complexity have been proposed to fabricate synthetic materials mimicking nacre [9, 10]. Some of these have focused on making transparent composites [11–13], resulting in thin films with enhanced mechanical and optical properties. To extend the applications beyond thin films, a new scalable nacreous composite was developed by infiltrating PMMA into a glass flake scaffold while matching refractive indices of the two phases [14]. Despite superior fracture resistance properties compared to glass, this composite sacrificed transparency, a key feature for widespread applications.

In contrast, others have employed top-down methods, including laser-engraving interlocking jigsaw-shaped 3D arrays in bulk glass [15], and glass lamination processes of thin glasses with laser-engraved cross-plied [16] and tablet-like architectures [17]. These approaches resulted in increased composite fracture toughness and impact resistance, but reduced stiffness and strengths. Stiffness and strength can be generally improved by decreasing the size of the patterns; however, this reduces transparency and scalability [17]. This highlights the general trade-off challenge that bio-inspired glasses have suffered from between mechanics, transparency, and fabrication scalability. While these diverse strategies have explored bottom-up and top-down approaches resulting in excellent mechanical, optical, and fabrication results, no method has successfully combined all three together in a tough glass.

In this paper, we demonstrate a bottom-up fabrication technique to produce a transparent brick and mortar structural composite possessing advantageous mechanical properties that improve upon those of normal glasses or their bio-inspired composite counterparts.

### 2.3 Results and discussions

The structure and composition of our transparent nacre-like material result from stringent requirements and careful material selection and preparation. For high mechanical performance, hard and stiff elongated inclusions must be bonded by a more deformable matrix. For high optical performance, the refraction index of the two phases must be identical. Finally, the bonding between hard and soft must be perfect to ensure strong interface strength, and also prevent light scattering that would reduce optical quality. To fulfill these mechano-optical requirements we chose glass flakes for the hard inclusions and Poly (methyl methacrylate) (PMMA) for the soft matrix. Glass flakes were utilized as the hard component due to their high diameter-to-thickness aspect ratio, transparency, high stiffness, and well-characterized surface chemistry for surface

functionalization. PMMA, an amorphous polymer which polymerizes through a free radical bulk polymerization process [18] was selected as the soft phase due to its deformability [19] and excellent optical properties [20]. The optical refraction indices of glass ( $n_{glass}$ =1.52) and PMMA ( $n_{PMMA}$ =1.49) do not exactly match, but this issue could be alleviated by adding an organic dopant, phenanthrene, to PMMA [21]. In order to achieve a strong and defect-free interface between glass and PMMA we functionalized the glass tablet surface with a silane. The prepared PMMA and glass flakes were then mixed, and then centrifuged to induce an aligned brick and mortar architecture and high volume-fraction of glass inclusions. As a final stage, PMMA polymerization was achieved by baking at 50° C (for 12 hours), 70° C (for 4 hours), and 100° C (for 2 hours).

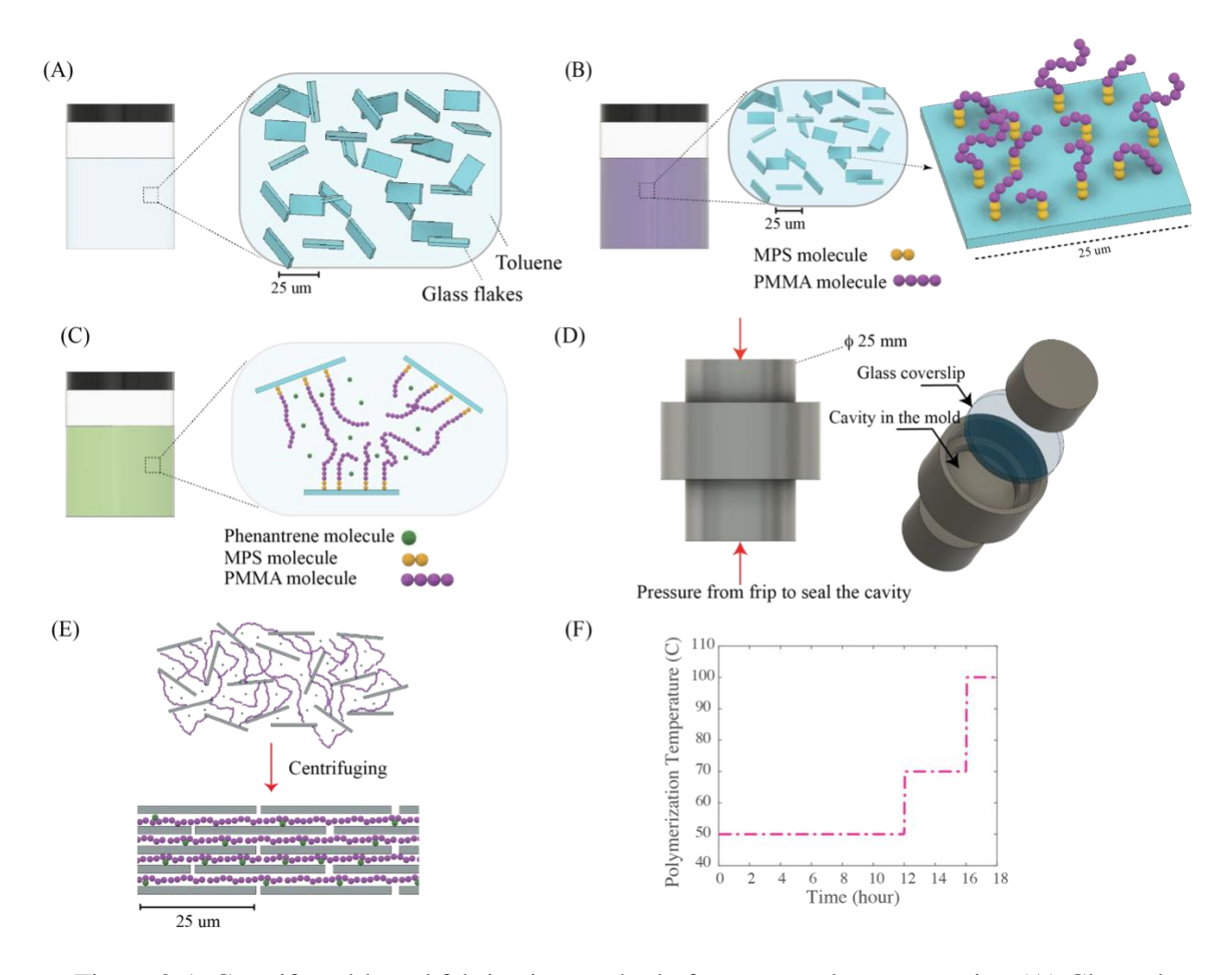


Figure 2-1. Centrifuged-based fabrication method of nacreous glass composite. (A) Cleaned glass flakes were dispersed in toluene. (B) Glass flakes surface-treated with γ-MPS and then with a solution of MMA in toluene to promote polymerization from the glass surface. (C) Surface-treated glass flakes were involved in free radical polymerization of PMMA at 50°C. (D) Glass-PMMA mixture transferred to a casting mold with a pre-designed cavity on the bottom (E) Glass-PMMA mixture was centrifuged to impose alignment in flakes and densify the mixture. (F) Polymerization process finalized in oven: 12 hours at 50°C, 4 hours at 70°C and 2 hours at 100°C.

We matched the refractive indices of the two phases using phenanthrene as a dopant to improve the transparency. We measured the refractive index of PMMA-dopant samples as a function of dopant weight percentage (Fig. 2-7-A), and then estimated the composition that leads to the highest level of transparency (Fig. 2-7-D). While the composite with no index-matching dopant was very hazy, and the sample was not transparent due to light scattering, our index-matched glass

composite demonstrated high levels of transparency (Figure 2-A). The optical transmittance of our glass composite compares well with both soda-lime monolithic glass and PMMA doped with 12% of phenanthrene (Fig. 2-B), and its average transmittance is only 16% less than the soda-lime glass (Fig. 2-7-E). It also has 24% higher transmittance than similar bio-inspired laminated composites [17] and has almost 100% higher transmittance than the recently reported nacre mimetic composite fabricated by *Magrini* [14]. Even the glass composite with 0% dopant has a similar optical transmittance to the bio-inspired glass composite fabricated by *Magrini* [14]. While our composite is hazier than the soda-lime glass with the same thickness, it is more than 70% less hazy than similar bio-inspired bulk fabricated composites [14] (Fig. 2-7-E and Fig. 2-7-F). This underlines a crucial difference between the current fabrication technique and the one presented in Ref. 14; while the method in Ref. 14 mimics other aspects of nacre by creating mineral bridges through a heat treatment process, this process also creates many potential light diffraction sites leading to the poor optical performance reported for that material.

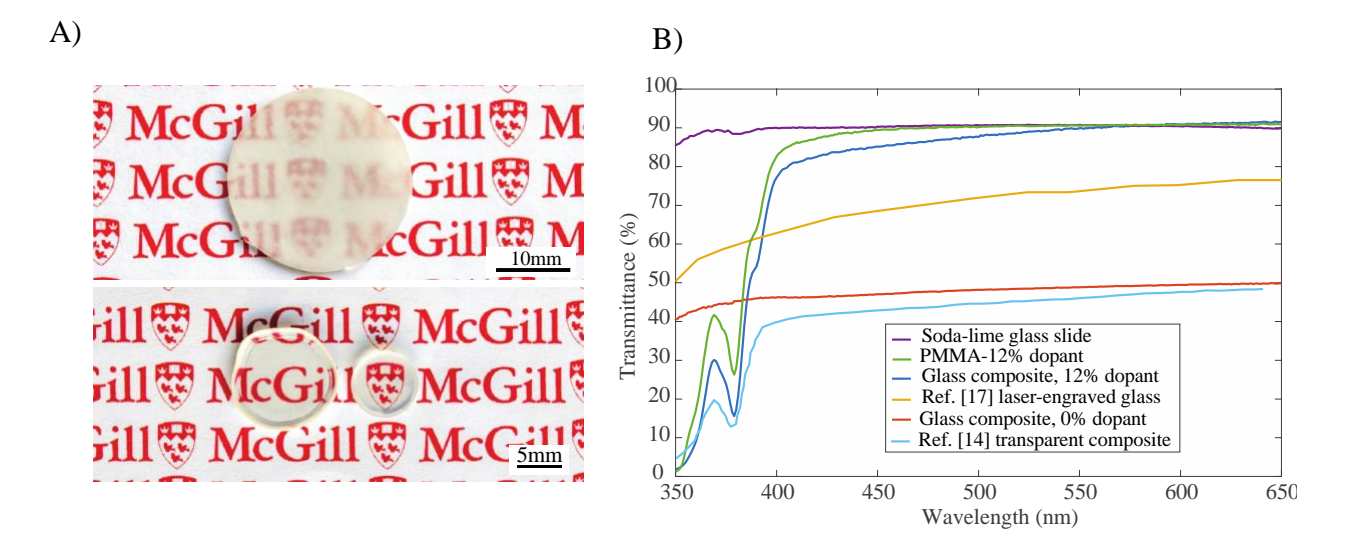


Figure 2-2. Dopant percentage and composite thickness affect composite transparency and haziness. (A) 1mm thick glass composites with 0% dopant (top), and 12% dopant (bottom). (B) Transmittance for the soda-lime glass, doped PMMA (12%), 12% glass composite, laser-engraved laminated glass [17], and bio-inspired transparent composite [14]. Our composite compares well with soda-lime monolithic glass and is superior to its bio-inspired counterparts.

In addition to high optical performance, our material needs to be stiff and strong, which requires high concentration of glass inclusions with a high alignment. As glass and PMMA have different densities, we used centrifugation to increase the fraction of glass in our composite, leading to a high volume fraction of the stiff (glass) phase and consequently a thin connective (PMMA) phase. The volume fraction of glass inclusions increased from about 24% for non-centrifuged composite to about 43% for the samples centrifuged with 2000g (Fig. 3-A). The thickness of the polymer layer between the flakes also decreased dramatically by applying centrifuge forces, from about 35μm for the simply mixed sample to about 17μm for the sample centrifuged with 2000g. Centrifugation homogenizes the distribution of flakes, preventing the formation of flake-free regions of PMMA (Fig. 3-B and Fig. 3-C top). Centrifugation also aligns the glass flakes (Fig. 3-B and 3-C bottom). By comparing the polar orientation distribution graphs of the non-centrifuged and centrifuged composites, we examined the role of the centrifuging process in inducing order in the structure of the composite. Centrifugation up to 2000g increased flake order and alignment, however further increasing the centrifugation speed did not seem to significantly improve flake alignment. Since no drastic change in volume fraction or mechanical testing data was observed with further increasing the centrifuging speed, we determined 2000g to be an optimal centrifugation force.

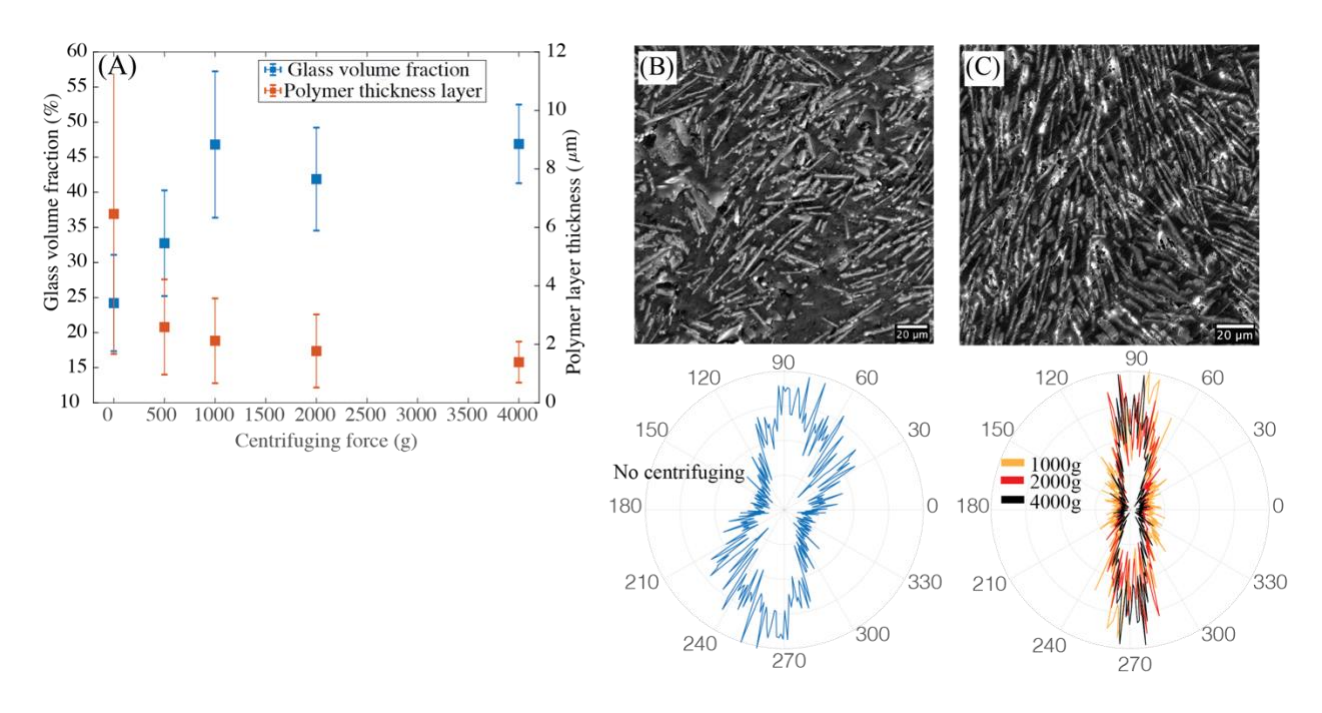


Figure 2-3. Centrifugation increases the glass volume fraction by decreasing the polymer thickness layer between tablets. (A) Glass volume fraction increases almost two-fold when the sample centrifuged (2000g). Also, polymer layer thickness decreases about 50% when centrifuged with 2000g force. (B) Section SEM image of a non-centrifuged composite (top, about 24% glass volume fraction). We observed a noticeable number of areas with no flakes, and also many flakes with random orientation in the material. Polar distribution of orientation in the flakes also confirms this observation (bottom). (C) Section SEM image of centrifuged composite (2000g, about 43% glass volume fraction). Flakes are more oriented in one direction, and areas with no flakes are rarely observed. Polar distribution of orientation in the flakes for different centrifuging speeds also shows insignificant difference between 1000g, 2000g and 4000g forces.

Data points and error bars are mean values and standard deviation respectively.

The mechanical performance of the composite was evaluated using 3-point bending tests. The glass composite displays two distinct linear and non-linear regimes in flexural response (Fig. 4-A). We attribute the non-linear regime to the large plastic deformation of the PMMA after yielding. All samples displayed evidence of inelastic deformation, with strains at failure in the 2.5 to 3.5% range. Flexural modulus and strength however varied significantly across the different designs we explored. The glass composite surface-functionalized with  $\gamma$ -MPS was 1.9 times stiffer than the glass composite without any surface treatment (Fig. 4-A and Table S1). The composite's flexural

strength also was increased about two-fold by functionalizing the glass flakes' surfaces by γ-MPS. This increase in strength, however, only produced a glass composite slightly stronger than pure PMMA (Table 2-1). The flexural strength was increased to about 140 MPa by including the centrifuging process as a part of fabrication process; this aligned the glass flakes into layers of parallel planes and also yielded a denser overall structure. The beneficial strengthening effects of centrifugation appeared to plateau at 2000g, with no significant increase in flexural strength for higher forces (Fig. 4-B). The flexural modulus was also increased from 4.7GPa for non-centrifuged sample to about 7.2Gpa for the sample centrifuged with 2000g force, with no significant increase of the modulus with higher centrifugation speeds. The effect of surface-functionalization and centrifugation appeared to be insignificant on the rupture strain, and most of the samples possessed a rupture strain of about 3% (Fig. 2-8 and Table 2-1).

In addition to modulus, strength and deformability, we measured fracture toughness using a single-Edge Notch Bending (SENB) configuration. Fig 4-C shows typical force-deflection results for these tests, showing a brittle response for pure PMMA, but a more "graceful" failure (more gradual decrease in force in the post-peak region) for the non-centrifuged glass composite. The centrifuged glass composite, on the other hand, not only lacked catastrophic fracture, but it demonstrated a higher peak force. From this experimental data we computed crack initiation fracture toughness  $K_{IC}$  using the maximum force [22] and the work of fracture (WOF), computed from the area under the force-deflection curve. Centrifuged glass composites outperformed the non-centrifuged ones in fracture toughness; By centrifuging (2000g), we increased the glass composite's crack initiation fracture toughness ( $K_{IC}$ ) and energy absorption (WOF) by about 30% (Fig. 4-D).

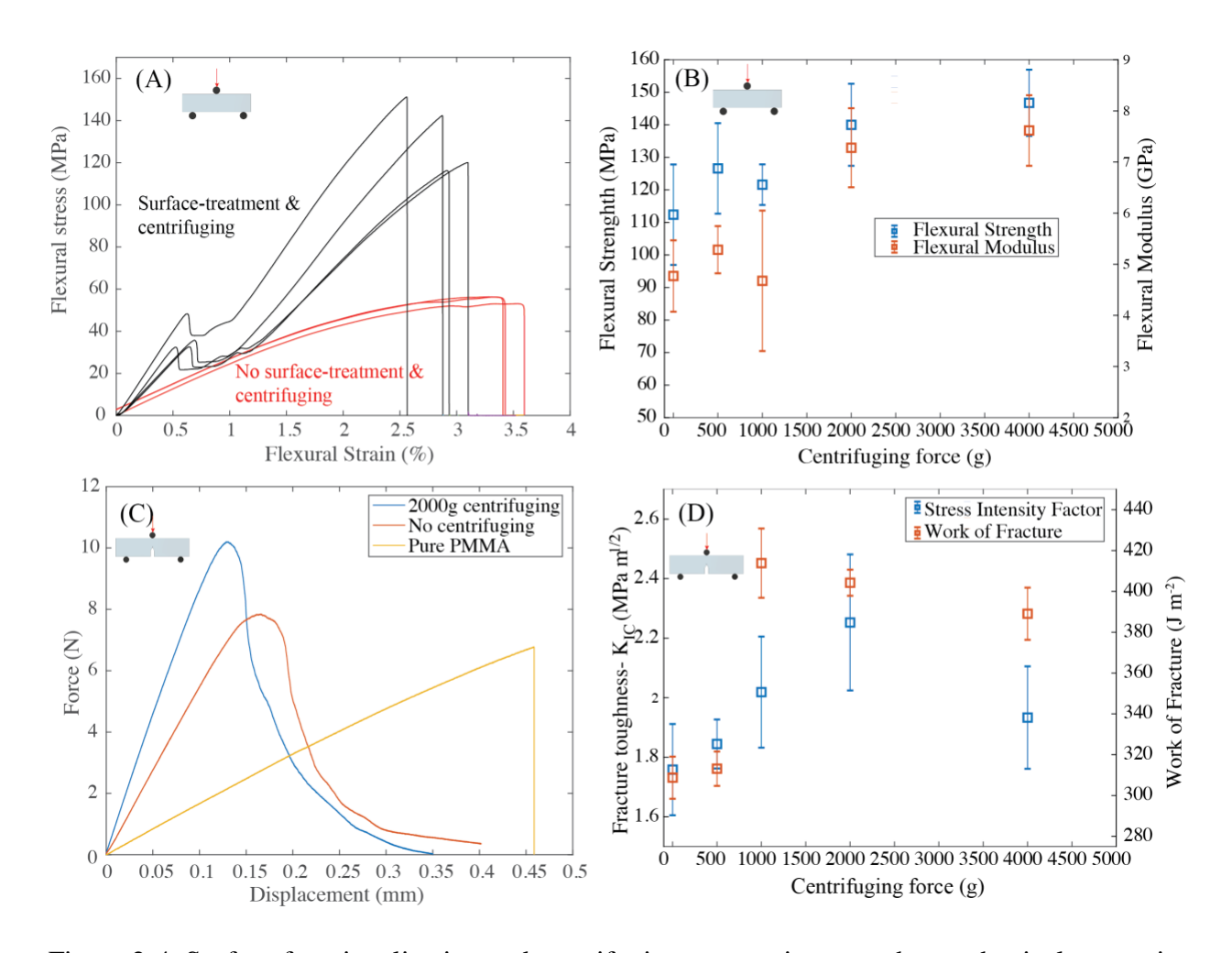


Figure 2-4. Surface functionalization and centrifuging process improve the mechanical properties of the glass composite. (A) Flexural stress-flexural strain curves for the composites with and without surface-functionalized glass and centrifugation. Surface-treated composite experiences a linear deformation regime followed by a non-linear one up to the failure, whereas the composite with no glass functionalization and centrifugation deforms non-linearly to the fracture while possessing lower strength and stiffness values. (B) strength and flexural modulus increase with centrifugation. While the higher centrifuging speed yields higher strength and flexural modulus, 2000g appears to be the saturation point. (C) SENB test load-displacement curves for pure PMMA, non-centrifuged and centrifuged composites, illustrating an increased fracture strength with composite formulation and subsequent centrifugation. (D) *KIC* and *WOF* values increase with increasing the centrifuging speed up to 2000g.

The results in Fig. 4 demonstrates that centrifuging improves the mechanical and fracture properties. This improvement is achieved by inducing order in the structure and creating a staggered structure of glass flakes and PMMA polymer similar to nacre (Fig. 5-A and Fig. 5-B).

Such order promotes some important extrinsic toughening mechanisms leading to the excellent performance of the composite under fracture. In the absence of mineral bridges and tablet interlocking, tablet sliding and delocalization of stresses are the most important mechanism responsible for the high fracture toughness in our composite. This deformation mode in large scales leads to the pull-out of glass tablets from the polymeric matrix, a critical toughening mechanism observed in biological nacre as well [23]. Another key toughening mechanism in our material is polymer bridging or formation of polymer ligaments between tablets, activated when the delamination of tablets occurs (Fig. 5-C). Also reported to occur in natural nacre (24), tablets experience delamination due to lateral displacements if (i) the interface material is deformable and (ii) the bonding between polymer and glass is strong [25]. This, again, highlights the role of glass surface treatment and consequent strong bonds between the soft and hard phases. PMMA large deformations in forms of stretching (polymer bridges) and shear (tablet sliding) cause yielding, and consequently, plastic deformation in the PMMA (non-linear part in Fig. 4-A). This gives rise to large deformations, and high levels of energy absorption manifest as high fracture toughness in the material. In addition, due to the activation of the mentioned toughening mechanisms, and consequently propagation of micro-cracks through the soft phase with many path diversions, many deflections in the crack propagation path are observed in the micro- and macro-scale (Fig. 5-D and Fig. 5-E).

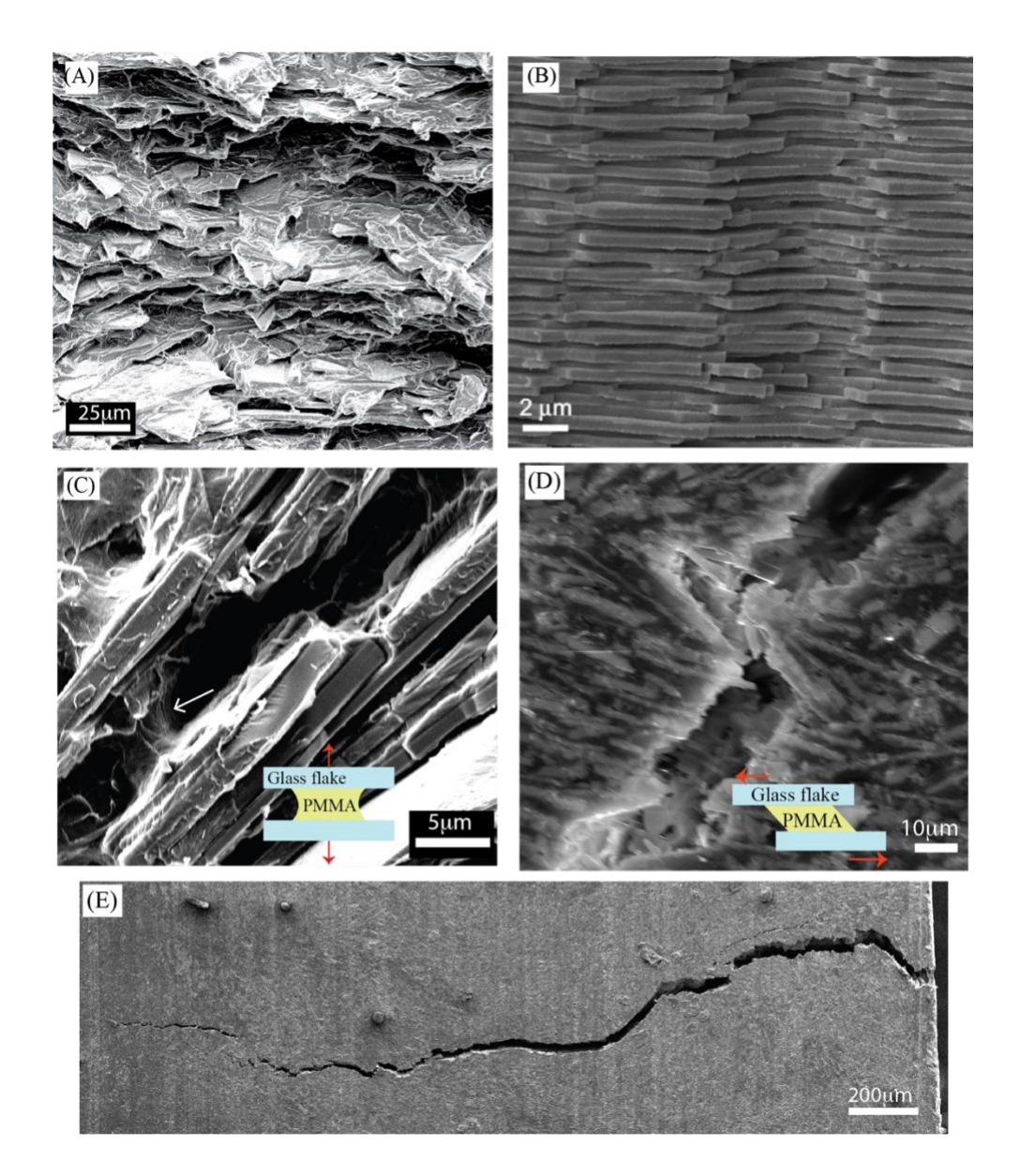


Figure 2-5. Transparent nacreous glass mimics key aspects of nacre's microstructure and toughening mechanisms. (A) SEM micrograph of the sample cross-section in a fractured surface in our glass composite. Staggered glass platelets with polymer layers in between and numerous pulled-out glass tablets due to fracture. (B) Fracture surface of natural nacre. (C) While tablets are experiencing delamination due to lateral deformation, the polymer layer acts as a bridge between tablets and contributes to the composite toughness (white arrow). (D) Tablet sliding in large scale leads to tablet pull-out and hence deflection of crack growth path. (E) Macroscopic crack deflection in the material as a result of microscopic toughening mechanisms.

Fig. 6 shows that our composite exceeds current state of the art materials in terms of fracture toughness and strength. It possesses a strength similar to thermally tempered glass [2] but has a

higher fracture toughness. Our glass composite also exceeds the previously reported bio-inspired glass composite [14] in both strength and fracture toughness (Fig. 2-9-A). The reason for this difference is likely in the glass tablet aspect ratios. For a fixed matrix shear strength, there is a range of aspect ratios for tablets that cause the material to experience tablet pull-out [27]. In this sense, too short and too long glass flakes cause vertical interface and tablet failure to be the prevailing modes of failure, respectively. In other words, keeping the interface shear strength constant while increasing the tablet aspect ratio would lead to a decrease in the WOF of the composite. The aspect ratio of the flakes in our material is about 25, or about 10 times smaller than the ones in Ref. 14, placing ours in an ideal range for strength and toughness, and explaining the difference in strength and fracture toughness values of the two materials. Considering the WOF as a non-linear measure of fracture resistance, our composite outperforms annealed [28] and laminated glasses [3], as well as pure PMMA (Fig. 2-9-B). The laser-engraved laminated glass structure [16] possesses a very high WOF, however, this has only been achieved with a corresponding compromise in reduced material strength.

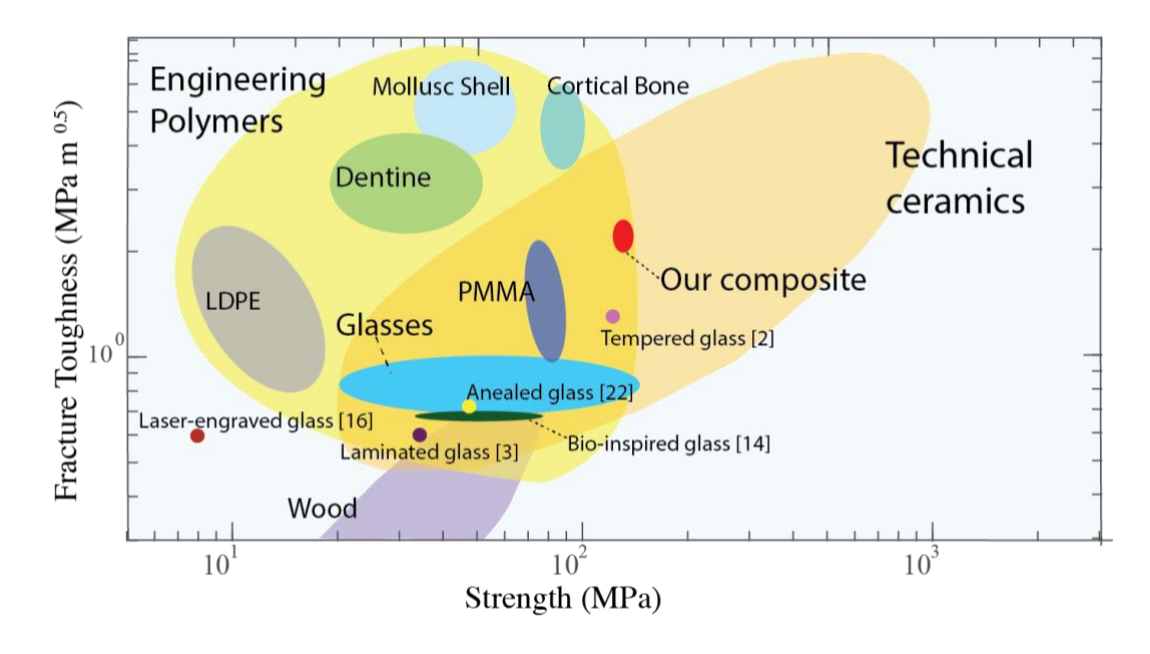


Figure 2-6. Ashby plot of fracture toughness versus strength for numerous synthetic and natural materials. Our transparent nacreous composite (centrifuged at 2000g) outperforms annealed soda-lime [28], tempered [2], laminated [3], bio-inspired transparent composite [14], and laser-engraved laminated [16] glasses in both strength and fracture toughness.

#### 2.4 Conclusions

Our novel nacreous composite structure displays previously unattained optical and mechanical properties and offers a potential alternative to tempered and laminated glasses. Hard phase alignment has long been recognized as a key strategy, often pursued from a serialized bottom up approach. Centrifugation is a methodological key advance enabling our composite fabrication concept. Centrifugation is a rapid and scalable approach useful for fabricating any composite geometry and dimensions and may be further enhanced by increasing the density differential between hard and soft phases. This is a fundamental advantage over the serialized layer by layer approaches which sacrifice production for precision. Additionally, this moves composite fabrication out of specialized nanofabrication facilities and into the realm of industrially approachable processes. The dependency of mechanical properties on centrifugation force

illustrates the importance of both aligning the hard phase tablets and minimizing the compliant PMMA phase in the overall composite structure, similar to the minimization of protein (~<5%) found in natural nacreous composites. This centrifugation imposed order on the structure also effectively enables the activation of toughening mechanisms such as tablet pull-out (as a result of large-scale tablet sliding), and polymer bridging (due to tablet delamination), which together cause micro- and macro-scale crack deflection in the material. These strategies enable our glass composite to mechanically outperform annealed, thermally tempered, and laminated glasses in fracture toughness and flexural strength.

Many other composites have structured glass flakes to create mechanically enhanced materials; to do so, however, they have also fundamentally sacrificed transparency or optical clarity in terms of scratches. This is not in principle due to a materials mismatch, required for a composite, but an *optical* mismatch in terms of the refractive index. By making the soft and hard phase with the same refractive indices, one can create any number of varied materials in structured composites, which have little to no optical defects. This methodology concept enabled us to tune the PMMA phase to that of glass, resulting in a uniform and single optical phase structure. We hope that the composite described here may find applications in high-performance scalable transparent composites that could replace glass where impact resistance is needed, or even to create transparent structural elements. Moreover, the strategies for mechanical enhancement and optical clarity presented here will allow researchers to explore new boundaries in composite fabrication.

## 2.5 Supplementary materials

#### 2.5.1 Materials and Methods

#### Materials

Glass flakes (GF001-10, d50 (median particle) diameter =27-32 μm, thickness =0.9-1.3 μm, refractive index = 1.524) were kindly supplied by Glassflake Ltd. Methyl methacrylate (MMA, 99%), azobis isobutyronitrile (AIBN, 98%), Phenanthrene (98%), (3-trimethoxysilyl) propyl methacrylate (γ-MPS, 98%), Methanol (ACS, 99%), hydrogen peroxide (30 wt. % in H2O), acetone (99.5%) and MMA inhibitor remover were acquired from Sigma . Toluene (reagent grade) and sulfuric acid (reagent grade) were purchased from Caledon Laboratories Ltd.

#### Glass surface functionalization

Glass flakes were cleaned in Piranha solution (3 parts of concentrated sulfuric acid, 1 part of water and 1 part of 30 wt.% hydrogen peroxide solution) for 30 minutes, and subsequently washed in DI water several times and dried in a vacuum oven at 120°C overnight. Cleaned and dried flakes (2 g) were mixed with a solution of toluene (15 ml) and the surface functionalization agent (5 ml), \(\gamma\)-MPS, (3:1 volume ratio) and gently stirred with a magnetic stirrer for 12 hours. The silane functional groups will react with hydroxyl groups on the glass surface. The surface-treated glasses were washed with toluene, methanol, and then washed with DI water several times and dried in a vacuum oven at 110°C for 2 hours. \(\gamma\)-MPS functionalized glass flakes were then involved in a free radical polymerization process to grow PMMA monolayer on their surface. This was performed in a two-step process: first, the glass flakes were added to a mixture of dry toluene and MMA (2:1 volume ratio) under gentle mechanical stirring at 70°C for 30 minutes with AIBN (1 wt.%) as initiator. This is to promote growing PMMA from the glass surface and decelerate the

polymerization in bulk MMA. After this step, we dried the flakes in a vacuum oven at 110°C for 2 hours prior to usage in the main composite fabrication process, which follows in the next section.

#### Glass composite fabrication

To adjust the refractive indices of the glass and PMMA, we dissolved an aromatic hydrocarbon, phenanthrene, in MMA as a dopant. Phenanthrene and AIBN (0.5 wt.%) were dissolved in MMA and added to the surface-treated glass flakes. The mixture was mechanically stirred at low speed for 45 minutes at 50°C under argon atmosphere and immediately cooled down in an ice-water bath afterward. The glass-polymer mixture then transferred to a 3D-printed polypropylene casting mold containing a cavity with desired shape and depth. The cavity's depth will be the glass composite's final thickness. To make a dense structure with well-aligned flakes, we centrifuged the glass-MMA compound. The centrifuging process involved two low-speed steps (100g RCF for 5 minutes and 300g RCF for 5 minutes) to induce alignment in the flakes. Then we performed the last step in high speed (more than 1000g RCF for 20 minutes) to make a denser structure. The top of the cavity was covered by a glass coverslip, and a gentle pressure applied from a small mechanical grip sealed the centrifuged glass-PMMA composite in the cavity. We finalized the polymerization process by exposing the composite to heat in the oven (50°C for 12 hours, 70°C for 4 hours, and 100°C for 2 hour).

Estimation of glass volume fraction, polymer layer thickness, and orientation distribution

We calculated the glass volume fraction by Archimedes' principle, assuming that the composite only consists of the hard and soft phases. The volume of the composite samples (7-10 samples for each data point) measured using a pycnometer (VWR, 25 ml, Gay-Lussac type), and by

knowing the densities of the glass flakes and the PMMA, we estimated the glass volume fraction in our composite.

The polymer layer thickness was measured by extracting data from several line scans on the SEM images of the composite cross-sections in ImageJ software. The orientation distribution was measured and plotted by analyzing the SEM images of the composite cross-sections using a Fourier transform based methods presented in [29].

#### Structural characterization of the composite (SEM images)

Samples were imaged using a scanning electron microscope (FEI Quanta FEG 450) at (20KV at secondary electron mode) to evaluate the ordering of the flakes with respect to the centrifugation speed. The samples were initially coated with a layer of platinum (4nm) using a sputter coating machine (Leica Microsystems EM ACE600 High Resolution Sputter Coater).

#### Optical characterization of the composites

PMMA samples doped with phenanthrene were dissolved in toluene and then coated on silicon wafers. Refractive index of the samples (3-5 samples for each data point) was then measured using a spectroscopic ellipsometer (Sopra GES-5E). The transmittance and haze factor of the glass composites measured using a UV-Vis-NIR spectrophotometer (LAMBDA 750 UV/Vis/NIR). For this purpose, cylindrical glass composite samples (3-5 samples for each data point) with the various diameters and thicknesses were prepared. Using two different configurations, total transmittance and diffuse transmittance values was measured. The haze factor then was calculated by dividing the diffuse to total transmittance values.

#### Mechanical characterization of the composite

To measure the elastic modulus, flexural strength, and rupture strain of the composites, 3-point bending tests were performed using a universal testing machine (Admet, eXpert 5000, MA US) [30]. Cubic samples (5-7 samples for each data point) with dimensions of 25x3.2x1.8 mm were prepared. Support span and displacement rate were 16 mm and 1 um/sec respectively.

Fracture toughness of the composites was evaluated using Single-Edge Notched Beam (SENB) test [31]. Cubic samples (5-7 samples for each data point) with 25x3.2x1.8mm dimensions were prepared, and a notch was created using a 450 µm diamond saw. The initial crack (40 µm in tip radius) then created on the tip of the notch using a thin blade covered with diamond paste. The samples then were used in a 3-point bending set up with a displacement rate of 1 um/s.

#### 2.5.2 Fracture mechanics calculations

The crack initiation fracture toughness,  $K_{IC}$ , was calculated from the load-displacement curves and based on the maximum force value and initial crack size from the following equation [31]:

$$K_{IC} = \left(\frac{P_c S}{W\sqrt{WB}}\right) f\left(\frac{a_c}{W}\right)$$

where  $P_c$  and  $a_c$  are maximum amount of load and initial crack size, respectively, and S, W and B are support span, specimen width and thickness, respectively. Also,

$$f(\frac{a_c}{W}) = \frac{3\sqrt{\frac{a_c}{W}}(1.99 - \frac{a_c}{W}(1 - \frac{a_c}{W})(2.15 - 3.93(\frac{a_c}{W}) + 2.7(\frac{a_c}{W})^2))}{2(1 + 2\frac{a_c}{W})(1 - \frac{a_c}{W})^{\frac{3}{2}}} \,.$$

The work of fracture (WOF) was calculated as a nonlinear measure of fracture toughness. WOF is defined as the total energy spent to create one unit of fracture surface area [22] and calculated as follow

$$WOF = \frac{U}{2(W-a)}$$

Where U is the area under the load-displacement curve in SENB test, and W and a are the width and initial crack length of the SENB sample respectively.

#### 2.5.3 Index-matching

To find the percentage of dopant that optically optimized the overall composite transparency, we first measured the refractive index of PMMA-dopant samples as a function of dopant weight percentage (Fig. 2-7-A). We estimated that between 12 to 16 % of dopant along with 0.5 % azobis isobutyronitrile (AIBN) as polymerization initiator would match the RI of PMMA to the one of our glass flakes (1.524). Knowing the refractive indices as a function of PMMA formulation and dopant, we can estimate the composition that leads to the highest level of transparency. To reach the optimum dopant percentage, composites with 1mm of thickness, 43% volume fraction, and various phenanthrene amounts were made. We measured the transmittance of the composites as a function of composition by a UV-Vis spectrophotometer (Fig. 2-7-A). We found the optimum dopant concentration to be 12%, yielding an average spectral transmittance of 76% for a 1 mm glass composites (Fig. 2-7-B). Despite the high transmittance values for the glass composite, this material also tends to diffuse light resulting in a hazy appearance (Fig. 2-C). The material appeared to have the lowest haziness for the optimal amount of dopant (Fig. 2-7-D). Although even 5% of dopant yielded a reasonably high average transmittance, the sample possessed an unsatisfactorily high haze factor of about 90% for almost the whole visible light spectrum. The haze factor for the composite with 12% of dopant, however, is not constant for the whole visible light spectrum and increases from about 10% for wavelengths greater than 500 nm to about 90% at the low end of the visible spectrum.

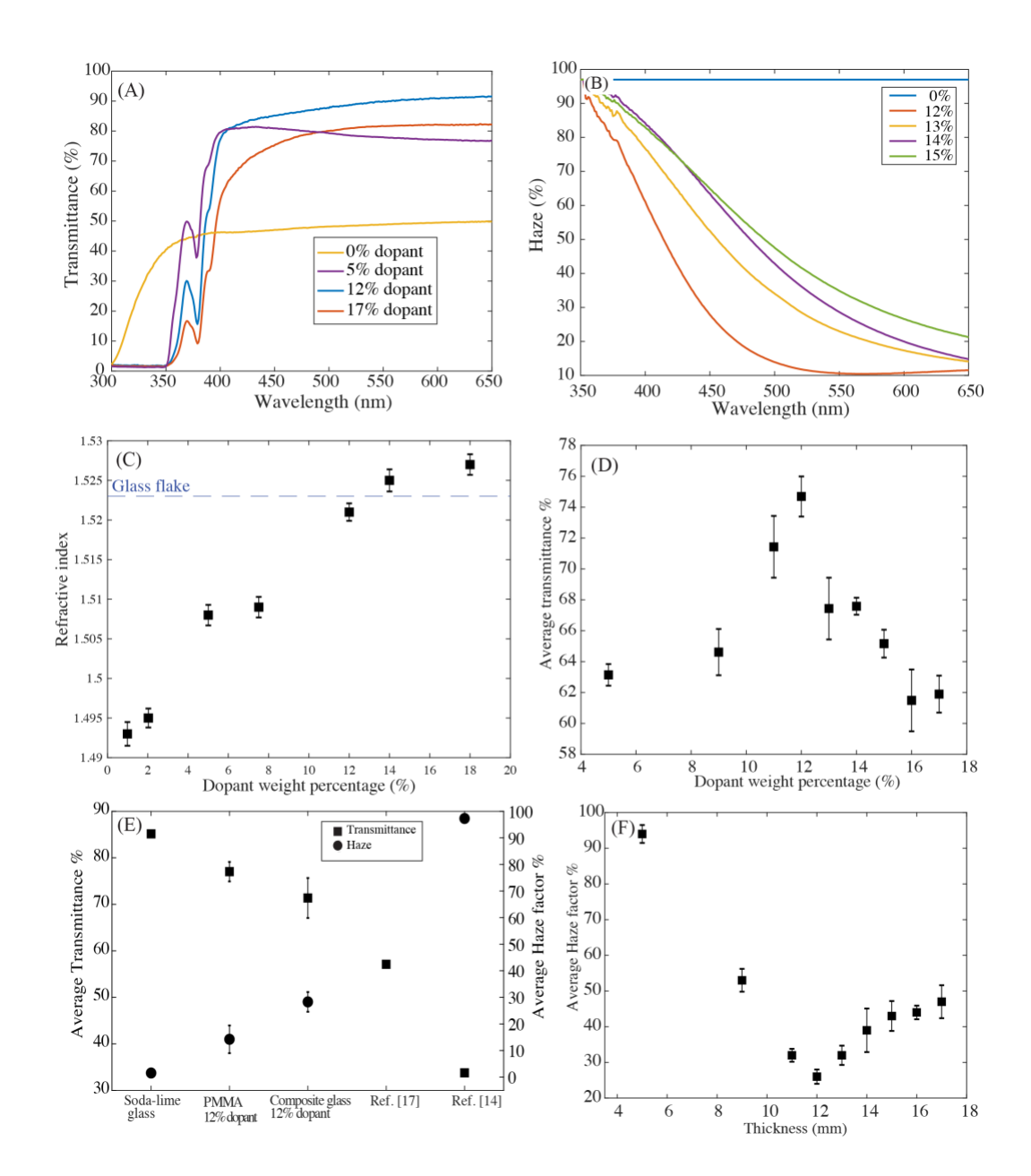


Figure 2-7. Glass composite doped with Phenanthrene is highly transparent, but hazy. (A) Transmittance values for 1mm thick samples and different phenanthrene weight percentages. (B) Haze factor values for 1mm thick composites and different dopant weight percentages. (C) PMMA refractive index increases linearly by increasing phenanthrene weight percentage. (D) Average transmittance values in terms of dopant weight percentage. 12% appears to be the optimum dopant amount. (E) Comparison of transmittance and haze factor for the 12% glass composite, doped PMMA (12%), soda-lime glass, bio-inspired transparent composite (14), and laser-engraved laminated glass [17]. Although the transmittance of our glass composite is similar to the soda-lime glass, its haze factor is higher by a factor of 20. Our glass composite, however, is superior to its bio-inspired rivals both in transmittance and haze factor. (F) Haze factor values for 1mm thick composites and different dopant weight percentages. 12 wt% of dopant yields the lowest haze factor value. Data point and error bars demonstrate the mean value and the standard deviation respectively.

### 2.5.4 Mechanical and fracture characterization supplementary results

Table 2-1. Strength, rupture strain, and flexural modulus values for composite with no surface functionalization and centrifuging, surface-functionalized and centrifuged, and PMMA samples.

	Strength [MPa]	Rupture strain [%]	Flexural modulus [GPa]
No surface functionalization and centrifuging	56.17 ± 4.30	$3.37\pm0.14$	2.46 ± 0.31
Surface-functionalizing and no centrifuging	112 ± 15.21	$2.77\pm0.88$	$4.77\pm0.75$
Surface-functionalized, centrifuged (2000g)	140.01 ± 12.62	$3.05\pm0.31$	$7.27 \pm 0.77$
PMMA	101 ± 2.85	$6.82\pm0.39$	1.41 ± 0.42

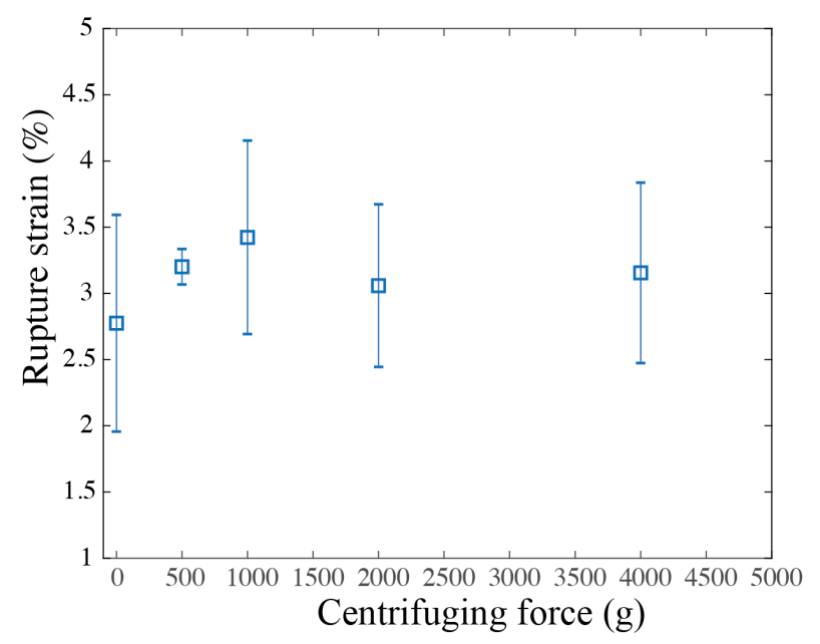


Figure 2-8. Effect of centrifugation on rupture strain of the composite. Centrifuging appears to have insignificant effect on the composite's rupture strain.

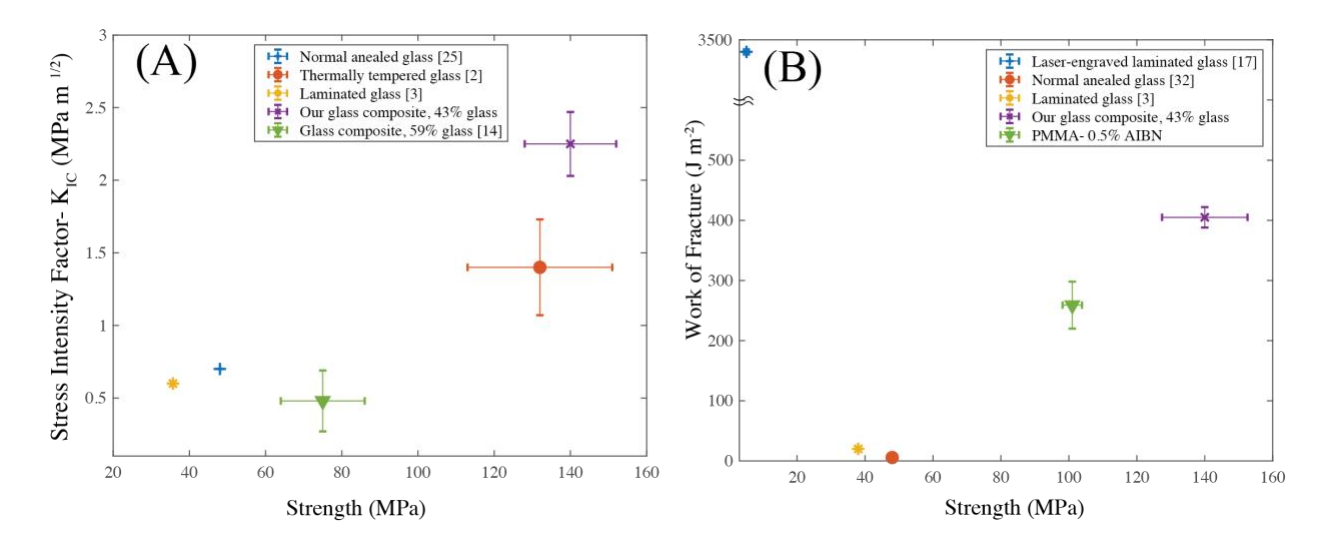


Figure 2-9. Nacreous glass composite outperforms normal, tempered and laminated glass under fracture. (A) Crack initiation fracture toughness vs final strength for normal annealed soda-lime [28], tempered [2], laminated [3], bio-inspired transparent composite [14], and our composite glass (2000g). The composite demonstrated here outperforms other state of the art glasses in both fracture toughness and final strength. (B) WOF versus final strength for normal annealed [32], laminated (3), and laser-engraved laminated [17] glasses, as well as the pure PMMA and our composite glass(2000g). The only glass that exceeds our composite in terms of WOF is Ref. 17, but it possesses far less strength compared to our composite. Data points and error bars demonstrate the mean value and the standard deviation respectively.

## 2.6 Acknowledgements

AJE acknowledges support from NSERC RGPIN/05843-2014 & EQPEQ/472339-2015, FRQNT team grant, Canadian Foundation for Innovation Project #32749, and the Canada Research Chairs Program. The authors thank Clayton Molter for helpful discussions and a critical review of the manuscript. Authors' contributions: Conceptualization, A.J.E., A.A.; Methodology- development, A.A., A.K., A.J.E.; Methodology-application, A.A.; Investigation, A.A., A.K.; Formal Analysis, A.A.; Software, A.A.; Visualization, A.A.; Writing- original draft, A.A.; Writing- review and editing, A.J.E., A.K., A.A.; Funding acquisition, A.J.E.; Resources, A.J.E; Supervision, A.J.E.

#### 2.7 References

- [1] F. M. Ernsberger, *Techniques of Strengthening Glasses* (ACADEMIC PRESS, INC., 1980), vol. 5.
- [2] F. Petit, A. C. Sartieaux, M. Gonon, F. Cambier, Fracture toughness and residual stress measurements in tempered glass by Hertzian indentation. *Acta Mater.* **55**, 2765–2774 (2007).
- [3] X. Huang, G. Liu, Q. Liu, S. J. Bennison, The flexural performance of laminated glass beams under elevated temperature. *Struct. Eng. Mech.* **52**, 603–612 (2014).
- [4] J. E. Minor, P. L. Reznik, Failure strengths of laminated glass. *J. Struct. Eng.* **116**, 1030–1039 (1990).
- [5] M. M. El-Shami, S. Norville, Y. E. Ibrahim, Stress analysis of laminated glass with different interlayer materials. *Alexandria Eng. J.* **51**, 61–67 (2012).
- [6] H. S. Norville, K. W. King, J. L. Swofford, Behavior and strength of laminated glass. *J. Eng. Mech.* **124**, 46–53 (1998).
- [7] H. D. Espinosa, J. E. Rim, F. Barthelat, M. J. Buehler, Merger of structure and material in nacre and bone Perspectives on de novo biomimetic materials. *Prog. Mater. Sci.* **54**, 1059–1100 (2009).
- [8] F. Barthelat, H. Tang, P. D. Zavattieri, C. M. Li, H. D. Espinosa, On the mechanics of mother-of-pearl: A key feature in the material hierarchical structure. *J. Mech. Phys. Solids*. 55, 306–337 (2007).
- [9] N. Almqvist, N. H. Thomson, B. L. Smith, G. D. Stucky, D. E. Morse, P. K. Hansma, Methods for fabricating and characterizing a new generation of biomimetic materials. *Mater. Sci. Eng. C.* 7, 37–43 (1999).
- [10] H. Le Ferrand, F. Bouville, T. P. Niebel, A. R. Studart, Magnetically assisted slip casting of bioinspired heterogeneous composites. *Nat. Mater.* **14**, 1172–1179 (2015).
- [11] P. Podsiadlo, A. K. Kaushik, B. S. Shim, A. Agarwal, Z. Tang, A. M. Waas, E. M. Arruda, N. A. Kotov, Can nature's design be improved upon? High strength, transparent nacre-like nanocomposites with double network of sacrificial cross links. *J. Phys. Chem. B.* **112**, 14359–14363 (2008).
- [12] T. Ebina, F. Mizukami, Flexible Transparent Clay Films with Heat-Resistant and High Gas-Barrier Properties. *Adv. Mater.* **19**, 2450–2453 (2007).

- [13] Y. Liu, S.-H. Yu, L. Bergström, Transparent and Flexible Nacre-Like Hybrid Films of Aminoclays and Carboxylated Cellulose Nanofibrils. *Adv. Funct. Mater.* 28, 1703277 (2018).
- [14] T. Magrini, F. Bouville, A. Lauria, H. Le Ferrand, T. P. Niebel, A. R. Studart, Transparent and tough bulk composites inspired by nacre. *Nat. Commun.* **10**, 2794 (2019).
- [15] M. Mirkhalaf, A. K. Dastjerdi, F. Barthelat, Overcoming the brittleness of glass through bio-inspiration and micro-architecture. *Nat. Commun.* **5**, 1–9 (2014).
- [16] Z. Yin, A. Dastjerdi, F. Barthelat, Tough and deformable glasses with bioinspired cross-ply architectures. *Acta Biomater*. **75**, 439–450 (2018).
- [17] Z. Yin, F. Hannard, F. Barthelat, Impact-resistant nacre-like transparent materials. *Science*. **364**, 1260–1263 (2019).
- [18] T. S. Balke, thesis (1972).
- [19] T. P. Niebel, F. Bouville, D. Kokkinis, A. R. Studart, Role of the polymer phase in the mechanics of nacre-like composites. *J. Mech. Phys. Solids.* **96**, 133–146 (2016).
- [20] T. Hanemann, J. Boehm, C. Müller, E. Ritzhaupt-Kleissl, in *Micro-Optics* 2008 (2008), vol. 6992, p. 69920D.
- [21] J. Böhm, J. Hausselt, P. Henzi, K. Litfin, T. Hanemann, Tuning the refractive index of polymers for polymer waveguides using nanoscaled ceramics or organic dyes. *Adv. Eng. Mater.* **6**, 52–57 (2004).
- [22] B. Lawn, Fracture of brittle solids (Cambridge university press, 1993).
- [23] F. Barthelat, R. Rabiei, Journal of the Mechanics and Physics of Solids Toughness amplification in natural composites. *J. Mech. Phys. Solids.* **59**, 829–840 (2011).
- [24] P. Jackson, J. F. V Vincent, R. M. Turner, The mechanical design of nacre. Proc. R. Soc. London. Ser. B. Biol. Sci. 234, 415–440 (1988).
- [25] F. Barthelat, Z. Yin, M. J. Buehler, Structure and mechanics of interfaces in biological materials. *Nat. Rev. Mater.* **1**, 1–16 (2016).
- [26] D. V Wilbrink, M. Utz, R. O. Ritchie, M. R. Begley, Scaling of strength and ductility in bioinspired brick and mortar composites. *Appl. Phys. Lett.* **97**, 193701 (2010).
- [27] M. R. Begley, N. R. Philips, B. G. Compton, D. V Wilbrink, R. O. Ritchie, M. Utz, Micromechanical models to guide the development of synthetic 'brick and mortar' composites. *J. Mech. Phys. Solids.* 60, 1545–1560 (2012).

- [28] S. M. WIEDERHORN, Fracture Surface Energy of Glass. *J. Am. Ceram. Soc.* **52**, 99–105 (1969).
- [29] E. A. Sander, V. H. Barocas, Comparison of 2D fiber network orientation measurement methods. *J. Biomed. Mater. Res. Part A An Off. J. Soc. Biomater. Japanese Soc. Biomater. Aust. Soc. Biomater. Korean Soc. Biomater.* **88**, 322–331 (2009).
- [30] ASTM D790-16, Standard Test Methods for Flexural Properties of Unreinforced and Reinforced Plastics and Electrical Insulating Materials, ASTM International, West Conshohocken, PA, 2016.
- [31] ASTM E1820-16, Standard Test Method for Measurement of Fracture Toughness, ASTM International, West Conshohocken, PA, 2016.
- [32] R. W. Davidge, G. Tappin, The effective surface energy of brittle materials. *J. Mater. Sci.* **3**, 165–173 (1968).

## Link between chapter 2 and chapter 3

In the previous chapter, we demonstrated an accessible technique for fabricating highly transparent nacre-inspired glass composites. Our composite successfully mimicked the natural nacre's microstructure and some of the essential mechanisms that lead to the high fracture toughness of such materials. Our composite consists of two phases: a soft connective one and a hard tablet phase. This gives us the great opportunity of improving or adjusting the composite to a specific need by modifying one of the building blocks. While there is little to change or modify with the glass flakes, there are numerous options for modifying the soft phase. As optical clarity and the simple fabrication method are two of the crucial elements of previous work, that would be more beneficial to develop a PMMA-based polymer with tunable mechanical and physical properties. In the next chapter, we will present a class of PMMA-based polymers with improved mechanical properties, fracture toughness, and impact resistance. Such a polymeric material would be an excellent candidate to be incorporated into our transparent glass composite for tuning the mechanics of nacreous material.

# Chapter 3

Poly(methyl methacrylate)-based polymers with improved toughness and impact resistance and tunable mechanical properties

# Poly(methyl methacrylate)-based polymers with improved toughness and impact resistance and tunable mechanical properties

Ali Amini<sup>1,2</sup>, Adele Khavari<sup>2</sup>, Pouria TirgarBahnamiri<sup>2</sup>, Allen J Ehrlicher\*<sup>1,2</sup>

- 1-Department of Mechanical Engineering, McGill University, Quebec, Canada.
- 2- BioActive Materials Lab., Department of Bioengineering, McGill University, Quebec, Canada.

\*Corresponding Author: <u>Allen.Ehrlicher@mcgill.ca</u>

**Keywords**: Poly(methyl methacrylate), toughness, impact resistance, copolymerization, crosslinking

#### 3.1 Abstract

Polymethyl methacrylate (PMMA) is a thermoplastic with a vast range of applications from glazing to biomedical purposes due to its excellent optical clarity, strength, and stiffness. The fabrication process (free radical polymerization) is straightforward, making it simple for bulk production. Although PMMA is brittle, there have been many studies improving its toughness and impact resistance. One disadvantage with the proposed techniques is the sacrifice of mechanical properties or fabrication simplicity to improve PMMA's toughness. Here, we propose a simple method to increase PMMA's fracture toughness and impact resistance without sacrificing mechanical properties, and with little modification to its simple fabrication method. With copolymerizing with acrylonitrile (AN), we were able to enhance PMMA's fracture toughness and impact resistance by 30% and 40%, respectively. The strength values also remained constant for lower concentrations of AN. By involving 1,4 butanediol dimethacrylate (BUT) as the crosslinking agent, the loss in flexural modulus from copolymerizing with AN was compensated, as well as the vulnerability against solvents was also improved tremendously. PMMA-based polymer comprising 10 mol% of AN and 10mol% of BUT has more than seven times less weight change than the neat PMMA when exposed to acetone at room temperature.

#### 3.2 Introduction

Polymethyl methacrylate (PMMA) is a transparent amorphous thermoplastic that has been widely used in different applications, from structural components to biomedical applications since its discovery in 1930. The reason for this wide range of applications is the simple fabrication processes and relatively high levels of stiffness and strength. It also possesses high optical clarity that make it a suitable alternative to structural glass in many applications. Being biocompatible, PMMA has also been used as a biomaterial in denture applications. Bulk free radical polymerization is one of the widely used techniques to make PMMA, along with many others, such as radical/anionic solution, suspension, and emulsion methods. In this technique, free radicals are generated by incorporating a suitable initiator molecule in proximity to heat/radiation. The PMMA chains are then formed across the double bonds in MMA monomer and grown by the successive addition of MMA monomers to the initial molecule.

Although PMMA is considered to be brittle, it has been extensively studied to improve its toughness and impact resistance. Incorporating micro- and nano-fillers into the PMMA matrix is one of the approaches to enhance the mechanical properties of PMMA. Rubber toughened PMMA is one of the most widely investigated filled PMMA composites. Rubber particles improve the fracture toughness of the PMMA matrix via cavitation and shear yielding mechanisms [1]. Despite the successful improvement of toughness and impact resistance, this approach entails a decrease in strength and stiffness[2][3]. Furthermore, care must be taken when making the rubber particles to prevent refractive index mismatch between matrix and filler to avoid transparency loss[2]. Effect of incorporation of many other micro- and nano- fillers into PMMA matrix, has been studied, such as carbon nanotubes[4][5] and nanofibers[6][7], graphene[8], graphene-oxide[9], alumina nanoparticles[10], polyhedral oligomeric silsesquioxanes nanocages[11], and Si-CaO

nano-particles[12],. The effect of adding these fillers to PMMA is not always beneficial: it varies from a neutral or even negative impact on mechanical properties [6][7][9]; improvement to one aspect of the mechanical properties while compromising the rest of them[10]; and the enhanced performance of PMMA under mechanical loading [4][5][12][11]. The latter, however, usually sacrifice the simplicity, the scalability of the fabrication process, or the optical transparency of the material.

Another way of modifying the polymeric materials is through copolymerization, involving at least two monomers in the polymerization process. Butyl acrylate (BA) [13], ethylene-vinyl acetate (EVA) [2], Dimethylsiloxane (DMS) [14], and Phenyl Maleimide[15] are some examples of monomers that have been reported to improve the mechanical properties of PMMA upon copolymerization. Like filled PMMA, copolymerization of MMA with other monomers does not necessarily lead to a mechanically superior material. For example, PDMS-PMMA copolymer is less strong and stiff compared to the neat PMMA[14]. Another similar example is PMMA/N-Phenyl Maleimide, where increasing the softening temperature and modulus of the material leads to a less strong yet more ductile polymer[15]. In many examples, however, some aspects of the material are improved by compromising some other material properties. PMMA and PBA copolymers, for instance, behave like elastomers and have a very high elongation at break, but this is achieved only by compromising the strength and stiffness[13] [16] [17]. PMMA/EVA grafted copolymer is another example where impact resistance and fracture energy is enhanced at the cost of strength and stiffness[2].

Copolymerization interconnects the PMMA chains, making a polymeric interlinked network. Such a process is called crosslinking, often achieved by using monomers with two end-functional vinyl groups. The crosslinking of PMMA has been reported to have a positive effect on chemical and

physical properties such as material's thermal stability[18] and solvent resistance[19]. However, its impact on the mechanical properties of the PMMA has been mostly negative. Butadiene acrylate as a crosslinker has no effect on the impact resistance of denture PMMA[20]. Ethylene glycol dimethacrylate (EGDM) and triethylene glycol dimethacrylate (TGDM) are two known crosslinking agents for the PMMA, the former has little to a negative effect on the strength and modulus of the PMMA, and the latter slightly improves the modulus while its effect on the strength is similar to TGDM[21]. Ethylene dimethacrylate (EDMA) also plays a similar role as EGDM in improving the mechanical properties of the PMMA[22].

Here, we employ the straightforward and simple method of free radical polymerization to make a crosslinked copolymer of PMMA in bulk, with improved fracture toughness and impact resistance, while retaining the strength, modulus and transparency. Acrylonitrile (AN) and 1,4 butanediol dimethacrylate (BUT) are used as the components for copolymerization and crosslinking, respectively. PMMA/AN copolymer and crosslinked PMMA with BUT have been synthesized and reported before, but to the best of our knowledge, no comprehensive study of their effect on mechanical properties, including fracture and impact resistance of individual components or their combination has been reported. The primary goal of using AN is to allow plastic deformation in brittle PMMA and hence increase the ductility, while BUT is utilized to crosslink the network and improve the modulus and chemical resistance of the polymeric matrix.

#### 3.3 Materials and methods

Methyl methacrylate, 1,4 butanediol dimethacrylate (95%), acrylonitrile (99%), 2,2'-Azobis(2-methylpropionitrile) (AIBN), and inhibitor remover column were purchased from Sigma (Ontario, CA).

#### 3.3.1 Copolymerization and crosslinking of PMMA

Inhibitors were removed from the monomers by passing them through the inhibitor removing columns. For the PMMA/Acrylonitrile (PA) copolymers, different molar percentages of the AN was added to the MMA along with 0.15 wt% AIBN as the polymerization initiator. MMA, BUT and 0.15 wt% AIBN were used for the crosslinked PMMA (PBDM). In both cases, the mixture was transferred to a mold consisting of two glass plates and a 3D-printed part in between, heated at 50°C for 12 hours, 60°C for 2 hours, and finally 75°C for 2 hours. For the crosslinked copolymer, MMA/AN/AIBN was first heated at 60°C for 2 hours in a glass flask. The mixture then was cooled down to room temperature and the BUT was added (PABDM). The system was then transferred to the mold and the same steps explained for PA copolymer was repeated. Different 3D-printing shapes were used to prepare samples for tensile, fracture and impact tests.

#### 3.3.2 Tensile test

Dumbbell-shaped samples were cast according to the ASTM standard D 1708. Tests were performed using a universal testing machine (Admet, eXpert 5000, MA US). Samples (5-7 samples for each data point) were put under load with a displacement rate of 0.5mm/min. Yield and rupture strengths and strains were calculated from the tensile test data and according to the ASTM standard.

#### 3.3.3 Three-point bending (3PB) test

3PB tests were performed using a universal testing machine (Admet, eXpert 5000, MA US). Cubic samples (5-7 samples for each data point) with dimensions of 50x12x1.5 mm were prepared based on standard ASTM D79. Support span and displacement rate were 16 mm and 1 um/sec respectively.

#### 3.3.4 Single-edge notched beam (SENB) test

Fracture toughness of the polymers was evaluated using the SENB test. Cubic samples (5-7 samples for each data point) with dimensions of 25x3.9x1.8mm were prepared, and a notch was created using a 450  $\mu$ m diamond saw. The initial crack (40  $\mu$ m in tip radius) then created on the tip of the notch using a thin blade covered with diamond paste. The samples were then used in a 3-point bending setup with a displacement rate of 1  $\mu$ m/s. Tests were performed on a universal testing machine (Admet, eXpert 5000, MA US).

The work of fracture (WOF) was calculated as a nonlinear measure of fracture toughness. WOF is defined as the total energy spent to create one unit of fracture surface area [23] and calculated as follows

$$WOF = \frac{U}{2(W-a)}$$

Where U is the area under the load-displacement curve in SENB test, and W and a are the width and initial crack length of the SENB sample respectively.

#### 3.3.5 Weight-drop impact test

Impact resistance of the glass composites was evaluated using a weight-drop impact test method according to the standard ASTM F3007. The tests were performed using a drop tower impact system (Instron, CEAST 9310). An impacting tool (round tip with a diameter of 5mm) and a 400 gr drop mass were installed on the machine. The velocity of the impact was 2.07 m/s. Circular samples (5-7 samples for each data point) with (25mm in diameter and approximately 1.6 mm thick) were placed under the machine while fully supported. Force-displacement curved were derived from raw data, and the impact energy was evaluated by calculating the area under force-

displacement curves. The energy values were normalized by the thickness of the samples to make up for the effect of sample thickness variation.

#### 3.3.6 Evaluation of solvent resistance

The material's solvent resistance was evaluated by exposing the polymeric samples to acetone and toluene for 24 hours at room temperature and 50°C. Samples' weight were measured before and after the process, and the weight change was recorded as a measure of solvent resistance.

#### 3.4 Results and Discussions

The schematic structure of neat, copolymerized with AN (PA), BUT-crosslinked PMMA (PBDM), and crosslinked P(MMA-co-AN) (PABDM) are illustrated in Fig. 3-1.

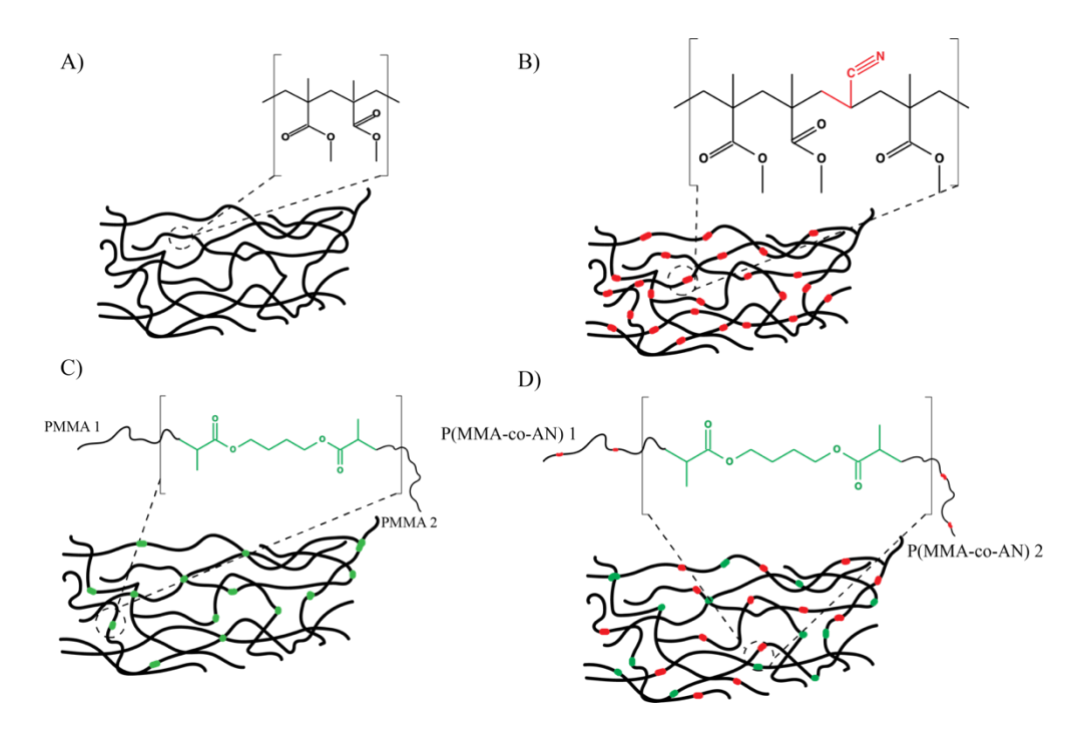


Figure 3-1. Chemical structure of polymers. A) Neat PMMA. B) PMMA copolymerized with acrylonitrile (PA polymer). C)PMMA crosslinked with 1,4 butanediol dimethacrylate (PBDM polymer). D) PA polymer crosslinked with 1,4 butanediol dimethacrylate (PABDM polymer).

Tensile, fracture, and impact tests were performed on 19 sets of samples, 5 samples each, with different molar concentrations of AN, BUT, and both. The details of the concentrations in samples are presented in Table 3-1.

Table 3-1. Monomer concentrations in polymeric samples

	AN molar percentage (%)	BUT molar percentage (%)
PA-N (N=1, 2, 5, 10, 20)	1, 2, 5, 10	
PBDM-N (N=1, 2, 5, 10, 20)		1, 2, 5, 10
PABDM-N-M	1	1, 5, 10
(N=1,5,10 & M=1,5,10)	5	1, 5, 10
	10	1, 5, 10

# 3.5 Optical clarity and solvent resistance

Copolymerization and crosslinking did not have an adverse effect on the transparency of the PMMA, and final products showed high levels of optical clarity for all the AN and BUT concentrations (Fig. 3-2-A). In terms of solvent resistance, PA polymers appeared to be the most vulnerable ones when exposed to solvents. Generally, the uncrosslinked polymers experience a two-step process when exposed to solvents, during the first of which the solvent diffuses into the polymer network and cause polymer swelling. It is after this stage that the dissolution process starts. In the case of PA polymers, exposure to acetone for 24 hours, either at room temperature or 50°C, dissolved a significant part of the polymer and left only a small portion of a soft gel-like polymeric network. We observed the same results when PA polymers were exposed to toluene at 50°C, but toluene at room temperature had a negligible effect on the PA polymers. For instance,

only 2 and 15 percent of weight loss was observed for PA-5 and PA-10, respectively. (Fig. 3-2-B).

In contrast, crosslinked PMMAs, either PBDM or PABDM, showed a similar swelling pattern to neat PMMA in solvents' vicinity. The degree of swelling, however, was significantly lower for crosslinked samples. For instance, when exposed to acetone at room temperature, PBDM-5 experienced seven times less weight change than pure PMMA.

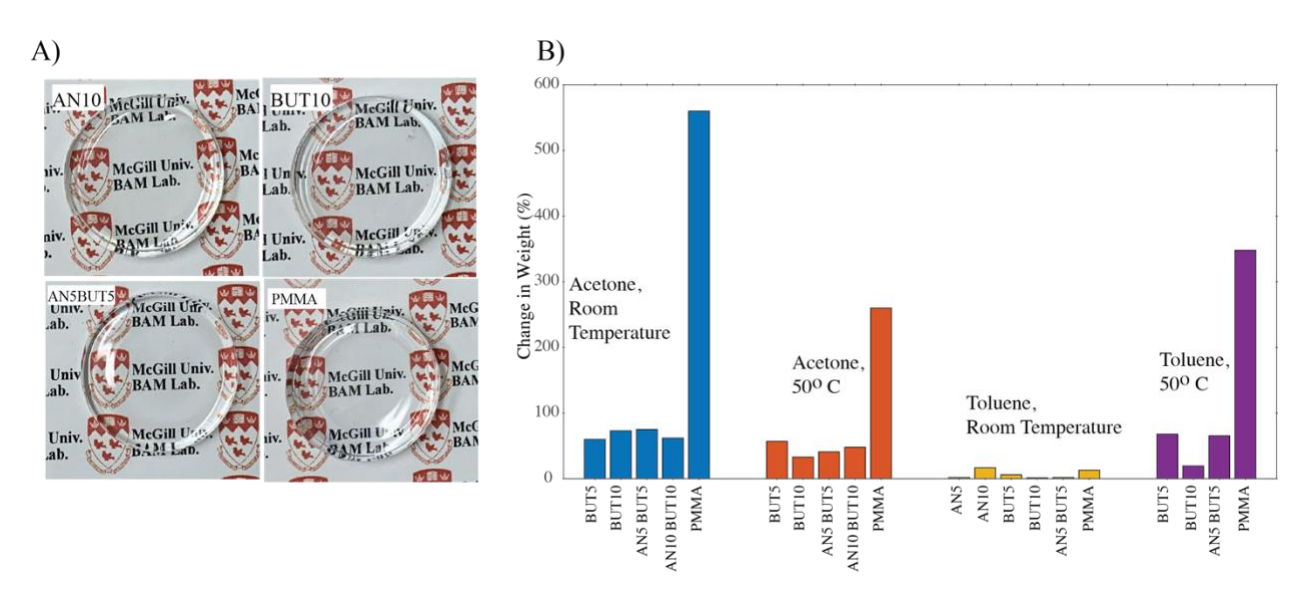


Figure 3-2. Optical transparency and solvent resistance of polymers. A) All synthesized polymers showed excellent optical clarity without any noticeable difference with PMMA. B) Unlike PA polymers that performed poorly when exposed to a solvent, the rest of polymers showed better solvent resistance that neat PMMA. The effect of toluene at room temperature, however, appeared to negligible even on PA polymers.

# 3.6 Mechanical properties

Copolymerization of PMMA with AN produced a material with a very distinct stress-strain profile from PMMA. Unlike PMMA that usually experiences rupture shortly after yielding, PA polymers underwent a drop in load-bearing capabilities and a relatively large deformation until rupture (Fig. 3-3-A). In other words, copolymerization of PMMA with AN allowed for a significant plastic deformation, and hence energy absorption, in the material after yielding. Another notable difference between the two polymers

was the formation of white regions in PA after yielding. These stress-whitened areas spread more as the extension continued in the material. Stress whitening, was also reported in the case of PMMA/EVA[2], and could be attributed to the formation of micro-voids and fibrils in the material, resulting in light diffraction. This region, also known as the craze area, has a significant contribution to the PA polymers' high toughness as more energy will be needed for formed micro-cracks to propagate in this area. PBDM polymers, on the other hand, exhibited a very similar behavior to PMMA under tensile loading, and for most of the samples, the difference between yield and rupture strains was insignificant. PABDM polymers, as was expected, showed a behavior in between the PA and PBDM polymers (Fig. 3-3-B). In general, the lower the concentration of crosslinking agent, the larger was the plastic region and amount of strain at rupture. The size and whiteness intensity of the stress-whitened area increased as the concentration of AN increased in PA polymers (Fig. 3-3-C). On the contrary, no such noticeable white area was observed for crosslinked polymers, even for the PABDM ones with high concentrations of AN (Fig. 3-3-D).

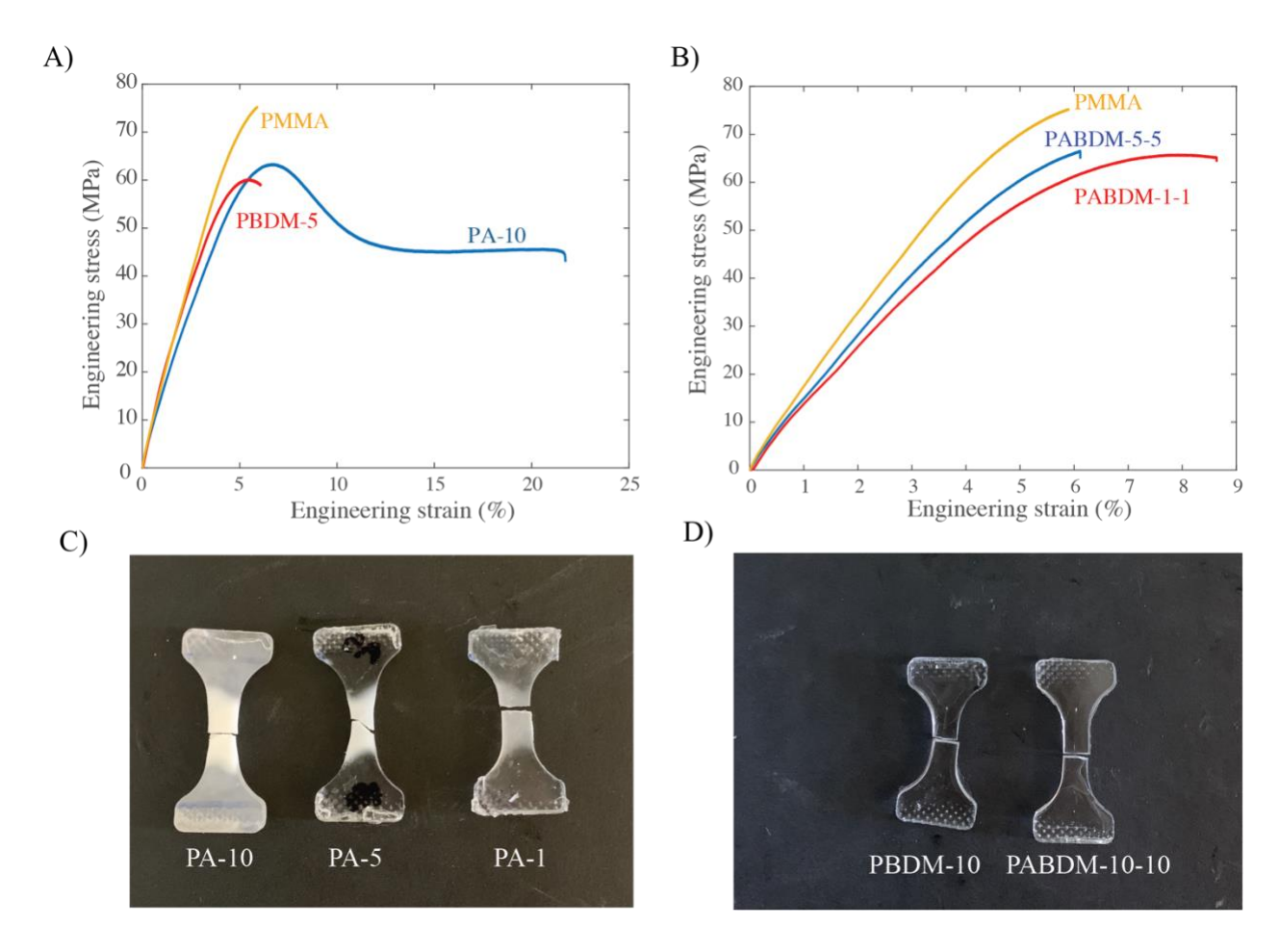


Figure 3-3. PA and PBDM show different behavior under tensile loading. A) PA polymers experience a huge plastic deformation after yielding, while PBDMS polymers are similar to PMMA and break shortly after yielding. B) PABDM polymers' stress-strain profile could be similar to PA or PBDM depending on the proportion of the chemical components. C) PA polymers experience stress whitening and craze after yielding. D) No stress-whitening was observed in PBDMS and even PABDM polymers with high AN content.

Focusing on the mechanical aspects of each individual polymer, PMMA's yield strength could be retained by using small portions of AN (in PA-1 and PA-2 for example). However, the strength values decline as the contribution of AN in the polymer increases (Fig. 3-4-A&B and Fig. 3-8-A). Retaining the strength values for low AN percentages is of great importance when considering the stresses and strains at the same time (Fig. 3-4-C&D and Fig. 3-8-B).

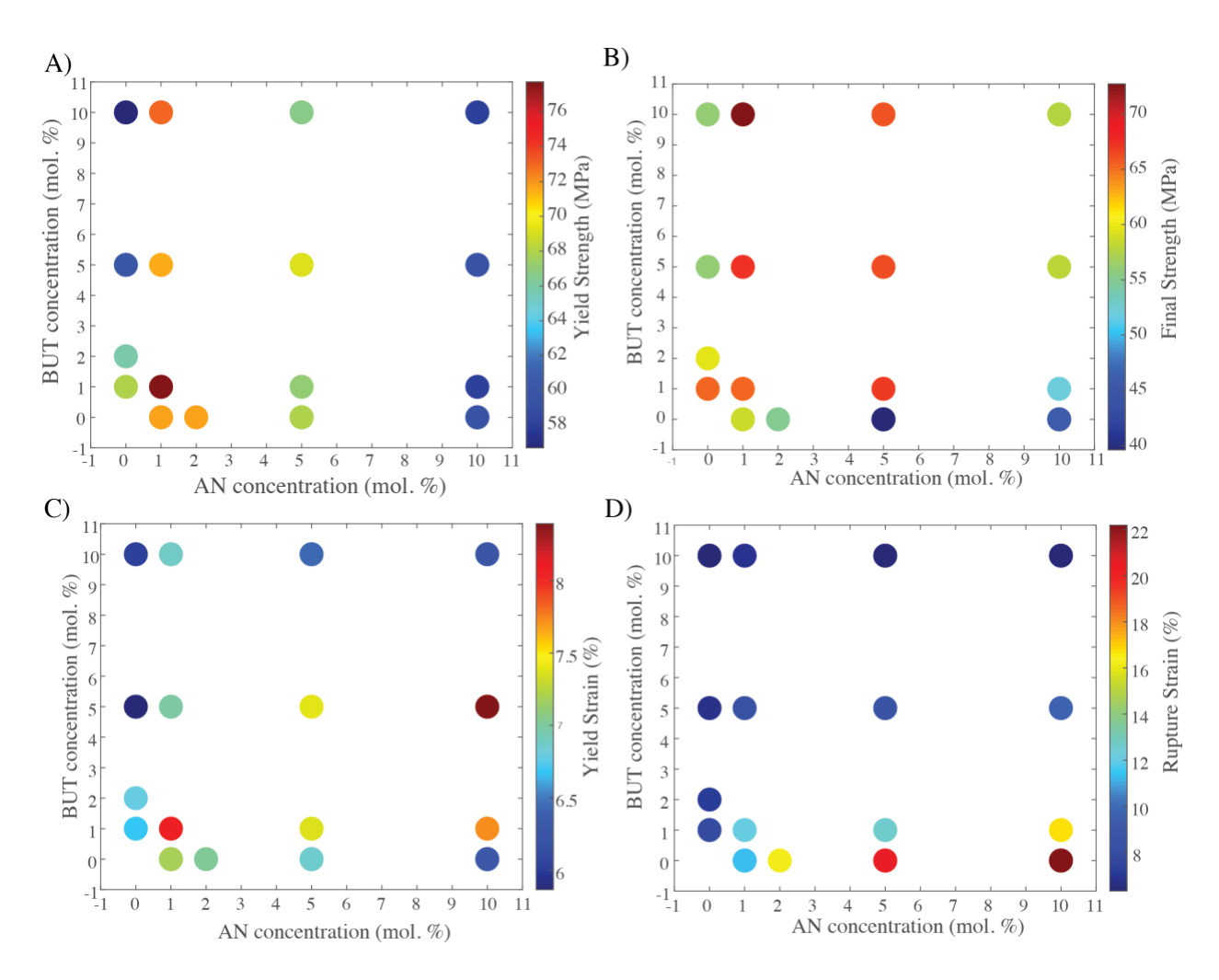


Figure 3-4. Mechanical properties of polymers from tensile testing. A) small molar percentages of AN almost retain yield/rupture strength, while similar to PBDM polymers, higher molar percentages of AN have a negative effect on strength values. PABDM polymers mostly show an improvement in strength values for higher BUT concentrations compared to the corresponding PA polymer. B) PA polymers undergo a huge plastic deformation and hence experience a considerable rupture strain. BUT crosslinker, on the contrary, does not affect the yield/rupture strain. All PABDM polymers with lower proportions of BUT showed high extensions at failure. However, increasing the BUT molar percentage diminishes the rupture strain.

The addition of AN did not weaken the material and made it tougher by absorbing a large amount of energy after the yield point. For instance, we observed a two-fold increase in rupture strain and almost no change in the yield strain for PA-2. No improvement was observed in PBDM's strength and yield/rupture strain values compared to neat PMMA. Strength values in general declined, and the difference between the yield and rupture strengths also decreased as the BUT molar percentage

increased. This implied that the polymer's ductility diminished, and a more brittle material was obtained as the contribution of BUT was increased. The effect of crosslinking PA polymers on strength and critical strain values was positive in general. This effect was pronounced for the polymers with higher molar percentages of AN and lower concentrations of BUT, where it yielded a stronger material with high elongation at break.

While incorporating a crosslinking agent in PA polymer might seem redundant, the usefulness of this approach comes to light when considering the positive effect of BUT on the flexural modulus of the polymer. In general, PA polymers possessed inferior modulus values to pure PMMA, and the decline in modulus values increased as the AN concentration increased (Fig. 3-5 and Fig. 3-9). In contrast, we observed an increase in modulus values for PBDM polymers, a 20% increase in PBDM-10, for instance. The improvement in modulus due to crosslinking with BUT was observed for PABDM polymers as well, and incorporating crosslinking agent compensated the adverse effect of AN on modulus. For example, PABDM-10-1 has a 15% higher flexural modulus than PMMA, and PABDM-1-5 and PABDM-1-10 polymers have similar flexural modulus values to the pure PMMA (Fig. 3-5 and Fig. 3-9). One other reason for using crosslinking agents is their positive impact on the polymer's chemical resistance that was discussed in detail in the previous section.

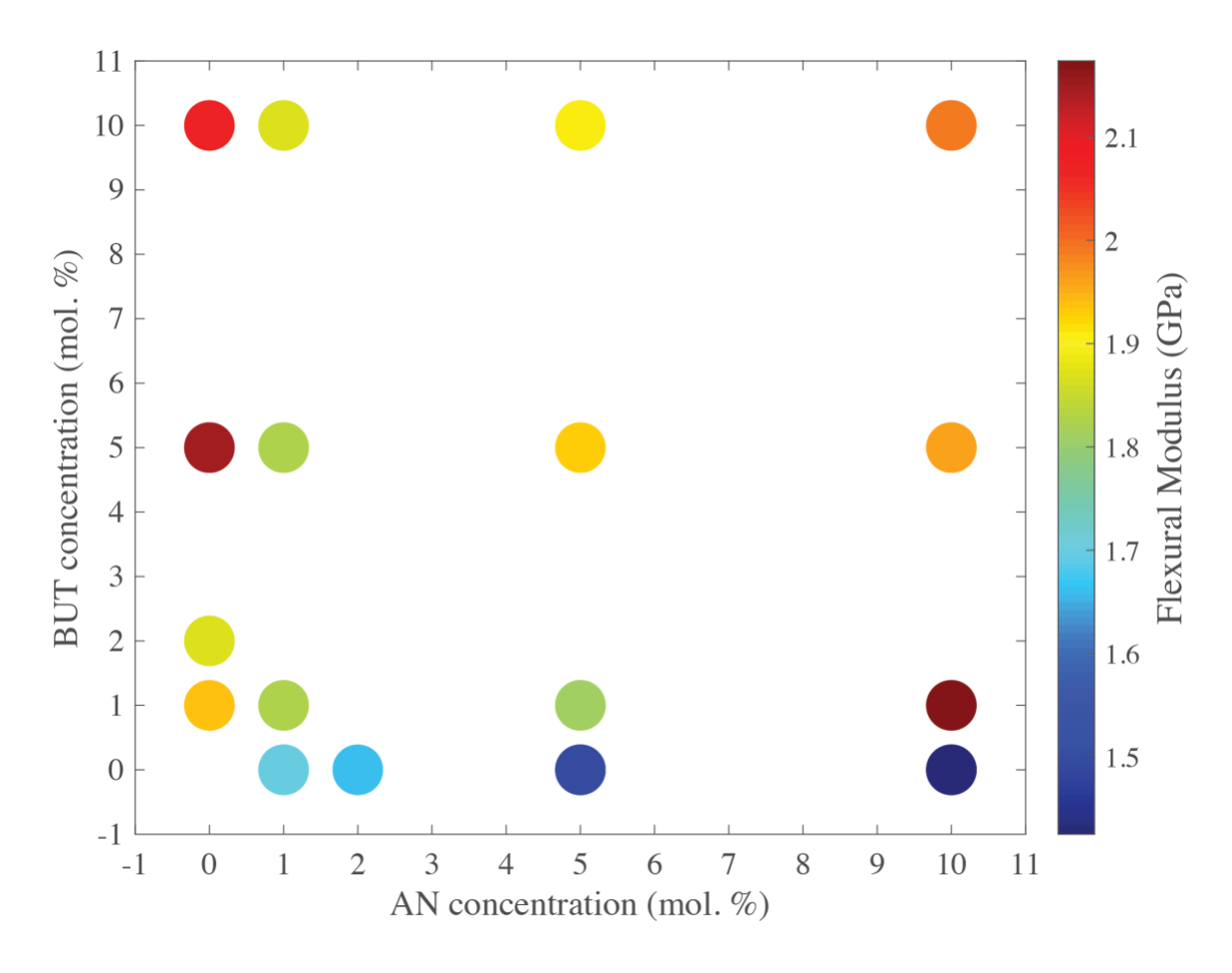


Figure 3-5. Crosslinking improves flexural modulus. increasing AN concentrations would decrease the flexural modulus of PA polymers. Increasing BUT concentration would increase the flexural modulus in PBDM polymers. Crosslinking with BUT compensates the negative effect of AN on modulus, and hence, PABDM polymers possess higher (or similar) modulus values compared to PA and PMMA polymers.

### 3.7 Fracture toughness

Copolymerization with AN and crosslinking with BUT appeared to have opposing effects on the performance of the final polymer before fracture. Only 1 mol% of AN increases the WOF by about 15% (Fig. 3-6-A and Fig. 3-10). This increase could go up to about 30% when using higher proportions of AN (10 mol%, for example). The increase of fracture toughness by involving AN in polymerization was expected because, as discussed in the previous section, PA polymers absorb

energy under tensile loading. On the other hand, crosslinking with BUT appears to have little to negative effect on the fracture toughness of PMMA. WOF generally decreases as the crosslinker mol% increases in PABDM. However, for moderate concentrations of BUT we observed an increase in WOF compared to the corresponding PA polymer. As discussed in the previous section, another reason that a crosslinked polymer is preferred over the copolymerized one (PA polymers) is the positive impact of crosslinking agent on the material's modulus and chemical resistance.

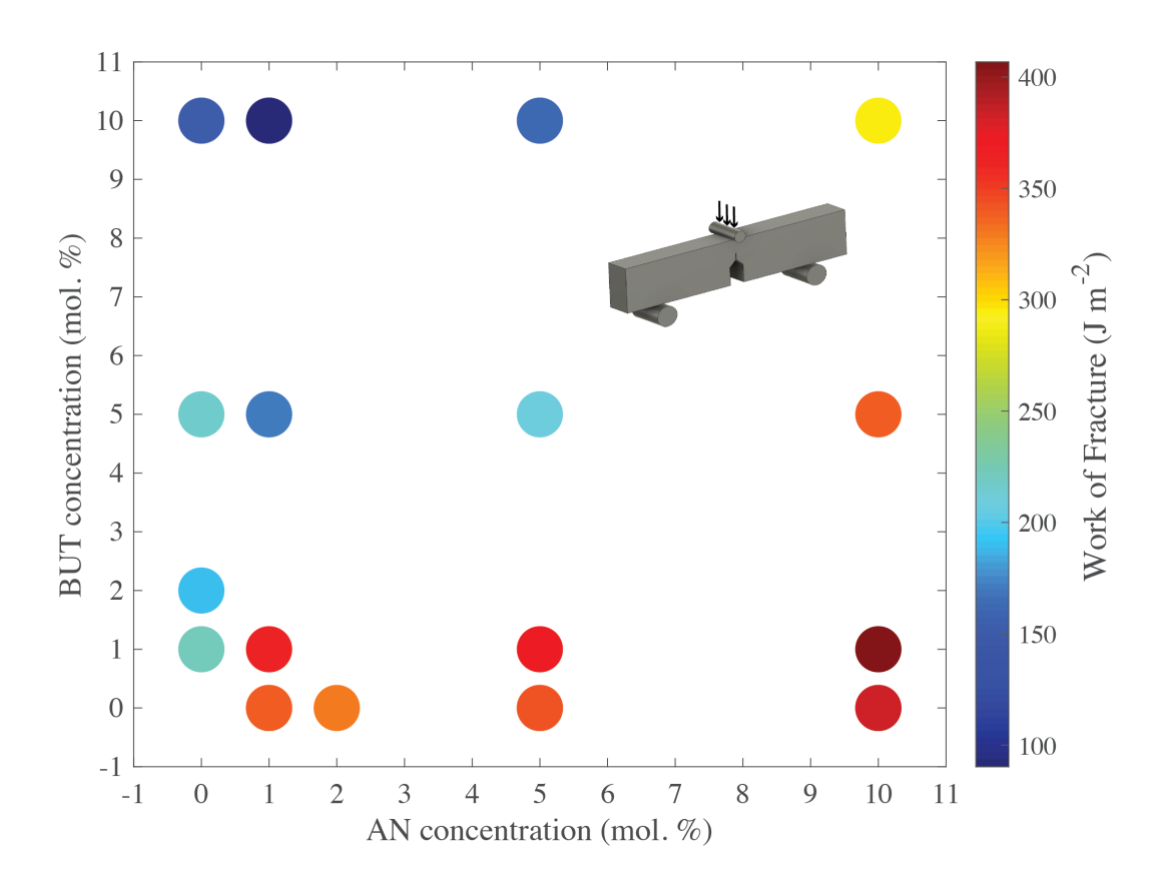


Figure 3-6. Effect of copolymerization and crosslinking on PMMA's fracture toughness. PA fracture toughness increases as the AN concentration increases in the polymer. Crosslinking, however, appeared to have an adverse effect on the fracture toughness. High AN content, along with low crosslinking agent concentrations, yielded a PABDM polymer with higher toughness than PA counterparts.

# 3.8 Impact resistance

All the PA polymers showed a modest improvement (from 25% for AN1 to about 40% for AN10) in impact resistance (Fig. 3-7-A and Fig. 3-11). Crosslinking with BUT, however, had an adverse effect on the impact resistance of PMMA and all the PBDM polymers showed an inferior performance in absorbing impact energy to the pure PMMA. For PABDM polymers, we observed the exact same trend as the one in fracture toughness section; although increasing the crosslinking agent would generally decrease the impact resistance of the material, moderate concentrations of BUT (for example 1 mol.%) lead to an increase in the impact energy compared to the corresponding PA polymer. For instance, PABDM-1-1 absorbed almost 15% more impact energy than PA-1 polymer. Images from a high-speed camera reveal another difference between PA and PBDM polymers. While there is no significant difference between the absorbed energy in PA and PBDM polymers, the former, similarly as PMMA, turns into fewer pieces after breaking (Fig. 3-7-B left and middle). PABDM and PBDM polymers, on the other hand, are alike in breaking patterns under impact loads (Fig. 3-7-B right).

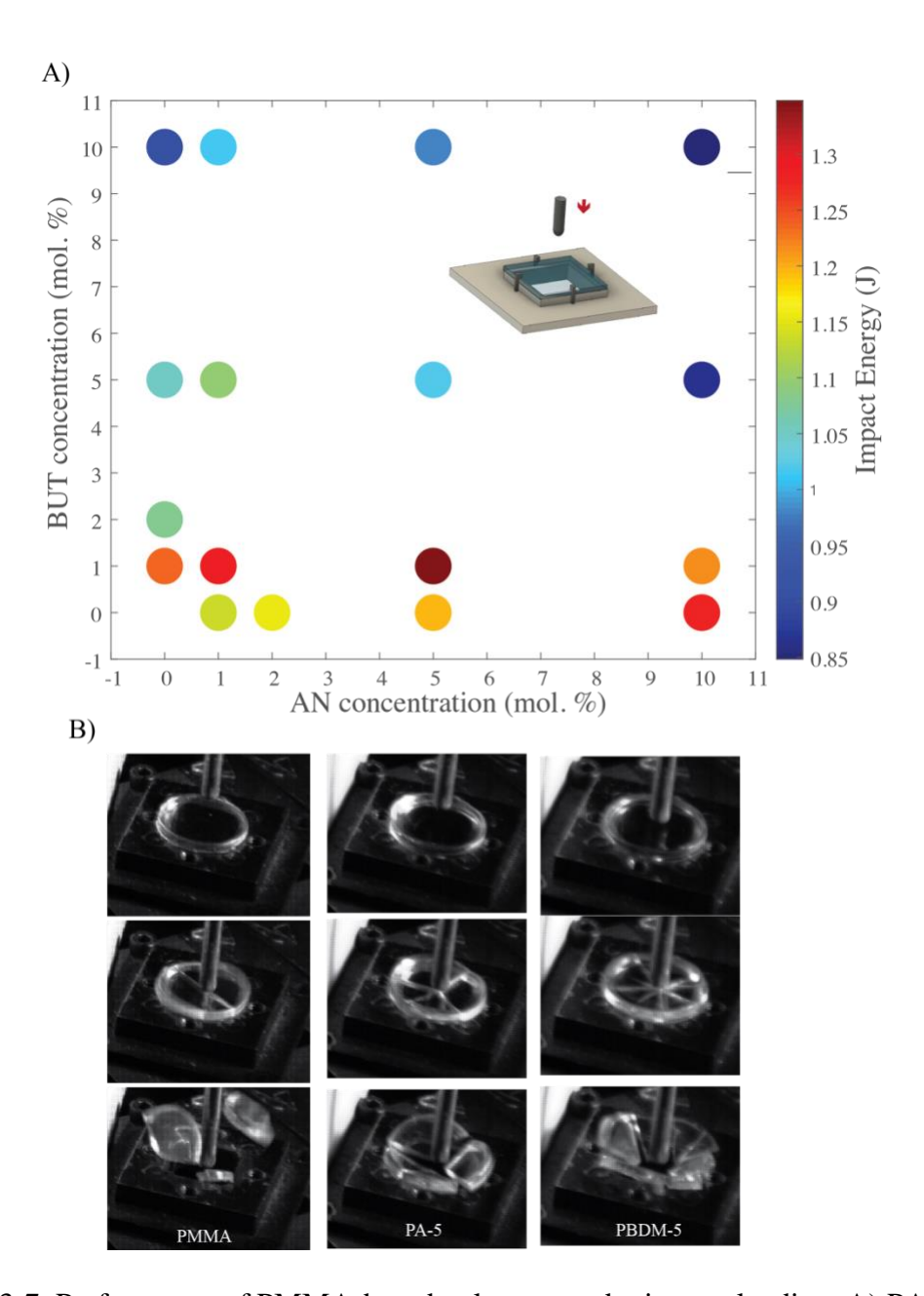


Figure 3-7. Performance of PMMA-based polymers under impact loading. A) PA impact resistance generally increases by increasing the AN content. The impact energy could be further increases by crosslinking the PA polymer with low amounts of BUT (PABDM polymer). BUT alone, however, has a negative effect on the impact resistance of PMMA B) PMMA (left) and PA polymers (middle) turn to fewer and bigger pieces when breaking under impact loads, compared to PBDM and PABDM (right) polymers, which turn to smaller and more fragments with the same loading and boundary conditions.

## 3.9 Conclusions

Here, we developed transparent PMMA-based polymers with improved chemical resistance, mechanical properties, fracture toughness, and impact resistance. PA polymers in low AN concentrations were shown to retain the yield strength with a significantly higher yield and rupture strains, allowing the material to dissipate more energy under mechanical loads. Copolymerization with AN also appeared to improve fracture toughness and impact resistance of pure PMMA. PA polymers, however, suffered from two drawbacks: poor performance when exposed to solvents and possessing lower flexural modulus compared to PMMA. In contrast, PBDM polymers have different advantages than PA ones. While PBDM polymers diminished the yield strength, fracture toughness, and impact resistance of PMMA without having any noticeable effect on PMMA's yield and rupture strain, they demonstrated a higher flexural modulus, and significantly higher solvent resistance. On the other hand, PABDM polymers with lower crosslinker concentrations seem to be the best option to take advantage of the positive aspects of PA and PBDM polymers. PABDM polymers with only 1mol. % of crosslinker, for instance, outperformed the corresponding PA polymers in terms of fracture toughness and impact resistance, flexural modulus and chemical resistance. Such improvements can be realized by adding only a small molar percentage of another monomer (AN or BUT) to the standard chemical synthesis of PMMA, without modifying the whole process.

# 3.10 Supplementary information

In this section, a more detailed set of data on performance of the polymers under tensile test, fracture, and impact loading is provided.

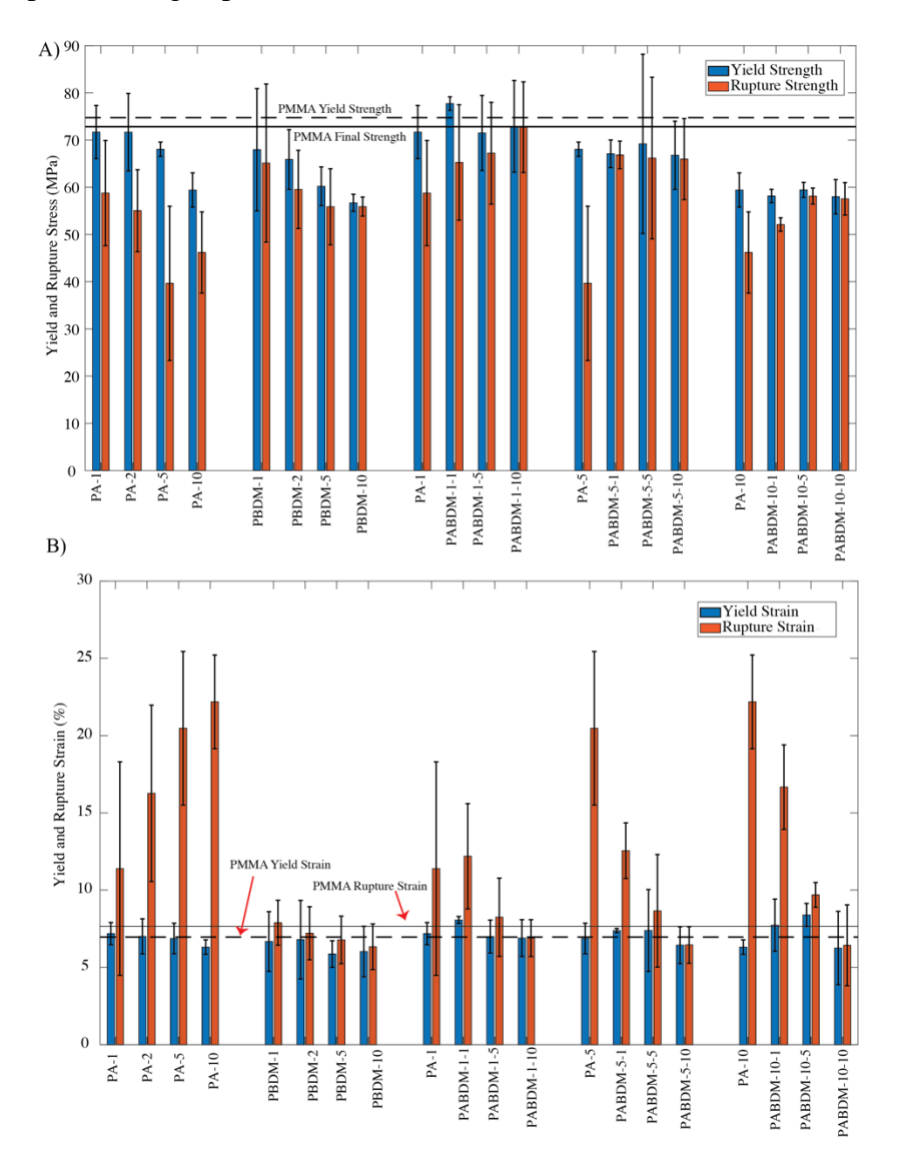


Figure 3-8. Mechanical properties of polymers from tensile testing. A) small molar percentages of AN could retain yield strength and cause a smaller decline in final strength. PBDM polymers also possess lower strength values compared to PMMA. PABDM polymers mostly show an improvement in strength values for higher BUT concentrations. B) PA polymers undergo a huge plastic deformation and hence experience a considerable rupture strain. BUT crosslinker, on the contrary, does not affect the yield/rupture strain. All PABDM polymers with lower proportions of BUT showed high extensions at failure. However, increasing the BUT molar percentage diminishes the rupture strain. Bar graphs are mean values, and error bars demonstrate standard deviation.

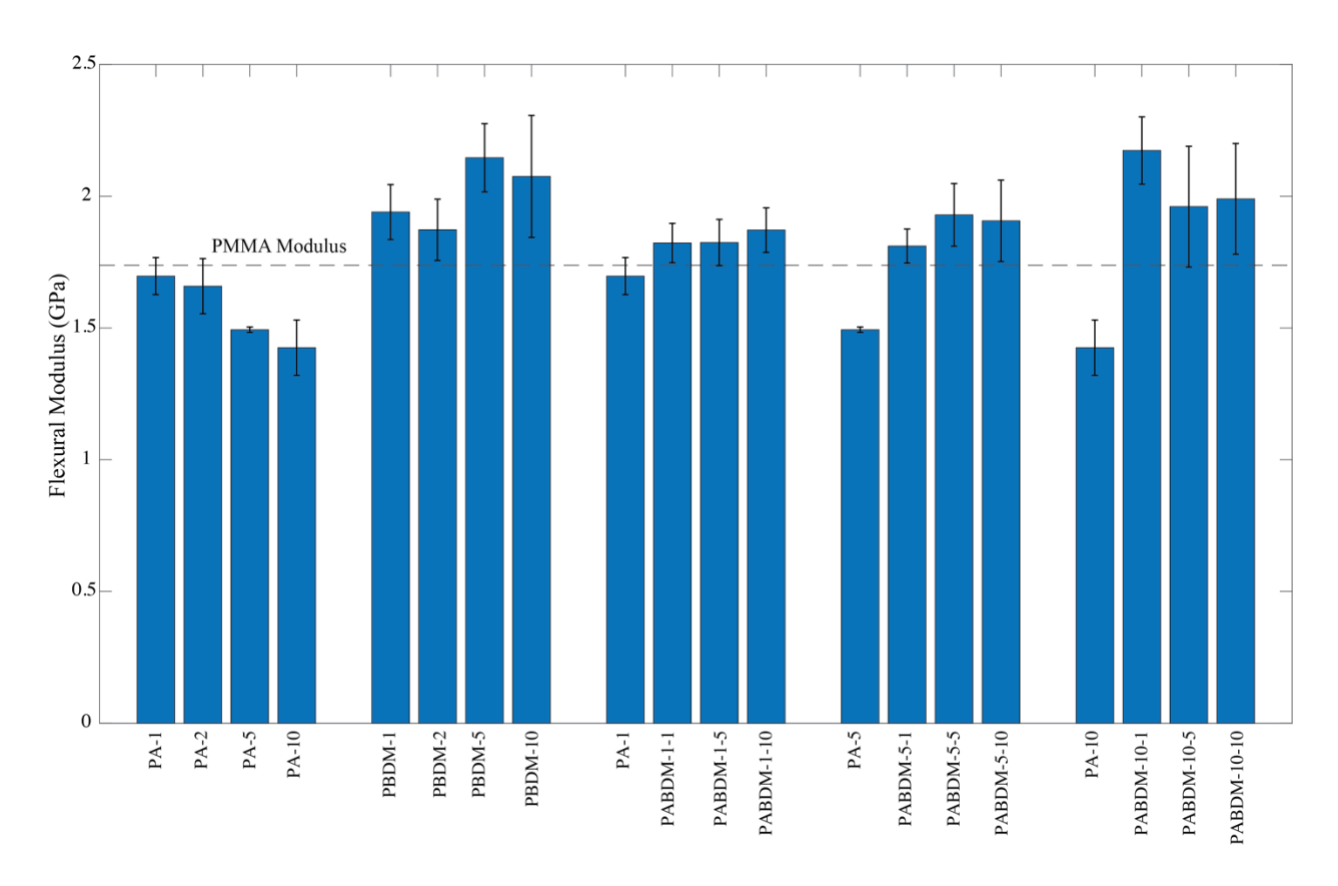


Figure 3-9. Crosslinking improves flexural modulus. PA polymers are inferior to PMMA in flexural modulus, and the decline in modulus values is more for higher AN concentrations. PBDM polymers, on the other hand, possess higher modulus compared to PMMA. Crosslinking with BUT compensates the negative effect of AN on modulus, and hence, PABDM polymers possess higher (or similar in some cases) modulus values compared to PA and PMMA. Bar graphs are mean values, and error bars demonstrate standard deviation.

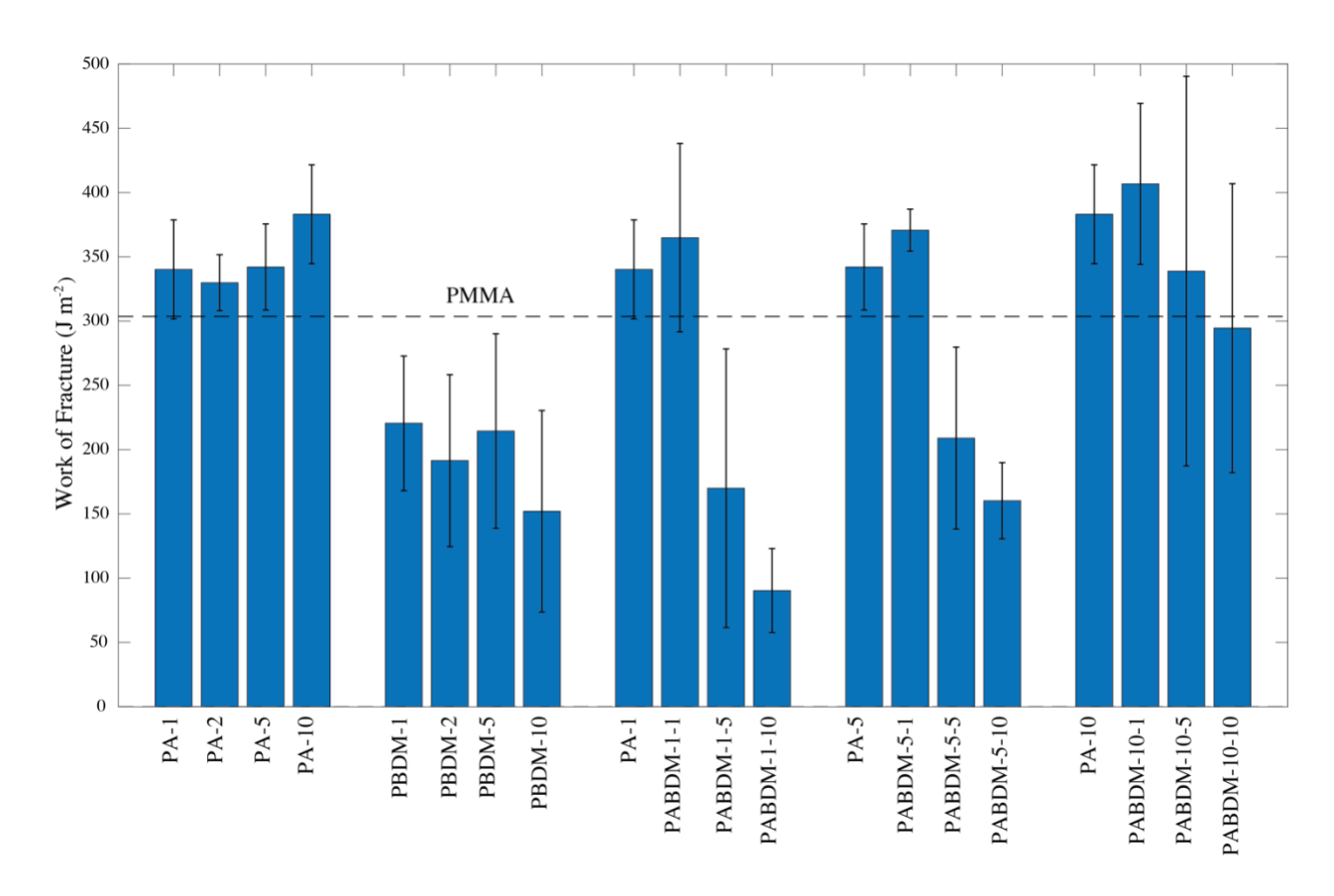


Figure 3-10. Effect of copolymerization and crosslinking on PMMA's fracture toughness. A) PA polymers appeared to have higher WOF compared to pure PMMA. Crosslinking, however, had a negative impact on WOF. High AN content, along with low crosslinking agent, yielded a PABDM polymer with higher toughness than PA counterparts. Data points are mean values and the error bars are standard deviation.

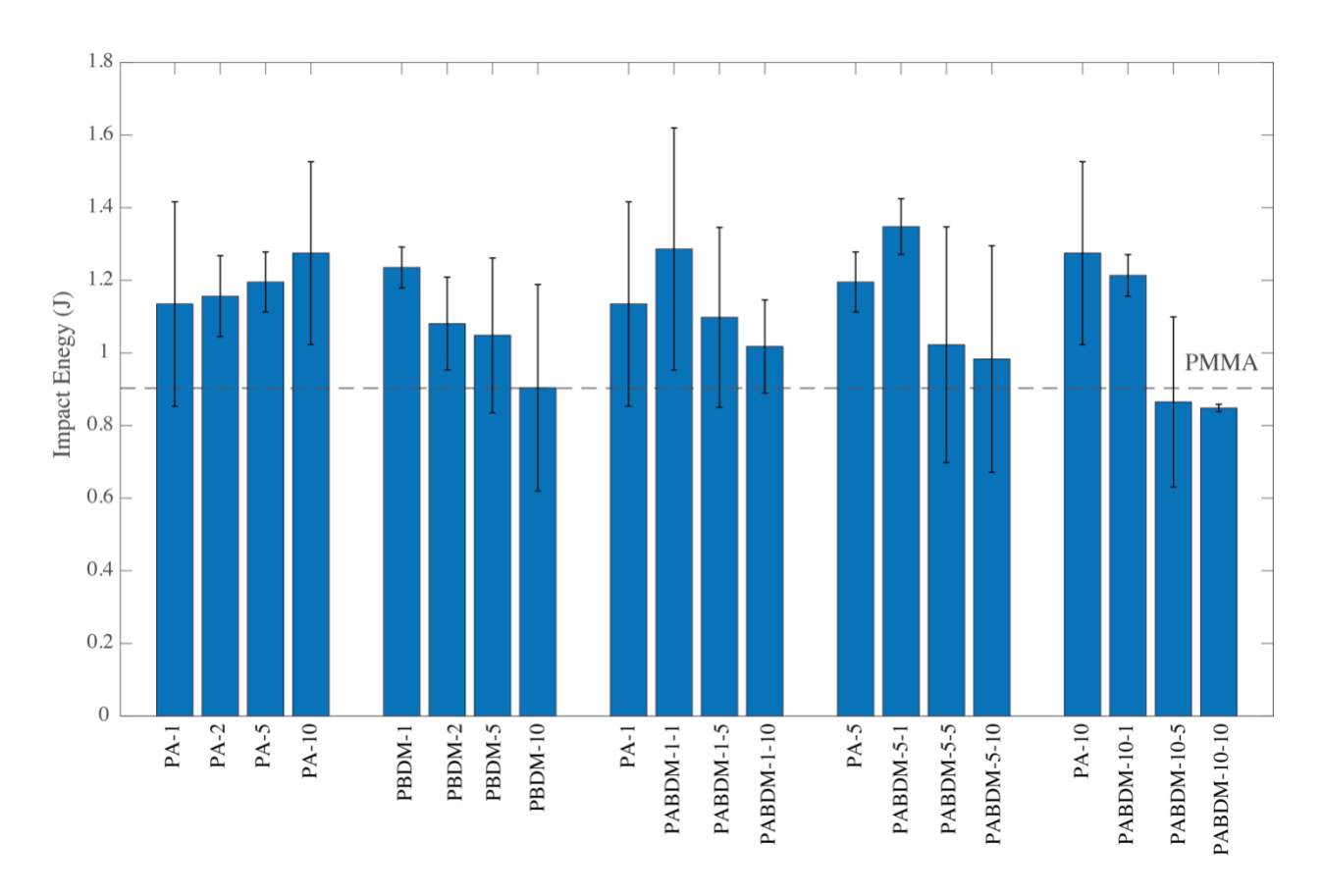


Figure 3-11. Performance of PMMA-based polymers under impact loading. Increasing AN content in PA would increase the impact resistance of the material. The impact resistance was further increase by incorporating low contents of crosslinking agent in PABDM polymers. BUT, however, appeared to have a negative effect on impact resistance of the PBDM polymers. Data points are mean values and error bars demonstrate standard deviation.

#### 3.11 Acknowledgements

AJE acknowledges support from NSERC RGPIN/05843-2014 & EQPEQ/472339-2015, FRQNT team grant, Canadian Foundation for Innovation Project #32749, and the Canada Research Chairs Program.

#### 3.12 References

- [1] E. B. Caldona, A. C. C. De Leon, B. B. Pajarito, and R. C. Advincula, "A Review on Rubber-Enhanced Polymeric Materials," *Polym. Rev.*, vol. 57, no. 2, pp. 311–338, 2017.
- [2] S.-K. Cheng and C.-Y. Chen, "Mechanical properties and strain-rate effect of EVA/PMMA in situ polymerization blends," *Eur. Polym. J.*, vol. 40, no. 6, pp. 1239–1248, 2004.
- [3] P. A. Lovell, J. McDONALD, D. E. J. Saunders, and R. J. Young, "Rubber-Toughening of Poly (Methyl Methacrylate) by Inclusion of Multiple-Phase Particles Prepared by Emulsion Polymerisation," in *Integration of Fundamental Polymer Science and Technology*—4, Springer, 1990, pp. 154–158.
- [4] D. Blond *et al.*, "Enhancement of modulus, strength, and toughness in poly (methyl methacrylate)-based composites by the incorporation of poly (methyl methacrylate)-functionalized nanotubes," *Adv. Funct. Mater.*, vol. 16, no. 12, pp. 1608–1614, 2006.
- [5] V. Skákalová, U. Dettlaff-Weglikowska, and S. Roth, "Electrical and mechanical properties of nanocomposites of single wall carbon nanotubes with PMMA," *Synth. Met.*, vol. 152, no. 1, pp. 349–352, 2005.
- [6] J. Zeng, B. Saltysiak, W. S. Johnson, D. A. Schiraldi, and S. Kumar, "Processing and properties of poly(methyl methacrylate)/carbon nanofiber composites," *Compos. Part B Eng.*, vol. 35, no. 3, pp. 245–249, 2004.
- [7] H. Varela-Rizo, M. Weisenberger, D. R. Bortz, and I. Martin-Gullon, "Fracture toughness and creep performance of PMMA composites containing micro and nanosized carbon filaments," *Compos. Sci. Technol.*, vol. 70, no. 7, pp. 1189–1195, 2010.
- [8] Q. Meng et al., "Effect of interface modification on PMMA/graphene nanocomposites," J.

- Mater. Sci., vol. 49, no. 17, pp. 5838-5849, 2014.
- [9] S. N. Tripathi, P. Saini, D. Gupta, and V. Choudhary, "Electrical and mechanical properties of PMMA/reduced graphene oxide nanocomposites prepared via in situ polymerization," *J. Mater. Sci.*, vol. 48, no. 18, pp. 6223–6232, 2013.
- [10] B. J. Ash *et al.*, "Mechanical properties of Al2O3/polymethylmethacrylate nanocomposites," *Polym. Compos.*, vol. 23, no. 6, pp. 1014–1025, 2002.
- [11] E. T. Kopesky, G. H. McKinley, and R. E. Cohen, "Toughened poly (methyl methacrylate) nanocomposites by incorporating polyhedral oligomeric silsesquioxanes," *Polymer (Guildf).*, vol. 47, no. 1, pp. 299–309, 2006.
- [12] K.-H. Lee and S.-H. Rhee, "The mechanical properties and bioactivity of poly (methyl methacrylate)/SiO2--CaO nanocomposite," *Biomaterials*, vol. 30, no. 20, pp. 3444–3449, 2009.
- [13] J.-D. Tong, G. Moineau, P. Leclere, J.-L. Brédas, R. Lazzaroni, and R. Jérôme, "Synthesis, Morphology, and Mechanical Properties of Poly (methyl methacrylate)-b-poly (n-butyl acrylate)-b-poly (methyl methacrylate) Triblocks. Ligated Anionic Polymerization vs Atom Transfer Radical Polymerization," *Macromolecules*, vol. 33, no. 2, pp. 470–479, 2000.
- [14] H. Inoue, A. Ueda, and S. Nagai, "Block copolymers derived from azobiscyanopentanoic acid. XI. Properties of silicone--PMMA block copolymers prepared via polysiloxane (azobiscyanopentanamide) s," *J. Appl. Polym. Sci.*, vol. 35, no. 8, pp. 2039–2051, 1988.
- [15] R. Bharel, V. Choudhary, and I. K. Varma, "Thermal and mechanical properties of copolymers of methyl methacrylate with N-phenyl maleimide," *J. Appl. Polym. Sci.*, vol. 49, no. 1, pp. 31–38, 1993.

- [16] B. Dufour, K. Koynov, T. Pakula, and K. Matyjaszewski, "PBA--PMMA 3-arm star block copolymer thermoplastic elastomers," *Macromol. Chem. Phys.*, vol. 209, no. 16, pp. 1686–1693, 2008.
- [17] H.-Q. Xie and S.-B. Zhou, "Copolymerization of polymethyl methacrylate macromers with n-butyl acrylate and mechanical properties of the graft copolymers," *J. Macromol. Sci.*, vol. 27, no. 4, pp. 491–507, 1990.
- [18] M. A. Hussein, R. M. El-Shishtawy, B. M. Abu-Zied, and A. M. Asiri, "The impact of cross-linking degree on the thermal and texture behavior of poly(methyl methacrylate)," *J. Therm. Anal. Calorim.*, vol. 124, no. 2, pp. 709–717, 2016.
- [19] A. R. K. Ralston, J. A. Tobin, S. S. Bajikar, and D. D. Denton, "Comparative performance of linear, cross-linked, and plasma-deposited PMMA capacitive humidity sensors," *Sensors Actuators B Chem.*, vol. 22, no. 2, pp. 139–147, 1994.
- [20] V. Jerolimov, R. G. Jagger, and R. Huggett, "Effect of Butadiene Acrylate Cross-Linking on Impact Strength of Poly Methyl Methacrylate," *Acta Stomatol. Croat.*, vol. 27, no. 1, pp. 11–15, 1993.
- [21] M. Atsuta and D. T. Turner, "Strength and structure of glassy networks formed from dimethacrylates," *Polym. Eng. Sci.*, vol. 22, no. 7, pp. 438–443, 1982.
- [22] H. B. Lee and D. T. Turner, "Influence of crosslinking on the tensile strength and fractography of poly (methyl methacrylate)," *Polym. Eng. Sci.*, vol. 19, no. 2, pp. 95–98, 1979.
- [23] M. Sakai and R. C. Bradt, "Fracture toughness testing of brittle materials," *Int. Mater. Rev.*, vol. 38, no. 2, pp. 53–78, 1993.

#### Link from chapter 3 to chapter 4

In the previous chapter, we presented a class of polymers based on methyl methacrylate by simply copolymerization and crosslinking the PMMA. The polymers showed improvements in various aspects such as chemical resistance, fracture toughness, and impact resistance. The ultimate motivation for developing such material was to use it as the soft phase in our previously introduced glass composite. It has been shown in several research works that the soft phase plays a vital role in the excellent performance of the nacreous materials. The soft phase is believed to be the component that triggers and activates the extrinsic toughening mechanisms in nacre. Hence, in the next chapter, we incorporate the PMMA-based polymers into the composite and study the effect of such modification on the glass composite's mechanics.

### Chapter 4

An impact resistant bio-inspired transparent composite material with tunable mechanical properties

# An impact resistant bio-inspired transparent composite material with tunable mechanical properties

Ali Amini<sup>1,2</sup>, Adele Khavari<sup>2</sup>, Francois Barthelat<sup>2,3</sup>, Allen J Ehrlicher\*<sup>1,2</sup>

- 1-Department of Mechanical Engineering, McGill University, Quebec, Canada.
- 2- BioActive Materials Lab., Department of Bioengineering, McGill University, Quebec, Canada.
- 3. Department of Mechanical Engineering, University of Colorado Boulder, Boulder, Colorado, US.

\*Corresponding Author: Allen.Ehrlicher@mcgill.ca

Keywords: Bio-inspired, composite materials, nacre, glass, PMMA, Impact resistance

#### 4.1 Abstract

Glasses are structural materials with a broad spectrum of applications due to their rigidity and excellent optical clarity. However, glass has low fracture toughness and impact resistance, thus limiting its applications. Besides the traditional methods of enhancing glass's toughness, some researchers have recently sought new pathways toward enhancing impact resistance and toughness of glass through bio-inspiration. While such methods usually suffer from a trade-off between toughness, rigidity, and fabrication complexity, we recently proposed a bottom-up methodology to overcome this problem. Our centrifuge-based methodology outcompeted the regular annealed glasses and other bio-inspired counterparts in strength, stiffness, and fracture toughness while possessing high optical transparency levels. Here, we study our composite glass's impact resistance, showing that our material absorbs more than 5 times more energy than annealed glass and neat PMMA. We also studied the soft phase's role on the structural properties of the glass composite by incorporating our previously developed PMMA-based polymers into the composite. Copolymerizing with acrylonitrile (AN) and crosslinking with 1,4 butanediol dimethacrylate (BUT), we increased the rupture strain of the composite by 30% while retaining (or in some cases slightly increasing) the flexural strength and modulus of the material. Employing such an approach, we also increase the Work of Fracture (WOF) as a measure of fracture toughness by 40%. Using PMMA-based polymers, however, appeared not to affect the impact resistance of the material.

#### 4.2 Introduction

Glasses are a class of structural materials with a wide range of applications due to their high levels of transparency, rigidity, and abundance. Although the theoretical strength of glass, based on the force needed to separate two atoms, is about 10GPA. This is due to the flaws introduced while processing and machining [1]. The real strength of glass is usually 100 times smaller than in theory. This, in addition to the low impact resistance and fracture toughness of glass, could greatly limit their applications.

In the search for addressing the challenges of the low toughness and impact resistance of glass, researchers have explored an alternative pathway to traditional glass strengthening methods through bioinspiration- by mimicking the design principles of natural materials that have experienced millions of years of evolutionary processes and refinements. Nacre, the tough material comprising the inner layer of mollusk shells, has been considered to be a source of inspiration in making a bio-mimetic glass structure. Nacre exemplifies how the right combination of soft and hard material phases in specific configurations can lead to remarkable mechanical properties far exceeding that of the individual resident materials [2]. While about 95% of its volume is comprised of brittle minerals (aragonite) and the remaining 5% is formed by biopolymers, the composite is 3000 times tougher than the components[3] and a yield strain of up to 1% of strain. This is a remarkable improvement relative to the individual ceramic building blocks, and a thousand-fold increase in elastic modulus of the connective proteins alone[2].

Nacre-inspired glass composites appeared to be promising improvements in mechanical properties while maintaining high levels of transparency. Techniques of varying complexity have been proposed to fabricate synthetic materials mimicking nacre[4], [5]. Some of these have focused on making transparent composites[6]–[8], resulting in thin films with enhanced mechanical and

optical properties. However, these methods generally suffer from a lack of simplicity and scalability.

Attempting to extend the application of transparent nacre-inspired material beyond thin films, one successfully tested bio-inspired strategy for improving impact resistance, and fracture toughness has been the top-down method of laser-engraving patterns in bulk glass. Barthelat's group was able to fabricate glass structures with interlocking jigsaw-shaped 3D arrays[9], laminated glasses with laser-engraved cross-plied pattern[10], and laminated glasses with tablet-like architectures[11]. The latter one was a successful effort to mimic the tablet sliding in nacreous materials. These approaches resulted in increased composite fracture toughness and impact resistance, however, they had to compromise the final product's strength and stiffness. The group improved the stiffness and strength values by decreasing the size of the patterns, however, this reduces transparency and scalability[11].

Magrini *et. al* approached the problem by employing a bottom-up strategy to make a nacreous glass structure[12]. They made a porous scaffold out of glass flakes and infiltrated it with a polymeric phase. To make the composite transparent, they matched the refractive indexes of the two phases. Their glass composite outcompeted regular annealed glass in fracture toughness, however, their composite sacrificed the transparency, which is a crucial element in glass-like materials.

Our group recently developed a bio-inspired glass composite using a scalable fabrication method out of glass flakes and PMMA as soft and hard components, respectively, with superior strength and fracture toughness to annealed and other bio-inspired glasses[13]. Surface functionalization of glasses created strong bonds between the two phases in the absence of mineral connective bridges. The method employed centrifugation to impose order in the microstructure, making a brick-and-

mortar structure, activating some important toughening mechanisms in the material (Fig. 4-1-A and Fig. 4-1-C). These two simple strategies together yielded a material with high levels of strength and fracture toughness. Our glass also appeared highly transparent with relatively low haziness due to matching the refractive indexes of the two building blocks by using a suitable dopant (Fig. 4-1-B).

One appealing feature of organic-inorganic composites in general, and our glass composite specifically, is the possibility of improving one or more aspects of the material by modifying the constituents. While there is not much to change about glass flakes, numerous options for polymeric materials allow us to tune one or more desired properties. Researchers have extensively studied the soft phase of nacreous structures and the critical role it plays in tuning the final mechanical properties and the pivotal role it plays in the toughening mechanism [14]. Thus, the possibility of adjusting the soft phase properties without changing the fabrication process of our glass composite would be intriguing. In this regard, we recently studied the effect of copolymerization and crosslinking on the mechanical properties of the PMMA[15]. The motivation behind that work was to tune the mechanical properties of the PMMA without changing the fabrication process tremendously and simply by involving new components in the original synthesis process.

Here, we first study the impact resistance of our previously developed glass composite and how it differs from the regular annealed glasses. Then, we evaluate the effect of using different PMMA-based polymeric material on mechanical properties, fracture toughness, and impact resistance of the composite.

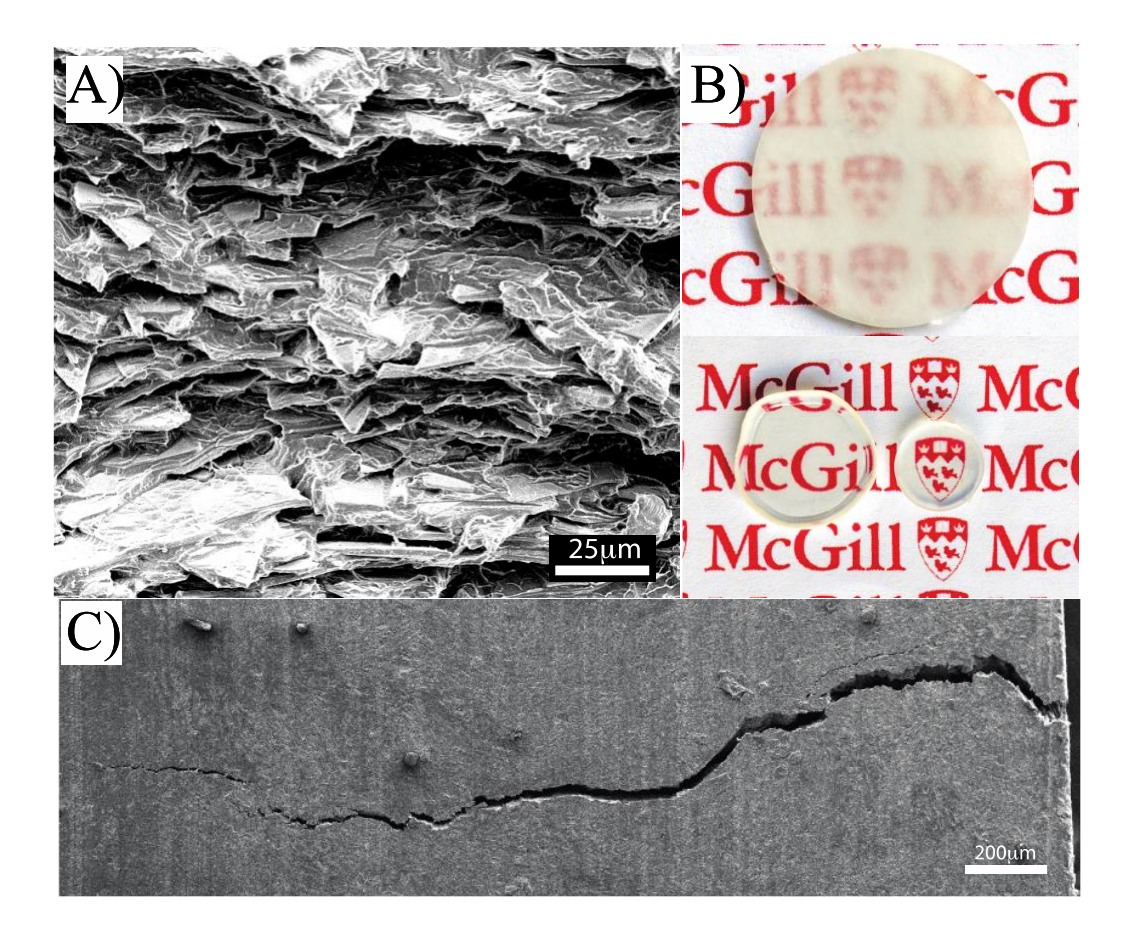


Figure 4-1. Our glass composite mimics the structure and toughening mechanisms of natural nacre. A) Centrifuging imposes order on the structure, and a brick-and-mortar structure is obtained. B) Due to our index-matching strategy, the glass composite possesses high levels of transparency, compared to the one without index-matching that is entirely white and hazy. C) Due to the activation of toughening mechanisms throughout the material, crack deflection is observed in macroscale.

#### 4.3 Materials and Methods

#### 4.3.1 Materials

Glass flakes (GF001-10, d50 (median particle) diameter =27-32  $\mu$ m, thickness =0.9-1.3  $\mu$ m, refractive index = 1.524) were kindly supplied by Glassflake Ltd. Methyl methacrylate (MMA), 1,4 butanediol dimethacrylate (95%) (BDM), acrylonitrile (99%) (AN), 2,2'-Azobis(2-methylpropionitrile) (AIBN),Phenanthrene (98%), (3-trimethoxysilyl) propyl methacrylate ( $\gamma$ -MPS, 98%), Methanol (ACS, 99%), hydrogen peroxide (30 wt. % in H2O), acetone (99.5%) and

MMA inhibitor remover were acquired from Sigma (ON, Canada). Toluene (reagent grade) and sulfuric acid (reagent grade) were purchased from Caledon Laboratories Ltd (ON, Canada).

#### 4.3.2 Glass composite fabrication

Detailed glass surface functionalization methods and glass composite fabrication are described elsewhere[13][15]. In brief, glass flakes were cleaned in the Piranha solution, subsequently washed in DI water several times, and dried in a vacuum oven. Glass flakes were then surface treated with a silane (y-MPS). Surface-functionalized glass flakes were then involved in a free radical polymerization process to grow PMMA monolayer on their surface in a two-step process. First, the components were added to a mixture of dry toluene and MMA (2:1 volume ratio) under gentle mechanical stirring at 70°C with an excess amount of AIBN as an initiator to promote growing PMMA from the glass surface and decelerate the polymerization in bulk MMA. After drying the flakes, they were used in the primary composite fabrication process, where a mixture of MMA, AIBN, flakes, and phenanthrene (for refractive index matching) were mixed and heated until a relatively thick mixture was obtained. The thick syrup was then transferred to the mold for centrifuging and polymerization processes. For the sake of tuning the composite's mechanical properties, the soft phase was copolymerized with AN and (or) crosslinked with BDM. Copolymerized and crosslinked PMMA polymer was obtained by simply adding the relevant chemical agents during the polymerization process, while the crosslinking agent was added to the mixture of MMA and AN after the polymerization started. Details of the process could be found elsewhere[15]. The copolymerized, crosslinked, and copolymerized/crosslinked final products are referred to as PA (poly (MMA-co-acrylonitrile), PBDM (PMMA/BDM), and PABDM (poly (MMA-co-acrylonitrile)/BDM), respectively. All glass composites prepared with PA, PBDM, and PABDM polymers were centrifuged at 1000g.

### 4.3.3 Mechanical, fracture toughness, and impact resistance characterization of the glass composite

To measure the flexural modulus, flexural strength, and rupture strain of the composites, 3-point bending tests were performed using a universal testing machine (Admet, eXpert 5000, MA US). Cubic samples (5-7 samples for each data point) with dimensions of 25x3.2x1.8 mm were prepared. Support span and displacement rate were 16 mm and 1 um/sec, respectively. Fracture toughness of the composites was evaluated using Single-Edge Notched Beam (SENB) test. Cuboid samples (5-7 samples for each data point) with approximate dimensions of 25x3.2x1.8mm were prepared and a notch was created using a 450 µm diamond saw. The initial crack (40 µm in tip radius) was created on the tip of the notch using a thin blade covered with diamond paste. The samples were then used in a 3-point bending set up with a displacement rate of 1 um/s. The work of fracture (WOF) was calculated as a nonlinear measure of fracture toughness. WOF is defined as the total energy spent to create one unit of fracture surface area and calculated as follow [16]

$$WOF = \frac{U}{2(W-a)}$$

Where U is the area under the load-displacement curve in SENB test, and W and a are the width and initial crack length of the SENB sample, respectively.

Impact resistance of the glass composites was evaluated using a weight-drop impact test method according to the standard ASTM F3007. The tests were performed using a drop tower impact system (Instron, CEAST 9310). An impacting tool (round tip with a diameter of 5mm) and a 400 gr drop mass were installed on the machine. The velocity of the impact was 2.07 m/s. Circular glass composites(5-7 samples for each data point) with (25mm in diameter and approximately 1.6 mm thick) were placed under the machine while fully supported. Force-displacement curved were

derived from raw data, and the impact energy was evaluated by calculating the area under forcedisplacement curves. The energy values were normalized by the thickness of the samples to make up for the effect of sample thickness variation.

#### 4.4 Results and discussion

#### 4.4.1 Impact-resistant nacreous glass composite

We evaluated the impact resistance of the glass composites using a weight-drop test method, where we calculated the puncture energy due to impact for our samples. Regular annealed borosilicate glass experienced an explosive failure with a sudden drop in load after reaching its peak in a loaddisplacement curve (Fig. 4-2-A and Fig. 4-2-C left). Our glass composite experienced several rises and drops in load over the course of impact loading, with a 35% larger maximum load than the annealed glass. Also, the maximum displacement at failure is almost 25 times bigger for our glass composite than the annealed glass. This leads to a more significant impact energy for the nacreous glass composite, making it a much more impact-resistant alternative to annealed glass. Due to such pronounced performance improvement during impact loading, our glass composite outperforms the annealed glass in its resistance to impact energy. For example, the glass composite centrifuged with 2000g has a normalized impact energy of almost 34 times larger than regular annealed glass (Fig. 4-2-B). Comparing our glass composite with the neat PMMA, which is usually considered a more impact-resistant alternative to regular glass panes, nacreous glass composite outperforms the PMMA with as much as five times higher impact energy. Centrifugation, a vital element from the present technique, was proven to have a significant effect on ordering the composite's microstructure, activating the extrinsic toughening mechanisms, and consequently, the excellent performance of the material under mechanical and fracture loads. Centrifugation appeared to significantly affect the glass composite's impact resistance, too, where the impact energy increased 100% by centrifuging the glass composite at 2000g. One possible reason for such improvement could be the resulting ordered and staggered microstructure due to the centrifugation process, extensively discussed in our previous work[13]. Such structure, as discussed elsewhere [11], could lead to a large-scale shearing of the tablets on top of each other, resisted by the thin inter-layers of polymer, resulting in absorption of high amounts of energy. The polymeric phase also undergoes different loading modes, including shear and stretching, causing even more energy dissipation.

We also tested the effect of using various PMMA-based polymers (PA, PBDM, and PABDM) on the glass composite's impact energy. We did not observe any significant improvement upon testing the mentioned materials, and only in a few cases, a material as formed using 1000g glass composite method was obtained. However, this method of improvement may prove useful as using different polymers could improve the performance of the material under other modes of loading, such as fracture.

Our glass composite also showed a different pattern of fracture under impact compared to the annealed glass. We reviewed the failure of glass under impact using a high-speed camera, where the regular annealed glass experienced an explosive fracture, forming many small pieces as it shattered (Fig. 4-2-C left). On the contrary, our glass composite experienced a failure similar to PMMA and broke into fewer pieces, and its failure was not as catastrophic as the annealed glass (Fig. 4-2-C middle and right).

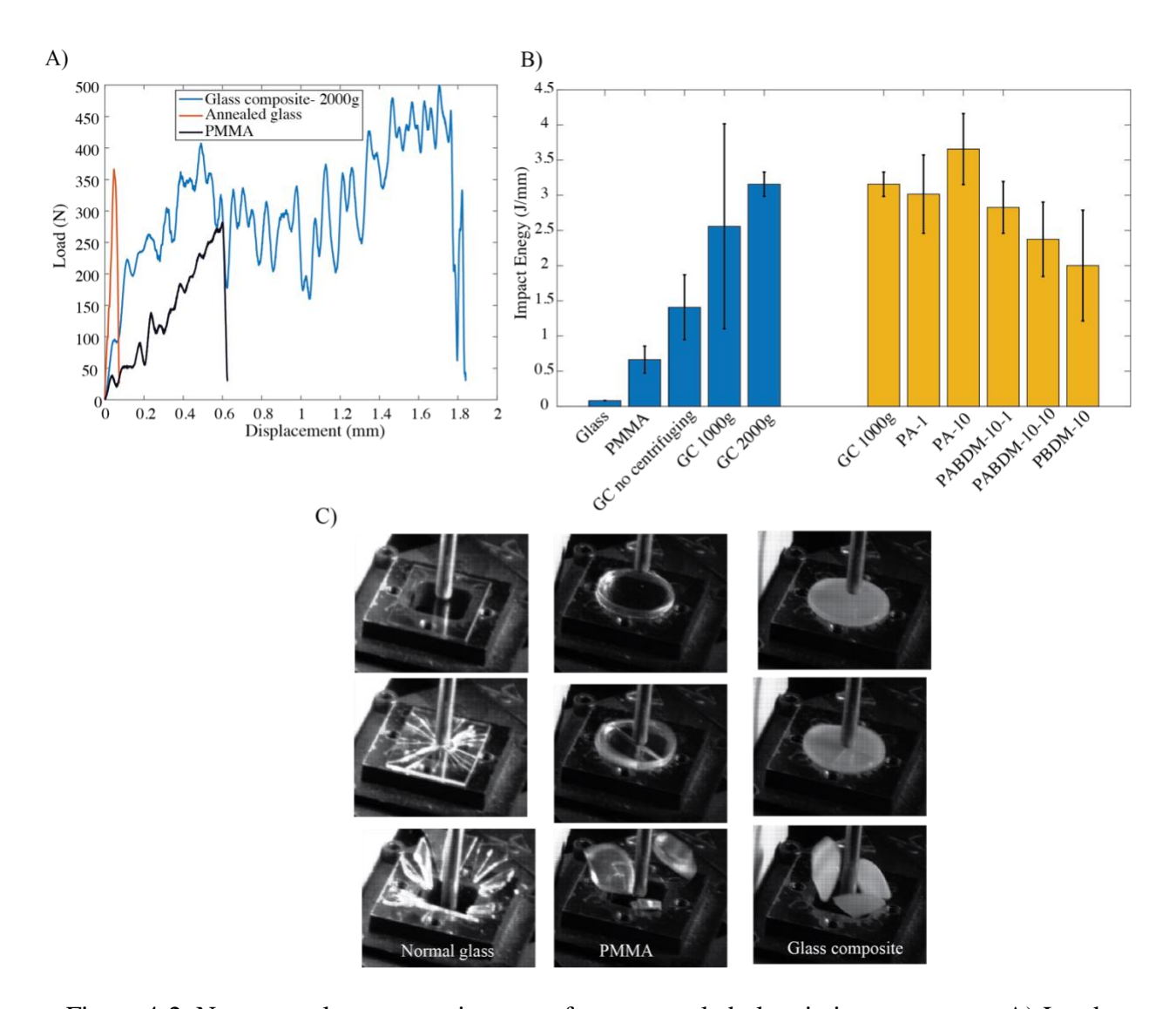


Figure 4-2. Nacreous glass composite outperforms annealed glass in impact energy. A) Load-displacement profiles of annealed glass, PMMA, and nacreous glass. Annealed glass and PMMA experience a sharp and sudden drop in load after reaching maximum load, while glass composite goes through numerous variations in load and possesses much larger displacement at the failure point. B) Centrifugation increases the impact energy. While centrifuging increases the impact energy by more than 100%, using crosslinked and co-polymerized PMMA does not affect the impact resistance of the glass composite. Bar graphs demonstrate mean energy values normalized by samples' thickness. C) Images of normal glass, PMMA, and composite glass with 2mm of thickness before (top), write after (middle), and after (bottom) impact, while simply supported. Bar graphs demonstrate mean values and error bars are standard deviation.

#### 4.4.2 Effect of soft phase on mechanical properties of the glass composite

The effect of copolymerized/crosslinked PMMA on the mechanical properties of the glass composite was studied. Moderate molar percentages (1 and 2%) of AN were previously demonstrated [15] to retain the yield strength of PMMA. This is of interest considering the significant increase in the PMMA's yield and rupture strain due to the presence of AN. The same effect on the flexural strength of the glass composite was observed. Using only 1 or 2 mol% of AN appeared to have an insignificant impact on composite's rupture strength, while further increasing the AN percentage appeared to have a negative effect on the strength of the composite (Fig. 4-3-A). Using PA as the soft phase, however, led to an increase in rupture strain, and in some cases up to 30%, compared to the glass composite with pure PMMA (Fig. 4-3-B). Unlike AN, crosslinking the soft phase with BUT yielded a less strong material for all the tested concentrations. The decline in strength showed a decreasing trend as we increased the crosslinking agent. While the moderate portions of crosslinking agent did not affect the composite's rupture strain, increasing the crosslinker concentration led to a decrease in rupture strain. We previously showed that PA and PBDM polymers have an opposing effect on the flexural modulus of PMMA [15]. The same effect was observed for the composite glasses; composites with PA as the soft phase had inferior modulus to the ones with PMMA, while the glass-PBDM composites demonstrated either no change or a slight increase in flexural modulus compared to the composites with pure PMMA. (Fig. 4-3-C). Glass composite with PBDM-10, for instance, possessed a higher flexural modulus of about 10% compared to PMMA-GC, while lower BUT concentrations such as 1 mol% had a modulus similar to the glass composite with pure PMMA. To take advantage of the positive aspects of crosslinked and copolymerized polymers in our composite, PABDM polymers were incorporated into our composite. However, no significant improvement was observed upon using PABDM polymers as

the soft phase in our composites and at best, a composite with similar mechanical properties to 1000g GC was obtained.

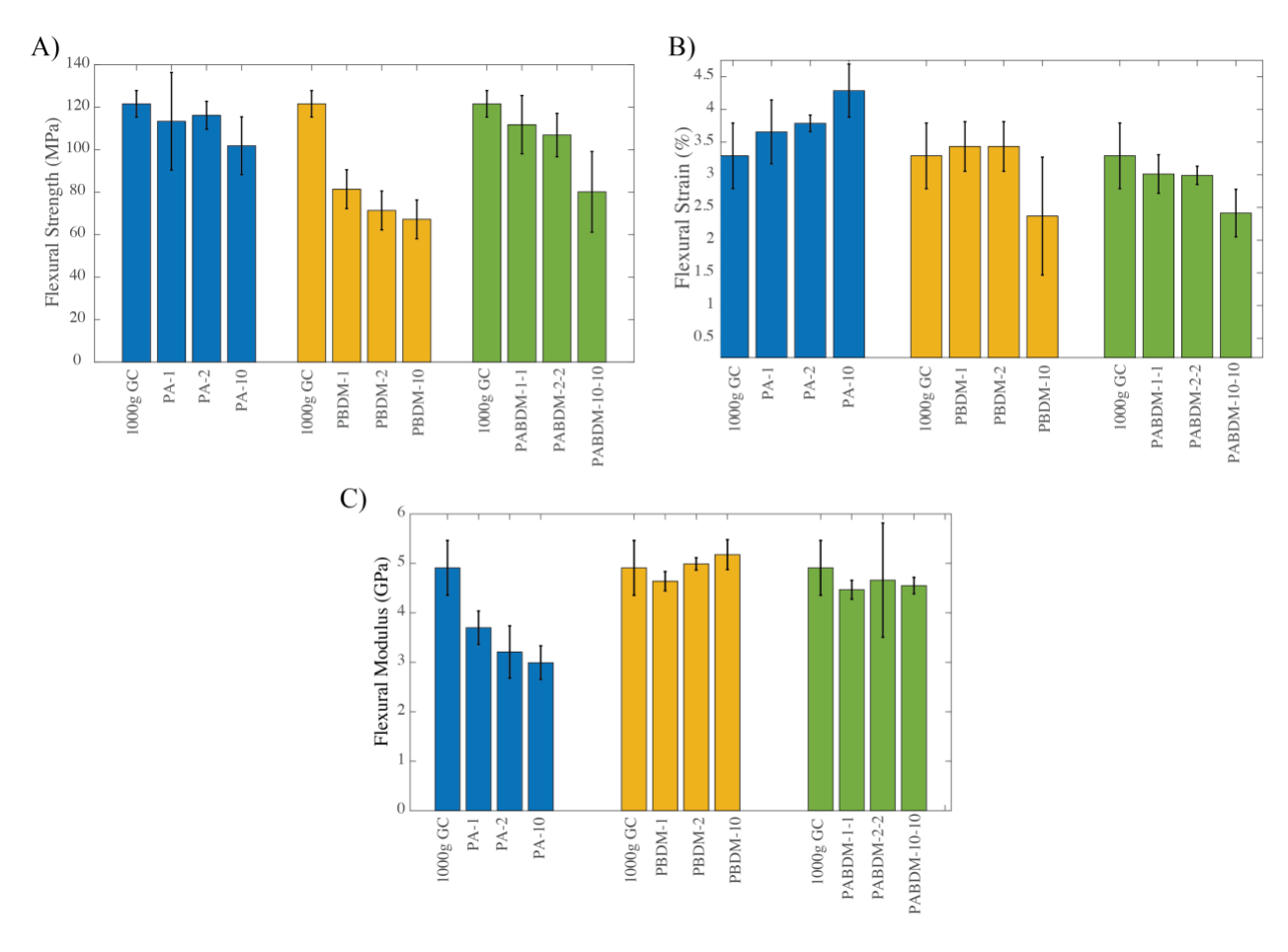


Figure 4-3. Effect of PMMA-based polymers on mechanical properties of glass composite. A) Low percentages of AN, along with PABDM (with moderate percentages of AN and BUT), appear to have no effect on the composite's strength. PBDM, however, negatively affected the composite's strength. B) Rupture strain increases as we increase the AN content in PA polymer. PBDM and PABDM polymers (in low BUT concentrations) do not have any adverse effect on the rupture strain. C) While PAs reduce the composite's flexural modulus, PBDM polymers slightly enhance the flexural modulus. Bar graphs demonstrate mean values and error bars are standard deviation.

#### 4.4.3 Effect of different soft phases on fracture properties of the glass composite

Another essential characteristic of the material is fracture toughness. Here we reported the work of fracture (WOF) as a measure of material resistance against crack growth and fracture. Annealed glass and PMMA usually go through a rapid crack growth and a catastrophic fracture. However,

these properties are different for our glass composite due to the extrinsic toughening mechanisms activated due to the material's brick-and-mortar microstructure. As thoroughly discussed in our previous work[13], large-scale shearing of tablets and as a result, tablet pull-out, the formation of ligaments of polymers between tablets, and consequently delamination at the micron scale. While at a larger scale, multiple changes in the path of crack growth (crack deflection), make the nacreous glass composite a tougher material compared to neat PMMA or annealed glass. As a result, the load-deflection curve of a single-edge notched sample also differs from the one for the PMMA (Fig. 4-4-A). Considering the pivotal role of the soft phase in nacre's toughening mechanisms, we tested different PMMA-based polymers to study the possibility of improving the glass composite's fracture toughness. As it was expected from the positive effect of PA polymers on strength and rupture strain of nacreous glass composite, glass-PA composites possessed a higher WOF compared to 1000g glass composite (Fig. 4-4-B). Increasing the AN portion in PA polymer yielded a glass composite with higher work of fracture. The highest value belonged to PA-10 with a WOF increase of about 35%. PBDM polymers, on the other hand, affected the composite's WOF negatively regardless of the concentration of BUT we used. Unlike PA and PBDM polymers, the effect of using PABDM polymers in our composite was not necessarily positive or negative. Moderate concentrations of BUT yielded a material with slightly higher fracture toughness compared to the corresponding PA/glass composite. However, further increasing the content of BUT decreased the WOF in the composite.

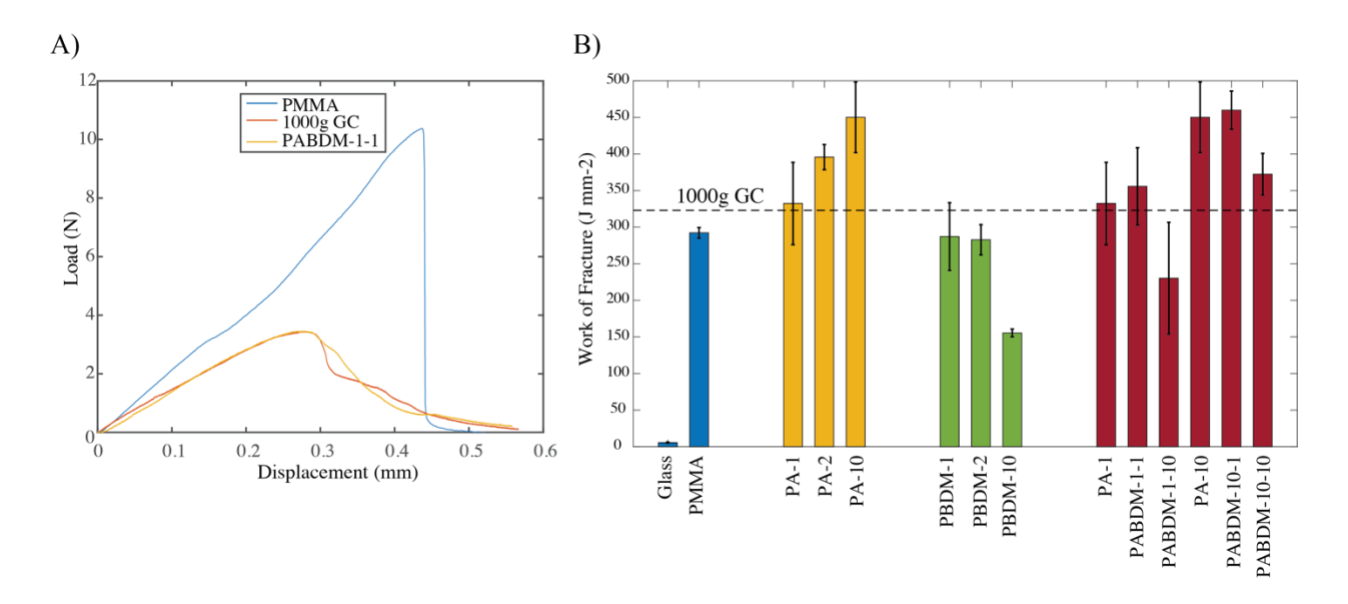


Figure 4-4. PA polymers increase the WOF. A) Glass composites experience non-catastrophic crack growth and fracture. As apparent from the load-deflection profiles, PMMA undergoes a sudden and rapid crack growth and fracture after reaching maximum load, while glass composites experience a smooth and slower crack growth till complete failure. B) PA polymers increase the WOF, and the increase is more significant for higher AN concentrations. PBDM polymers affect the WOF negatively regardless of the molar percentage of BUT. A notable increase in WOF was observed when high amounts of AN with a low amount of BUT was used in PABDM.

#### 4.4.4 Conclusions

In conclusion, our tough and strong nacre-inspired glass composite shows superior performance under impact loads compared to regular annealed glass. Our glass not only absorbed more energy under impact, but its failure was also less explosive as it formed larger pieces upon fracture than traditional glass. This makes our glass composite a suitable alternative to standard glass as it outcompetes them in all the essential mechanical aspects for which glass's performance matters. Yet, our material shows acceptable levels of transparency, one critical element of any glass structure.

We also investigated the possibility of tuning the glass composite's mechanical properties by using different PMMA-based polymers. Since our simple and straightforward fabrication method is one

of the main features of this work, we used our previously developed polymers in the fabrication process, which did not entail any extra complication or change to the whole process.

In general, substituting PMMA with PA increased the rupture strain and fracture toughness, while had no effect on the strength (when moderate concentrations were used) and impact resistance of the composite material. PA also appeared to decrease the flexural modulus of the composite. In contrast, PBDM polymers, except for a minor positive effect on flexural modulus, negatively affected the performance of the glass composite under fracture, bending, and impact loadings. In the case of PABDM polymers, they appeared to have an insignificant impact on the composite's mechanical properties (strength, rupture strain and impact resistance). However, they improved the glass composite's fracture toughness when used with a low concentration of crosslinker. Having both options of PA and PABDM to improve the mechanics of our material, the latter one seems to be a better option. Crosslinked PMMA could be extremely useful as, based on the results presented in [15], it significantly enhances the polymer's resistance against solvents and improves the polymer's stiffness. This also shows the enormous potential of adjusting the glass composite's mechanical, physical, and chemical properties by employing the different soft phases.

#### 4.5 Acknowledgements

AJE acknowledges support from NSERC RGPIN/05843-2014 & EQPEQ/472339-2015, FRQNT team grant, Canadian Foundation for Innovation Project #32749, and the Canada Research Chairs Program.

#### 4.6 References

- [1] S. W. Freiman, Fracture Mechanics of Glass, vol. 5. ACADEMIC PRESS, INC., 1980.
- [2] F. Barthelat, H. Tang, P. D. Zavattieri, C. M. Li, and H. D. Espinosa, "On the mechanics of mother-of-pearl: A key feature in the material hierarchical structure," *J. Mech. Phys. Solids*, vol. 55, no. 2, pp. 306–337, 2007.
- [3] H. D. Espinosa, J. E. Rim, F. Barthelat, and M. J. Buehler, "Merger of structure and material in nacre and bone Perspectives on de novo biomimetic materials," *Prog. Mater. Sci.*, vol. 54, no. 8, pp. 1059–1100, 2009.
- [4] N. Almqvist, N. H. Thomson, B. L. Smith, G. D. Stucky, D. E. Morse, and P. K. Hansma, "Methods for fabricating and characterizing a new generation of biomimetic materials," *Mater. Sci. Eng. C*, vol. 7, no. 1, pp. 37–43, 1999.
- [5] H. Le Ferrand, F. Bouville, T. P. Niebel, and A. R. Studart, "Magnetically assisted slip casting of bioinspired heterogeneous composites," *Nat. Mater.*, vol. 14, no. 11, pp. 1172–1179, 2015.
- P. Podsiadlo *et al.*, "Can nature's design be improved upon? High strength, transparent nacre-like nanocomposites with double network of sacrificial cross links," *J. Phys. Chem. B*, vol. 112, no. 46, pp. 14359–14363, 2008.
- [7] T. Ebina and F. Mizukami, "Flexible Transparent Clay Films with Heat-Resistant and High Gas-Barrier Properties," *Adv. Mater.*, vol. 19, no. 18, pp. 2450–2453, 2007.
- [8] Y. Liu, S.-H. Yu, and L. Bergström, "Transparent and Flexible Nacre-Like Hybrid Films of Aminoclays and Carboxylated Cellulose Nanofibrils," *Adv. Funct. Mater.*, vol. 28, no. 27, p. 1703277, 2018.
- [9] M. Mirkhalaf, A. K. Dastjerdi, and F. Barthelat, "Overcoming the brittleness of glass

- through bio-inspiration and micro-architecture," Nat. Commun., vol. 5, pp. 1–9, 2014.
- [10] Z. Yin, A. Dastjerdi, and F. Barthelat, "Tough and deformable glasses with bioinspired cross-ply architectures," *Acta Biomater.*, vol. 75, pp. 439–450, 2018.
- [11] Z. Yin, F. Hannard, and F. Barthelat, "Impact-resistant nacre-like transparent materials," *Science*, vol. 364, no. 6447, pp. 1260–1263, 2019.
- [12] T. Magrini, F. Bouville, A. Lauria, H. Le Ferrand, T. P. Niebel, and A. R. Studart, "Transparent and tough bulk composites inspired by nacre," *Nat. Commun.*, vol. 10, no. 1, p. 2794, 2019.
- [13] A. Amini, A. Khavari, F. Barthelat, and A. Ehrlicher, "Centrifugation of index-matched acrylic and glass flakes yields a strong and transparent bioinspired nacreous composite," *Submitt. to Sci. Mag.*, 2020.
- [14] T. P. Niebel, F. Bouville, D. Kokkinis, and A. R. Studart, "Role of the polymer phase in the mechanics of nacre-like composites," *J. Mech. Phys. Solids*, vol. 96, pp. 133–146, 2016.
- [15] A. Amini, A. Khavari, P. Tirgarbahnamiri, and A. Ehrlicher, "Tough and impact resistant poly(methyl methacrylate)-based polymers with tunable mechanical properties," *Under Prep.*, 2020.
- [16] M. Sakai and R. C. Bradt, "Fracture toughness testing of brittle materials," *Int. Mater. Rev.*, vol. 38, no. 2, pp. 53–78, 1993.

# Chapter 5

Conclusions

#### **5.1** Summary of accomplishments

In this thesis, we addressed the problem of general trade-off between mechanics, transparency, and fabrication scalability in many bio-inspired glass materials, and developed a bio-inspired glass composite with the following accomplishments and findings:

#### -Simple and straightforward fabrication method to mimic nacre:

There are numerous fabrication techniques with different levels of complexity that mimic the different aspects of bio-inspired materials, including nacre, and some of them accomplish the job through overly complicated methods. We presented a simple technique based on fundamental physical principles to make a material with a brick-and-mortar structure similar to natural nacre. Our centrifuged-based technique took advantage of density difference between glass and polymer to create a compact structure of glass flakes, highly oriented in one direction, with relatively thin layers of polymer in between. A proper surface functionalization technique created strong bonds between the two phases and played the integral role of mineral connective bridges in natural nacre. Overall, our composite not only mimicked the microstructure of the nacre, but it also showed high levels of fracture toughness that were achieved by activation of toughening mechanisms similar to those observed in natural nacre.

#### - Employing index-matching as a strategy to make a transparent structure:

To develop a transparent nacreous composite, either the size of the glass particles should be smaller than the light wavelength or the refractive indexes (RI) of the two phases should match. The former condition is not ideal considering the basic size requirements for glass platelets in nacreous structures. On the other hand, increasing the RI of the soft phase to the glass's through conventional ways such as incorporating nanoparticles into the polymer matrix would raise many new complexities. Hence, we employed a more straightforward yet efficient method for matching the

RIs of the two phases by adding a dopant to the soft phase. In this way, the polymeric phase's mechanical properties would remain unchanged, while at the same time, we could considerably increase the polymer's RI and match it to the glasses. The index-matching strategy eventually yielded a composite structure with high levels of transparency, comparable to normal glasses.

#### -A transparent, strong, tough, and scalable glass composite:

We addressed the general trade-off challenge that bio-inspired glasses have suffered vis-à-vis its mechanics, transparency, and fabrication scalability. Our glass composite possesses high levels of optical transparency comparable to regular glass and far beyond its bio-inspired counterparts. It is also easily scalable through a straightforward fabrication method, and its application is not limited to thin films. Additionally, it outcompetes the normal glasses in all the essential structural aspects; it is more than five times tougher, and about 80% stronger than the annealed glass.

#### -An impact-resistant and safer glass composite:

One of the most critical aspects of glass structures is the resistance to impact loads. Our bio-inspired glass composite exceeds annealed glass and PMMA's impact resistance, absorbing more than 34 and 5 times more energy than glass and PMMA. Also, when it breaks under impact loads, our glass composite appeared to be much safer than normal annealed glass due to the fact that it turns to just a few pieces as compared to the normal glass, which experiences an explosive fracture and turns into dangerous fragments.

#### -A simple strategy to tune the mechanics of PMMA:

we employed copolymerization and crosslinking techniques to make a new class of PMMA-based polymeric materials, aiming to modify and tun the mechanical, physical, and chemical properties of neat PMMA. The main goal was to produce such a material by adhering to the straightforward synthesis process of PMMA. In this regard, by adding a copolymerization agent (AN) and/or one

crosslinking agent (BUT), we successfully developed a class of polymers comprising more than 90 mol% of methyl methacrylate, with the possibility of improving polymer's several essential material properties. Our methodology maintained the transparency of the PMMA and significantly improved the polymer's chemical resistance. Also, depending on the polymer's composition, up to several structural aspects of the polymer could be improved. For instance, copolymerization with only 2 mol% of AN increased the rupture strain, fracture toughness, and impact resistance at the same time while retaining the material's strength.

#### - Adjusting the structural properties of the composite glass by tuning the soft phase:

The soft phase plays a vital role in the performance of the nacreous structures under mechanical loads. Besides, the polymeric phase is the only component in such materials whose properties could be tuned. In this regard, we incorporated our PMMA-based polymers into our glass composite to make a material with tunable structural properties. In this way, we could increase the glass composite's flexibility, increasing the rupture strain by 30% while retaining the strength and flexural modulus. Additionally, we could increase our bio-inspired composite's fracture toughness by as much as 40%.

#### 5.2 Thesis contributions

The contributions of the present work to the study of material science can be summarized as below:

- Developing a straightforward and scalable methodology based on centrifugation for fabricating transparent bio-inspired nacreous glass composites.
- Fabrication of a bio-inspired glass composite possessing high levels of optical transparency, strength, and toughness at the same time.

- Fabrication of a nacreous glass composite with superior impact resistance compared to annealed glass and PMMA.
- Studying the effect of centrifugation on the nacreous glass composite's microstructure (volume fraction, polymer layer thickness, and glass flake orientation)
- Studying the impact of the centrifugation process on the mechanical properties and fracture toughness of the glass composite.
- Identification of prevailing extrinsic toughening mechanisms responsible for high levels of fracture toughness in the glass composite fabricated using the centrifuged-based technique.
- Developing a simple methodology based on copolymerization with Acrylonitrile and crosslinking with 1,4 Butanediol dimethacrylate in a free radical polymerization process for improving the mechanical properties of PMMA.
- Improving PMMA's fracture toughness, impact resistance, and flexural modulus using small concentrations of copolymerizing and crosslinking agents in a free radical polymerization process.
- Improving PMMA's chemical resistance as a result of crosslinking the polymer network while retaining the optical transparency of the material.
- Studying the role of soft phase on mechanical properties of the nacreous glass composite by incorporating the family of crosslinked and copolymerized PMMA polymers into the composite.
- Improving the glass composite's fracture toughness and chemical resistance while retaining its high levels of strength and impact resistance using a crosslinked and copolymerized PMMA as the soft phase.

#### 5.3 Future work

In this study, we proposed a straightforward methodology for the fabrication of a bio-inspired nacre-like composite material. We used glass flakes and PMMA as the soft and hard phases,

respectively. Our fabrication method is based on simple physical principles: it employs centrifugation to make an ordered and compact structure, and index-matching for the sake of optical clarity. Our nacreous glass composite outperformed annealed and other bio-inspired glasses in strength, fracture toughness, and impact resistance. We also demonstrated that the choice of soft phase is of great importance and can vastly affect the final composite's mechanical, physical, and chemical properties. Our findings are show promise and great potential in this class of materials. Based on this, the following suggestions are proposed as future work:

-Seeking other self-assembly methods:

In this study, we employed centrifugation as a means of self-assembly of glass flakes. We demonstrated that even a moderate centrifugation force could lead to a relatively dense structure that resembles natural nacre. In this regard, finding other simple methods for making such a structure could lead to an even more approachable fabrication technique. Self-assembly of the flakes using sound waves could be the topic of the next study. The goal is to obtain a system which is comprised of glass flakes and monomer in minimum energy state with sound waves. This could be achieve either with high-frequency waves found in ultrasonic cleaning baths or low-frequency waves accessible from traditional speakers could give the system such energy. Another source of energy for self-assembly of flakes is through vibration. This simple mechanism can be implemented even with a simple shaker that has the potential to give the system enough energy for assembling the glass flakes in a brick and mortar manner.

-Role of flake size on optics and mechanics of the composite:

Although index-matching yields a transparent structure, our composite's haziness is relatively high compared to the normal glass. This is partly due to the many tiny glass particles that are potential light diffraction sites in the material. In this regard, an effective filtering mechanism to obtain the

narrowest size distribution would be a first step. Subsequently, studying the effect of different flake sizes on the optics is of great importance to achieve acceptable levels of transparency. On the other hand, glass flake size affects the mechanics of the composite as well, and too big flakes could prevent the activation of extrinsic the glass composite's toughening mechanisms. Hence, the optimum flake size should be chosen in a way that the highest optical clarity, mechanical properties, and the lowest haziness is obtained.

-Smart soft phase, smart glass composite:

Our glass composite is comprised of two phases. Chapter 4 showed that by adjusting the polymeric phase, we could improve some desired aspects of the glass composite. Considering the potential of the soft phase, we can seek more than just improved mechanical properties. A wide range of polymeric materials could be actuated by being exposed to external stimulation sources. For instance, electrochromic polymers, a class of polymeric material that change color when exposed to an electric potential, could be a candidate for incorporating into our glass composite to make a smart glass structure that can change color or turn to a non-transparent structure as desired. The same concept could be implemented using a thermochromic (change color by heat), mechanochromic (change color by pressure) or photochromic (change color by light) polymers.

-Lamination, an approach toward a safer glass composite:

Glasses are brittle materials and under impact loads, experience an explosive fracture, forming many small fragments. Chapter 4 showed that our glass composite is much safer than regular glass as it only forms a few pieces during failure from impact loads. To further improve the glass composite's safety, the old yet reliable method of lamination could be employed where glass sheets and thin layers of polymers are sandwiched into one piece. In the case of fracture, the polymeric layers hold the glass pieces together and prevent the broken pieces becoming dangerous

projectiles. This strategy could be used for our glass composite as well. However, this might lead to a decline in the mechanical properties of the final product. Hence, a study on the effect of lamination and polymeric layers' choice is necessary to obtain an overall improvement in the glass composites mechanical properties.

## Chapter 6

Supplementary experimental information

The journey of my PhD research has been a very challenging and adventurous one, and what is presented here is only a part of my research activities at Professor Ehrlicher lab. The primary goal of the project was to **self-assemble** some plate-like micron-size particles with a **layer of polymer** in between to eventually have a **transparent**, **tough**, **strong** nacreous structure. To accomplish each part of that goal, I tried many different solutions and changed my path several times. Although the main objective of the project is accomplished, I believe briefly describing the steps I took to this point would be very beneficial to anyone who wants to continue this work or is simply interested in this field of study.

I tried several different methods for self-assembly of particles, three of which took more time and energy. First, the DNA self-assembly; I coated the surface of two groups of particles, i.e. glass flakes, with two different pre-designed DNA strands through a click chemistry process. The DNA strands were designed in a way that could hybridize in a proper condition. In other words, I was trying to self-assemble some micron-sized particles with an excessive layer of nanometer-sized DNA polymer on the surface. This, of course, raised many problems and questions, including if the DNA strands are long enough to hybridize despite huge repelling forces between flakes. As a solution to this concern, I purified some plasmids to obtain longer chains of DNAs for this purpose. Since we were looking for a simple and scalable technique and considering many problems regarding the DNA assembly technique, I decided to change the path. The next important technique was the freeze-casting method. Freeze casting is a great technique to assemble ceramic/glass particles in a lamellar way, make a brick-and-mortar structure, and obtain high levels of toughness and strength. Despite successful implementation of the technique and even making some structures with pre-designed local anisotropy, attempts to make the samples transparent were not successful. This, I believe, was due to the existence of many pocket holes and bridges between

matched polymer to the freeze-cast sample, we could at best make a translucent structure. Another method I tried was to orient and assemble the glass flakes using the magnetic field. For that, I coated the surface of the glass flakes with proper magnetically sensitive nanoparticles and exposed a solution of flakes to a weak magnetic field. In this way, I could successfully orient the flakes in one direction and assemble them under gravity. This process, however, raised many new problems such as, how to add the polymeric phase to the system. There were also some concerns about the adverse effect of nanoparticles on the transparency of the final product.

Before starting to use PMMA as the soft phase in our composite, I spent a great amount of time using silicones (PDMS) as the soft phase. Despite having some great properties such as transparency, flexibility, and toughness, some problems made me look for other options such as PMMA. Firstly, PDMS's inertness made it harder for chemical processes such as nanoparticle addition. Also, unlike the PMMA, there was no dopant for silicones. Also, in absence of mineral bridges in our material, the soft phase should have some high levels of strength and contribute more to the strength and integrity of the whole structure. But the strength of silicones, because of their chemical structure, could go up to only 10 MPa. Another interesting goal we pursuit was to induce some weak and secondary interactions in the silicone network to induce huge deformations while retaining the strength of the structure. Despite some successful attempts, we never used that network in our glass composite due to the inherent problems with PDMS was mentioned earlier. Another challenging task was to mix two phases and obtain a transparent structure, where our strategy was based on matching the refractive indexes of the two phases. While there is nothing much we can do about glass flake's RI, we could tune the RI of the polymeric phase. The first attempt, for both silicones and PMMA, was to incorporate some nanoparticles into the polymeric

network. Out of many options and based on the requirements of the project, I chose the simple addition method, where the surface-treated nanoparticles were added to and dispersed in the polymeric phase. I synthesized titanium oxide and zirconium oxide nanoparticles and successfully increased the RI of silicones and PMMA. But the problem was the very hard and time-consuming process of making nanoparticles and surface treating them, where a simple change in humidity of the lab would make all the nanoparticles agglomerate. The other problem was the need for a high concentration of nanoparticles in my polymer to increase its RI to one of the glass, which added greatly to the complexity of the whole process. Due to all of the mentioned reasons, we eventually came up with the idea of using the dopants for increasing the RI.

In addition to the method presented in this thesis in chapter 2, I tried a more sophisticated technique named Atom Transfer Radical Polymerization (ATRP). Unlike free radical polymerization, in which there is no control over the formation and growth of the polymeric chains, in ATRP the chain growth is controlled and can be started from a target surface (glass flake surface in our case). After going through the complicated ATRP chemistry and growing PMMA chains from the surface of the glass flakes, I did not see any change in terms of mechanical properties of the glass composite and hence, I opted to use the conventional free radical polymerization process.